DIAMINOPOLYTHIOL COMPLEXES OF TECHNETIUM AND RHENIUM

By

HOSEN I ALARABI, B.Sc.

A Thesis

Submitted to the School of Graduate Studies

in Partial Fulfilment of the Requirements

for the Degree

Doctor of Philosophy

McMaster University

December 1993

DIAMINOPOLYTHIOL COMPLEXES OF TECHNETIUM AND RHENIUM

By

HOSEN I ALARABI, B.Sc.

DOCTOR OF PHILOSOPHY (1993) MCMASTER UNIVERSITY

(Chemistry) Hamilton, Ontario

TITLE: Diaminopolythiol Complexes of Technetium and Rhenium

AUTHOR: Hosen I Alarabi, B.Sc (Brock University, St.Catharines, Ont.)

SUPERVISOR: Professor C. J. L. Lock

NUMBER OF PAGES: xx, 166

ABSTRACT

Interest in technetium chemistry is derived from the fact that it is a recently-discovered element and from the use of the isotope ^{99m}Tc as a radioactive label in diagnostic nuclear medicine. Rhenium belongs to the same group in the periodic table as technetium, which makes the two elements similar in terms of chemical properties. Diaminopolythiol ligands designed for chelation with technetium and rhenium have been synthesized and characterized. Methods of characterization included ^{1}H NMR, ^{13}C NMR, IR, Raman and mass spectroscopy. Double resonance NMR experiments were carried out for confirmation of the NMR assignments. Single crystal X-ray diffraction was used in cases where suitable crystals could be isolated.

The unexpected formation of oxo(2-(1'-methyl-1'-mercaptoethyl)-3-(5''-methyl-5''-mercapto-3''-dehydroazahexyl)-thiazolidinato-N^{3},$N^{3''}$,$S^{1'}$,$S^{5''}$)technetium(V) (7) was reinvestigated. The complex was prepared previously and was thought to have the technetium atom bound to two nitrogen and three sulfur atoms giving a novel TcO(N2S3)[1] complex. The crystal structure determination of the complex showed that the third sulfur atom was not bound to technetium instead it formed a S-C bond to give a five-membered thiazolidine ring. It was shown in this work

[1]Throughout this thesis the nomenclature NXSY, where X and Y are not subscripts, indicate an organic ligand with X nitrogen atoms and Y sulfur atoms.

that the unexpected thiazolidine ring formation had taken place during the ligand synthesis and before the complex formation.

The ligand N10-(thioethanoyl)-2,2,5,5-tetramethy-3,4-dithia-7,10-diazabicyclo[5.3.0]decane **(10)**, was synthesized in a multi-step procedure. The reaction of **(10)** with $ReO(P(Ph)_3)_2Cl_3$ led to the unexpected formation of the novel asymmetric Re(V)ON2S2 complex, oxo(1,1-dimethyl-3-aza-6-amidooctane-1,8-dithiolato)rhenium(V) **(11)**. Complex **(11)** was characterized by single crystal X-ray diffraction and IR and Raman spectroscopy.

ACKNOWLEDGEMENTS

I would like to express my gratitude to Professor Colin Lock for his guidance and friendship throughout the course of this study.

I am grateful to my committee members Prof. R. A. Bell and Prof. M. J. McGlinchey for their help with various aspects of this work.

I gratefully acknowledge Dr. D. W. Hughes, Mr. B. Sayer for their technical assistance on the NMR spectrometers and Dr. J. Britten for his help with the X-ray work.

I wish to thank Theresa Fauconnier, Daren Leblanc, and John Valliant for their friendship and Z. Wang and Y. Wei for their cooperation. Thanks to Dr. Alan Guest for his encouragement.

abbreviations

Ab	antibody
BAT	bis-aminothiols
BBB	blood brain barrier
bipy	2,2'-bipyridine
BNL	Brookhaven National Laboratories
CAT	computer assisted tomography
CCD	charge coupling device
CIMS	chemical ionization mass spectrometry
DADS	diamidodisulfides
DADT	diaminodithiol
DCC	1,3-dicyclohexylcarbodiimide
DCIM	N,N'-carbonyldiimidazole
DCIMS	direct chemical ionization mass spectrometry
DEIMS	direct electron impact mass spectrometry
DCU	dicyclohexylurea
DMF	N,N-dimethylformamide
DMG	dimethylglyoxime
dmpe	1,2-bis-(dimethylphosphino)ethane
DMSO	dimethyl sulfoxide

edt	ethane-1,2-dithiolato
e=dt	ethene-1,2-dithiolato
EIMS	electron impact mass spectrometry
FA	fatty acid
H_2edt	ethane-1,2-dithiole
HOMO	highest occupied molecular orbital
HPLC	high performance liquid chromatography
hr	hour
Hz	hertz
IPA	isopropyl alcohol
IPPA	p-iodophenyl pentadecanoic acid
IR	infra red
MAMA	monoaminemonoamidedithiol
mdtc	morpholine-N-carbodithioate
mer	meridional
min	minute
MRI	magnetic resonance imaging
MS	mass spectrometry
NMR	nuclear magnetic resonance
NOE	nuclear Overhauser effect

NXSY	an organic ligand with X nitrogen and Y sulfur atoms
Ph	phenyl
phen	1,10-phenanthroline
ppm	parts per million
SPECT	single photon emission computerized tomography
tdt	toluene-3,4-dithiolate
terpy	2,2':6',6"-terpyridine
THF	tetrahydrofuran
TLC	thin layer chromatography
TMS	tetramethylsilane
tu	thiourea
USA	The United States of America
yr	year

TABLE OF CONTENTS

LIST OF TABLES

LIST OF FIGURES

APPENDIX

Numbering Scheme

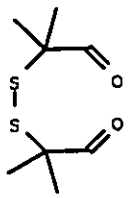

(1)

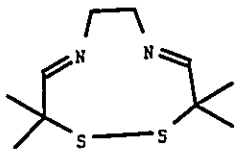

(2)

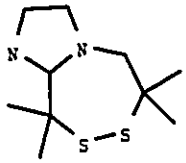

(3)

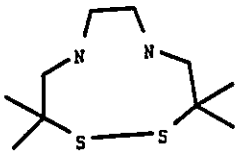

(4)

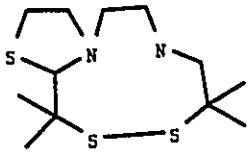

(5)

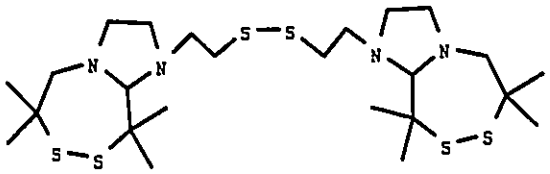

(6)

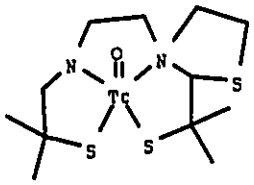

(7)

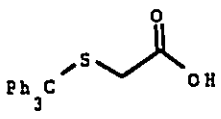

(8)

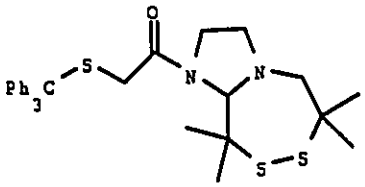

(9)

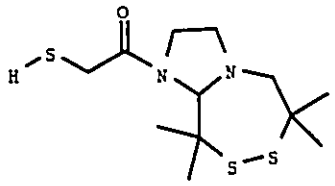

(10)

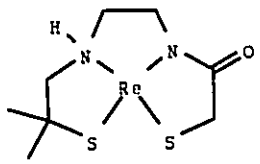

(11)

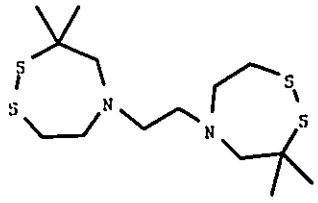

(12)

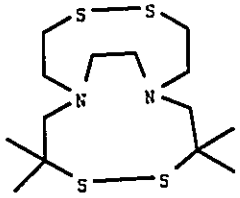

(13)

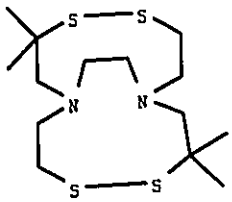

(14)

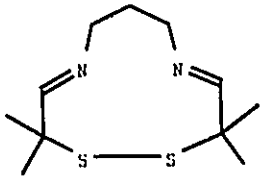

(15)

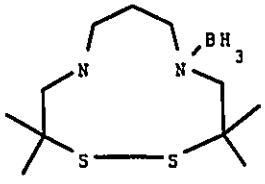

(16)

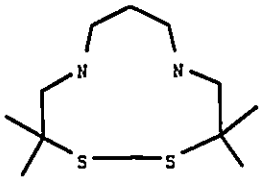

(17)

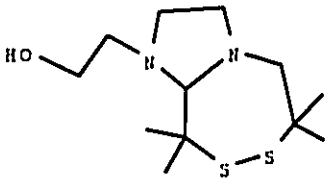

(18)

Chapter 1

Introduction

1.1 Introduction

Technetium has a very diverse chemistry. Because of the lanthanide contraction there are close similarities between the chemical properties of technetium and its third-row congener rhenium, whereas the chemistries of both elements differ considerably from that of the first row element manganese. In compounds, technetium is known to exist in oxidation states from -I to VII, with coordination numbers ranging from 4 to 9 [1]. As far as simple salts are concerned, TcO_4^- is the most stable chemical form of technetium, followed by TcO_2 in which the oxidation states of technetium are +7 and +4, respectively. The remaining oxidation states of technetium gain stability through complex formation. The coordination complexes of technetium containing organic ligands are numerous. Mono- and polydentate ligands that form technetium complexes include compounds with N, O, S, P and As donor atoms. In addition, mixed atom donor ligands that form technetium complexes are well known. This work describes studies which have been undertaken to investigate the use of diamine and diamide polythiolate (N2S2, N2S3, N2S4) chelates as a potential starting point for making new technetium radiopharmaceuticals.

1.2. The Element Technetium

Technetium was the first element to be produced artificially. Despite earlier claims, the first conclusive experimental evidence for its production was provided by Perrier and Segré when they isolated minute amounts in 1937 [2-4]. Their procedure involved subjecting a molybdenum plate to deuteron irradiation from a cyclotron. The element is a bright silvery grey metal which can be obtained in the form of rods, strips, foil and wires. It crystallizes in a hexagonal closest packed arrangement. The metallic radius of technetium is 1.261 Å and the metal has a density of 7.47 g cm^{-3} and a melting point of 1247 °C [5]. Technetium is unique among the *d*-block elements in that it has no stable isotope. All isotopes of this element are unstable on a geological time scale, and thus throughout the early history of chemistry there was no technetium available for study. For this reason the chemistry of technetium is relatively new.

Currently ^{99}Tc, the most stable isotope of technetium, is produced in kilogram amounts by extraction from a mixture of uranium fission products. ^{99}Tc presents only minor radiation hazard ($t_{1/2}$= 2.1 x 10^5 yr, β^- = 292 KeV) and can be safely handled in milligram quantities. For these reasons, the chemistry of technetium is being investigated by employing ^{99}Tc. During the last two decades, technetium chemistry has been a very active field of research because ^{99m}Tc is used extensively diagnostic nuclear medicine procedures. Progress in this field depends upon basic research into the chemistry of technetium.

1.3. Technetium in Nuclear Medicine:

^{99m}Tc is the most widely used isotope in the practice of diagnostic nuclear medicine. The potential for use of ^{99m}Tc in diagnostic imaging was first recognized by Richards in 1960 [6], and its first actual use in humans was reported by Harper in 1962 [7]. Currently, in the USA, it is used in greater than 85% of all nuclear medicine studies [8]. There are three reasons why ^{99m}Tc is extremely useful in diagnostic medicine:

(a) the nuclear properties of this isotope are ideal. The γ-ray energy, 140 KeV, of ^{99m}Tc is well-suited for the Auger camera and gives excellent resolution and efficiency with low energy collimators. ^{99m}Tc does not emit α or β particles, it has low γ-ray energy and a short (6hr) half-life which all allow its use in large quantities with only low radiation dose to the patient. While a portion of the technetium may remain in the tissues for considerable periods, the gamma emitting ^{99m}Tc decays to ^{99}Tc which emits negligible radiation because of its long half-life.

(b) ^{99m}Tc is inexpensive and readily available to hospitals *via* $^{99}Mo/^{99m}Tc$ generators. The technetium generator was originally developed in 1958 by Walter Tucker and Margret Greene at the Brookhaven National Laboratories (BNL) [9]. Current generators contain $[^{99}MoO_4]^{2-}$ adsorbed onto an alumina ion exchange column. Figure 1.1 shows a typical arrangement for a ^{99m}Tc generator. Figure 1.2 shows that continuous β^- decay of $^{99}MoO_4^{2-}$ yields $^{99m}TcO_4^-$ which in turn decays

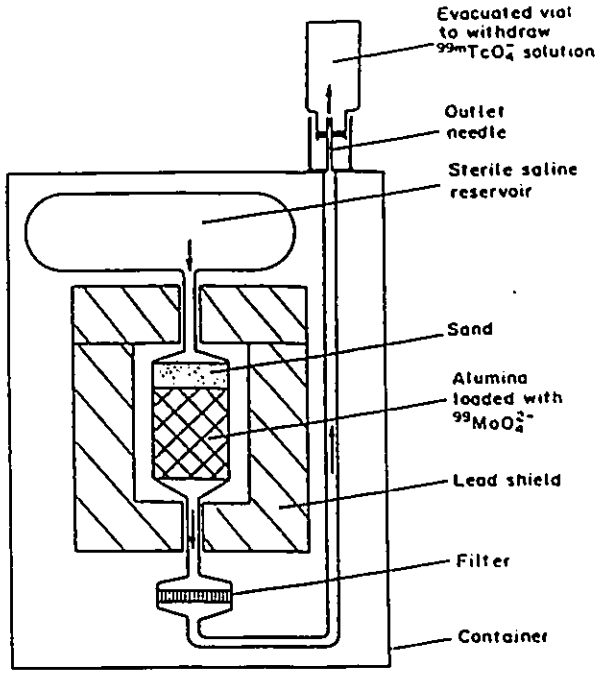

Figure 1.1. A typical ^{99m}Tc generator

to $^{99}TcO_4^-$. The parent ^{99}Mo has a half-life of 66hr which allows time for shipment from the manufacturer to hospitals. In addition, the 6hr half-life of ^{99m}Tc allows rapid build-up of activity allowing for frequent milking of the generator. At clinical facilities, both forms of pertechnetate, $^{99m}TcO_4^-$ and $^{99}TcO_4^-$, are eluted from the column with 0.15M NaCl solution, leaving behind the parent $^{99}MoO_4^{2-}$. The activity of the eluent and the relative quantities of ^{99m}Tc and ^{99}Tc depend upon the age of the column and the period of time since it was previously eluted. The total technetium concentration in the eluent is usually in the range of 10^{-6} - 10^{-8}M [10].

(c) The diverse chemistry of technetium in its several oxidation states allows it to

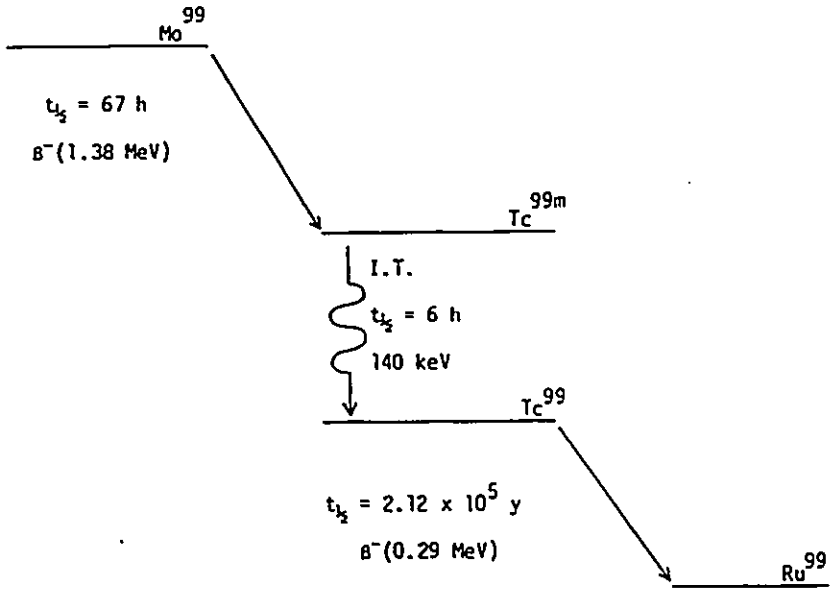

Figure 1.2. Decay scheme for technetium

be incorporated in a variety of organic molecules that are specific for different organs.

1.4. ^{99m}Tc Radiopharmaceuticals:

Unlike magnetic resonance imaging (MRI), CAT scanning or ultrasonic imaging which are often superior in terms of resolution, radioimaging shows not only the structure of the organ but also aspects of its physiological function. The visualization of the metabolism or clearance of a radiopharmaceutical in real time provides the physician with clear evidence of the ability of the organ to carry out its function. An unusually high or low accumulation of the radiopharmaceutical

in a certain organ or part of the body is normally taken as a strong indication of an organ failure or tumour growth. A large number of technetium compounds are used to image various organs including the brain, kidneys, liver, lungs, heart, bones, *etc.* [11-17]. These radiopharmaceuticals can be divided into four broad categories:

(a) simple technetium complexes which have the tendency to localize in a particular organ. These are called technetium essential radiopharmaceuticals,

(b) proteins and macromolecules whose biological distribution is predictable and where the technetium label causes no major change in their behaviour,

(c) ^{99m}Tc tagged colloidal particles,

(d) whole blood cells labelled with ^{99m}Tc.

1.5. Methods of Synthesis:

Because of the diversity of technetium chemistry, a very large number of synthetic routes, which use a variety of starting materials have been reported. In general, however, the methods of synthesis of technetium complexes can be divided into two broad categories which are: the reduction of TcO_4^- and by ligand substitution reactions.

1.5.1. The Reduction Route:

The reductive methods for the syntheses of technetium complexes start from the pertechnetate ion TcO_4^-, in which technetium is in the +VII oxidation state. Tc(VII) is easy to purify either by sublimation of Tc_2O_7 or extraction of TcO_4^-

in nonaquous solvents. TcO_4^- is also the most readily available chemical form of technetium. It can be readily prepared by oxidation of the metal with concentrated nitric acid. Salts of pertechnetate are, therefore, the most convenient starting materials for the study of technetium chemistry. Pertechnetate is a relatively mild oxidant (E_o = 0.738V) and is initially reduced to $[TcO_4]^{2-}$ [18, 19].

$^{99m}TcO_4^-$ is the starting material for all nuclear medicine applications of technetium since this is what is produced by $^{99}Mo/^{99m}Tc$ generators. In nuclear medicine preparations, $^{99m}TcO_4^-$ is reduced in the presence of a ligand or a biomolecule that is to be labelled:

$$[^{99m}TcO_4]^- + \text{reductant/ligand} \text{ ------> product complex} \qquad \text{eq.1.1}$$

Reactions of this type are controlled by the 6hr half-life and the low concentration of $^{99m}TcO_4^-$ (10^{-6} to 10^{-8}M). In most cases, the reaction produces a mixture of reduced technetium complexes. Commercial "kits" for the rapid preparation of ^{99m}Tc radiopharmaceuticals almost invariably use Sn(II) as the reductant, and this may lead to problems associated with the chemistry of tin and the fact that Sn(IV) and Tc(IV) are physically very similar. The extent to which Tc(VII) is reduced depends on whether excess Sn^{2+} is used, the pH, and whether air is excluded [20]. If a large excess of stannous ion is used, tin might compete with technetium for the ligand. The reaction of the N3S3 hexadentate ligand, shown in figure 1.3, with

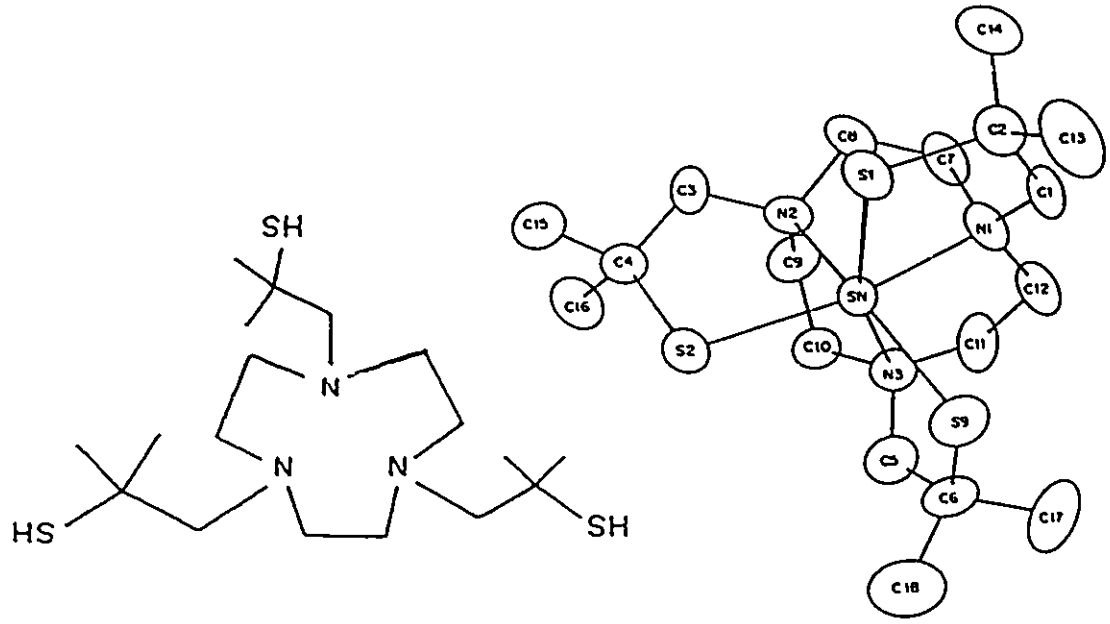

Figure 1.3. N, N',N''-tris[2-methyl-(2-mercapto)propyl]-1,4,7-triazacyclononane and its tin(IV) monocationic complex

ammonium pertechnetate in the presence of tin(II) tartrate provided the cationic six coordinate tin(IV) complex shown in figure **1.3** [21]. Pertechnetate was incorporated into the complex as counter anion. This illustrates that the incorporation of tin instead of technetium in the compound is possible when stannous ion is used for pertechnetate reduction. The isolation of $[Tc(DMG)_3SnCl_3(OH)].3H_2O$ (DMG = dimethylglyoxime), figure **1.4**, is clear evidence for the possible incorporation of both tin and technetium into complexes that are prepared by stannous reduction of TcO_4^- [22], and care should be taken when predicting structures of proposed radiopharmaceuticals.

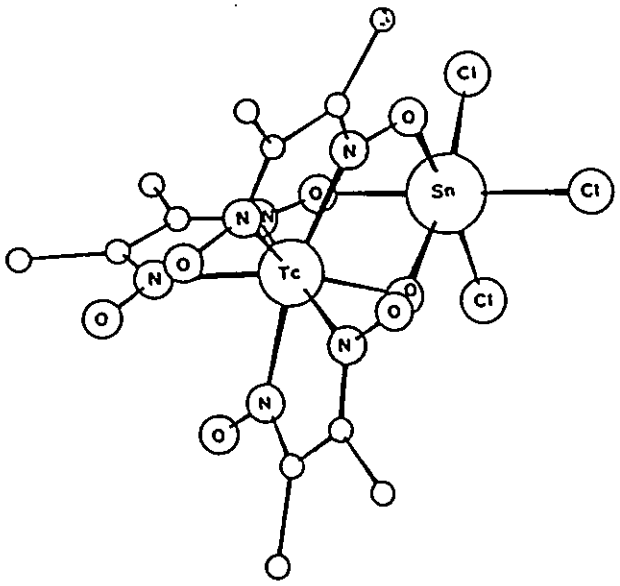

Figure 1.4. The structure of $[Tc(DMG)_3SnCl_3(\mu\text{-}OH)]$

When dealing with macroscopic amounts of ^{99}Tc the reduction of pertechnetate is not always the most useful synthetic route since it leads to a variety of products. In the absence of a strong acid or a good complexing agent, the undesirable formation of the insoluble oxide $TcO_2.xH_2O$ rapidly takes place. In addition, many organic reductants, such as thiols, tend to work slowly or only at high pH, which promotes hydrolysis of the reduced technetium species and the formation of TcO_2. Extensive work-up of the product mixture and chromatographic separation, however, can lead to the isolation of complexes of analytical purity.

1.5.2. The Substitution Route:

The substitution method is useful in the synthesis of Tc(V), Tc(IV) and Tc(III) complexes because the starting materials $Tc(V)OCl_4^-$, $Tc(IV)Cl_6^{2-}$ and $Tc(S\text{-thiourea})_6^{3+}$ can be prepared readily. Synthetically useful materials should contain fairly labile ligands and be readily soluble in organic solvents in which hydrolysis to $TcO_2.xH_2O$ is prevented. The substitution method has not been commonly used in the synthesis of ^{99m}Tc radiopharmaceuticals because it is not easy to produce such intermediates in high purity from 10^{-6} - 10^{-8}M solutions of $^{99m}TcO_4^-$.

$TcOCl_4^-$ [23, 24] represents a useful synthetic starting material for Tc(V) complexes. It has a square pyramidal geometry in which the oxo ligand sits in the apical position and the basal plane is defined by the four chlorine atoms. The technetium oxygen bond is short (1.610(4)Å) [23], and is formally considered a triple bond. Figure 1.5 shows a molecular orbital diagram for $[TcOCl_4]^-$. This diagram is by no means quantitative; nevertheless, it gives a rough picture of the bonding between the five ligands and the technetium centre. There are two important features in this diagram that should be pointed out. First, there is a π overlap between the oxygen p_x and p_y orbitals and the technetium d_{xz} and d_{yz} orbitals. This overlap leads to the set of π and π^* orbitals in the complex and is the cause of the triple bond character of the Tc-O bond. Second, the highest occupied molecular orbital (HOMO) is a singly degenerate (d_{xy}, b_2) orbital that is essentially non-bonding. This orbital is fully occupied by two electrons, which is

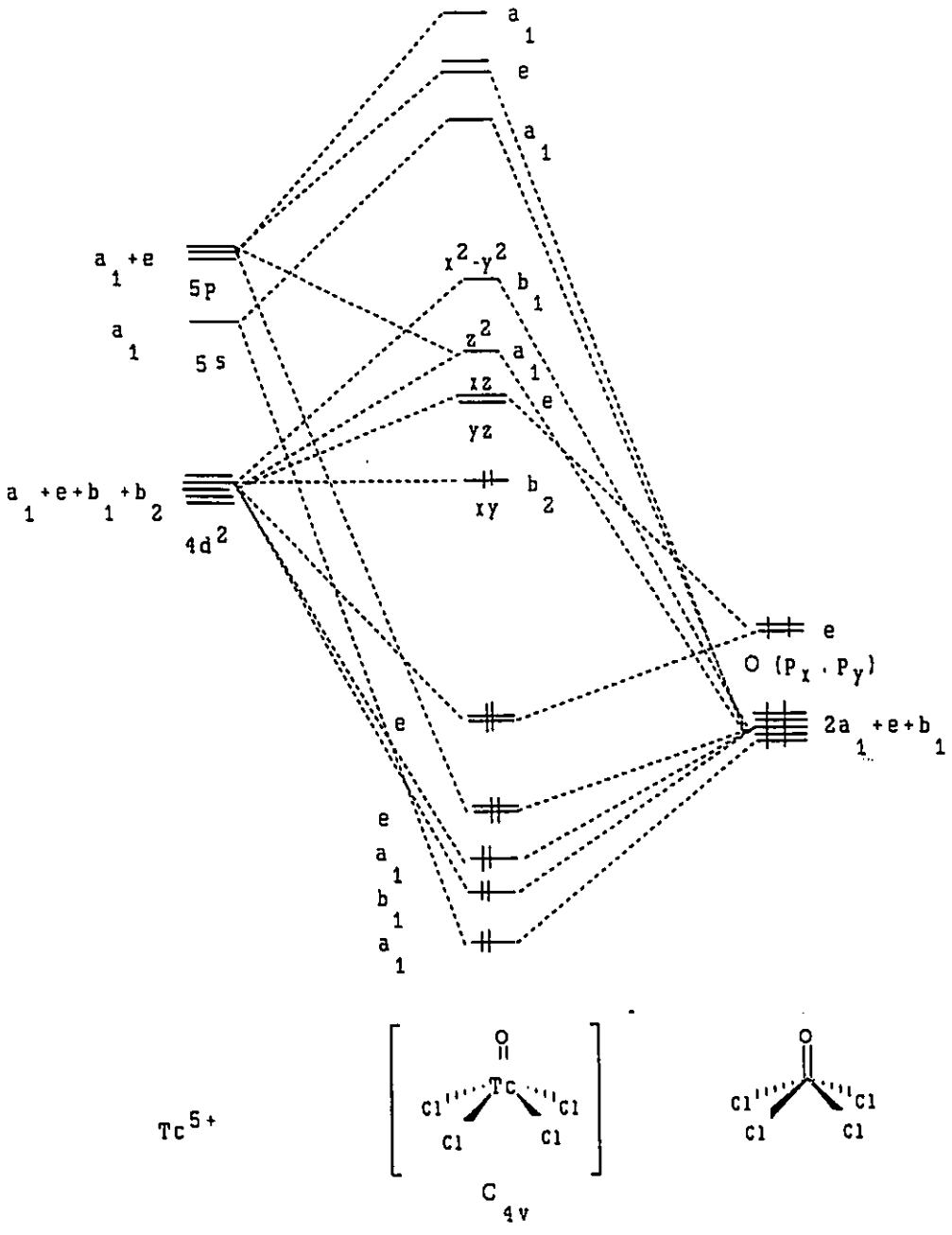

Figure 1.5. A qualitative molecular orbital diagram for $[TcOCl_4]^-$

consistent with the fact that the ion is diamagnetic. For electron-count purposes,

it should be mentioned that Tc^{5+} has a $4d^2$ electronic configuration.

$TcOCl_4^-$ is prepared by the reaction of TcO_4^- with cold concentrated HCl:

$$TcO_4^- + 6\ HCl \longrightarrow TcOCl_4^- + 3\ H_2O + Cl_2 \qquad \text{eq.1.2}$$

The anion can be precipitated easily from acid solution as $[(C_4H_9)_4N][TcOCl_4]$ by the addition of excess tetrabutylammonium chloride. Tetrabutylammonium tetrachlorooxotechnetate(V) is a light grey-green solid that dissolves readily in polar organic solvents such as, methanol, dichloromethane, acetone and acetonitrile [25]. It can be easily identified by IR spectroscopy. It has a Tc=O IR stretching absorption that occurs at 1019 cm^{-1}. With the use of the n-Bu_4N salt, substitution onto $TcOCl_4^-$ is usually carried out in organic solvents to prevent the hydrolysis and disproportionation of the starting material to TcO_4^- and TcO_2, which takes place in neutral aqueous solutions. The majority of Tc(V) complexes have been prepared from $TcOCl_4^-$ [26, 27]:

$$TcOCl_4^- + \text{ligand} \longrightarrow \text{Tc(V) complex} \qquad \text{eq.1.3}$$

Normally the Tc=O bond remains intact while the labile chlorine atoms are replaced by the donor atoms from the ligand(s). This process results in the formation of a Tc(V) complex that contains the characteristic $[Tc=O]^{3+}$ unit which

is readily identified by its IR stretching absorption that occurs at 930-1020 cm^{-1}. Although less common, it is possible to break the Tc=O bond in $TcOCl_4^-$ as in the case of the synthesis of $Tc(mdtc)_4$ (mdtc = morpholine-N-carbodithioate) [28] and $Tc(P(Ph)_3)(S_2COC_4H_9)_3$ [29].

$TcCl_6^{2-}$ is another useful starting material for the synthesis of technetium complexes. It can be prepared by the reaction of TcO_4^- with hot concentrated HCl

$$TcO_4^- + HCl \longrightarrow TcCl_6^{2-} \qquad \text{eq.1.4}$$

Substitutions onto $TcCl_6^{2-}$ are also carried out in organic solvents in which sufficient solubility is provided by the tetraalkylammonium salts.

$$TcCl_6^{2-} + \text{ligand} \dashrightarrow \text{Tc(IV) product} \qquad \text{eq.1.5}$$

The octahedral compound mer-$[Cl_3(Me_2PhP)_3Tc]$ was synthesised through the reaction of $(NH_4)_2[TcCl_6]$ with dimethyl phenyl phosphine in absolute ethanol [30]. The reaction of $K_2[TcCl_6]$ with ethane-1,2-dithiol (H_2edt) provided the novel complex $[AsPh_4][Tc(S)(edt)_2]$, edt = ethane-1,2-dithiolato, and the dimeric Tc(IV) complex $[Tc_2(edt)_2(\mu\text{-}e{=}dt)_2]$, e=dt = ethene-1,2- dithiolato, shown in figure 1.6 [31]. The anion $[Tc(S)(edt)_2]^-$ constitutes the first example of a technetium complex containing a terminal Tc=S bond, whereas, the dimer $[Tc_2(edt)_2(e{=}dt)_2]$ represents

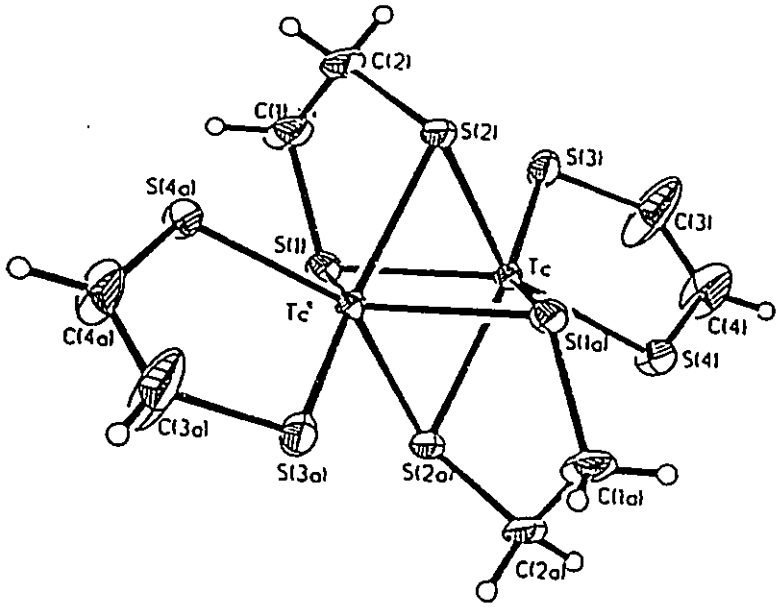

Figure 1.6. The structure of the dimer $[Tc_2(edt)_2(\mu\text{-e=dt})_2]$

a novel example of a technetium complex containing two terminal dithiolene and two bridging dithiolato ligands.

$Tc(tu\text{-}S)_6^{3+}$, (tu = thiourea), has also proven to be a useful synthetic starting material. It decomposes in water but is stable in alcohol. It can be made by the reaction of TcO_4^- with thiourea in HCl/ethanol or HBF_4/ethanol [32]. The structure determination of $[Tc(SC(NH_2)_6]Cl_3.H_2O$ has shown that the Tc-S bond distances range from 2.412(1) Å to 2.440(1) Å [32]. The thiourea complex has been used in the synthesis of several low-valent technetium species, including the hexakis isocyanide complex $[Tc(NCC(CH_3)_3)_6]PF_6$ and the hexakis trimethyl phosphite complex $[Tc(P(OCH_3)_6]PF_6$ by reflux with the appropriate ligand in

methanol [32]. A neutral technetium(III) complex with Ph.CO.CH_2.CS.Ph has also been made from the thiourea species [33].

Another technetium complex that has been successfully used in substitution reactions is $[Tc(V)(OH)O(dmpe)_2]^{2+}$, where dmpe = 1,2-bis(dimethylphosphino)ethane. Deutsch *et al.* [34] have used this compound in the synthesis of a series of compounds of the form $[Tc(SR)_2(dmpe)_2]^{+/0}$ and $[Tc(tdt)(dmpe)_2]^+$, tdt = toluene-3,4-dithiolate, [35-38]. In these reactions the technetium atom is reduced by excess thiol.

The complex $[TcCl_3(MeCN)\{P(C_6H_5)_3\}_2]$ has been reported as a good technetium(III) precursor [39]. It can be prepared either by the reduction of $[TcCl_4(PPh_3)_2]$ with zinc metal in acetonitrile in the presence of triphenylphosphine [39] or by the reaction of $[n\text{-}Bu_4N][TcOCl_4]$ with triphenylphosphine in acetonitrile [40]. Technetium complexes with the chelating imine ligands 2,2'-bipyridine, $[Tc(bipy)_3][BPh_4]_2$, 1,10-phenanthroline, $[Tc(phen)_3][BPh_4]_2$, and 2,2':6',2''-terpyridine $[Tc(terpy)_2][BPh_4]_2$, were prepared with the use of this precursor [39]. The labile MeCN ligand in $[TcCl_3(MeCN)\{P(C_6H_5)_3\}_2]$ was shown to be replaced effectively by the small π-accepting ligands NO and CO, which resulted in the isolation of $TcCl_3(PPh_3)_2(NO)$ and $TcCl_3(PPh_2)_2(CO)$ [40].

1.6. The N2S2 Systems:

N2S2 chelating agents are now very well known to form stable complexes

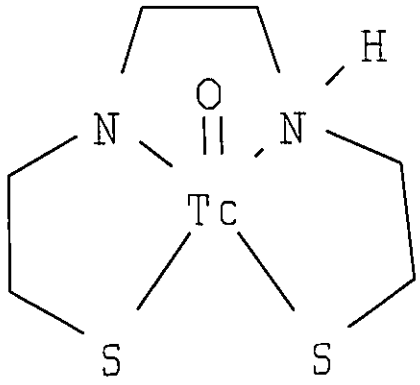

Figure 1.7. (TcO)(N2S2) complex

with technetium(V), [(TcO)(N2S2)]. These complexes have the general structure in which the technetium centre is five-coordinate in a square-pyramidal geometry with an oxo ligand at the apical position and the N2S2 chelate occupying the basal plane figure 1.7. The first (TcO)(N2S2) complex was reported in 1981 [41]. Since then the number of technetium complexes containing the N2S2 backbone has increased dramatically. Studies of those complexes include synthesis [41, 42], X-ray structure determination [43], and the investigation of their potential as imaging agents for single photon emission computerized tomography (SPECT) [44, 45]. N2S2 systems can be divided into two classes of ligands; diamido disulfides (DADS) and bis-aminoethanethiols (BAT).

1.6.1. The N2S2 (DADS) :

Davison and co-workers [41, 46] prepared and characterized the first ^{99}Tc

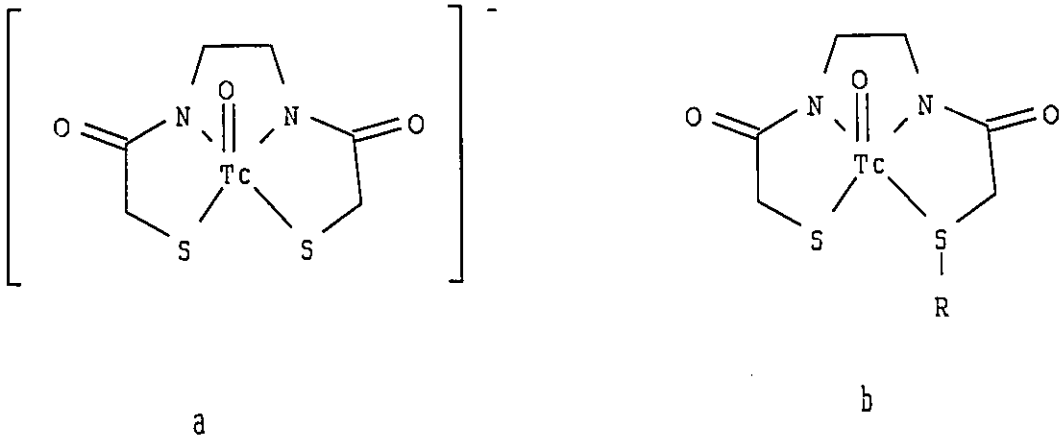

a b

Figure 1.8. $[TcO(DADS)]^-$ (a) and [TcO(DADS-R)] (b)

complex of 1,2-di(mercaptoacetamido)ethane (DADS, for diamide disulfide). The anionic complex, shown in figure 1.8 (a), was formed in high yield and was found to be highly stable with the ligand forming three 5-membered chelate rings about the TcO^{3+} core. Bryson *et al.* [47] modified the chelate (DADS) to give a series of mono-S-alkylated derivatives (DADS-R), R = CH_3, CH_2Ph, $(CH_2)CO_2H$ or $(CH_2)_2(NC_4H_8O)$; see figure 1.8 (b). Unlike the parent DADS ligand, which forms an anionic technetium complex, these S-alkylated ligands react to give five-coordinate neutral oxo-technetium(V) complexes, TcO(DADS-R).

With respect to nuclear medicine, the $[^{99m}TcO(DADS)]^-$ complex, shown in figure 1.8 (a), was found to be rapidly excreted by the kidney in a manner consistent with tubular secretion. Animal and clinical evaluations of $[^{99m}TcO(DADS)]^-$, however, indicated that its biological properties are inferior to

those of ^{131}I-o-iodohippurate [48, 49], which is routinely used to evaluate renal function.

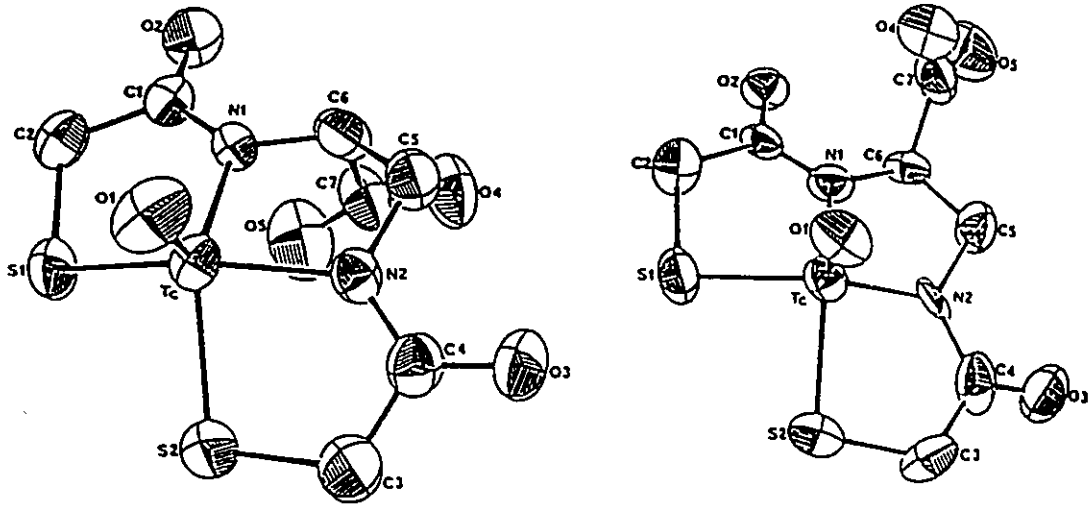

Figure 1.9. *Syn* and *anti* $[TcO(DADS\text{-}CO_2)]^{2-}$

In order to improve its biological properties, the DADS ligand was modified. A series of N2S2 (DADS) ligands were synthesised by Kasina *et al.* [6], Fritzberg *et al.* [50] and Schneider *et al.* [7]. These compounds included a variety of functional groups that were added to the ethylene bridge of the parent ligand. Functionalization of the ethylene bridge, however, leads to the formation of *syn* and *anti* isomers, figure 1.9. Addition of a carboxylate group to the DADS ligand to give 2,3-bis(mercaptoacetamido) propanoate and complexation of the ligand by technetium led to the formation of two complexes separable only by high performance liquid chromatography (HPLC). It was shown by mass spectroscopy that both components had the same molecular weight and were chelate ring

epimers [51]. The stereoisomers differ in the position of the carboxylate group on the chelate ring *syn* or *anti* to the Tc=O group. Both isomers and their rhenium analogues have been characterized by X-ray [52] and NMR spectroscopy [53].

Biological tests in mice [54] showed that the *syn* epimer had a higher excretion rate than the *anti* epimer. The clearance rate of *syn*-$[^{99m}TcO(DADS(CO_2))]^{2-}$ was even higher than that of the parent $[^{99m}TcO(DADS)]^-$ complex. Similar results were observed in humans and dogs, but with more pronounced differences between the two epimers [55].

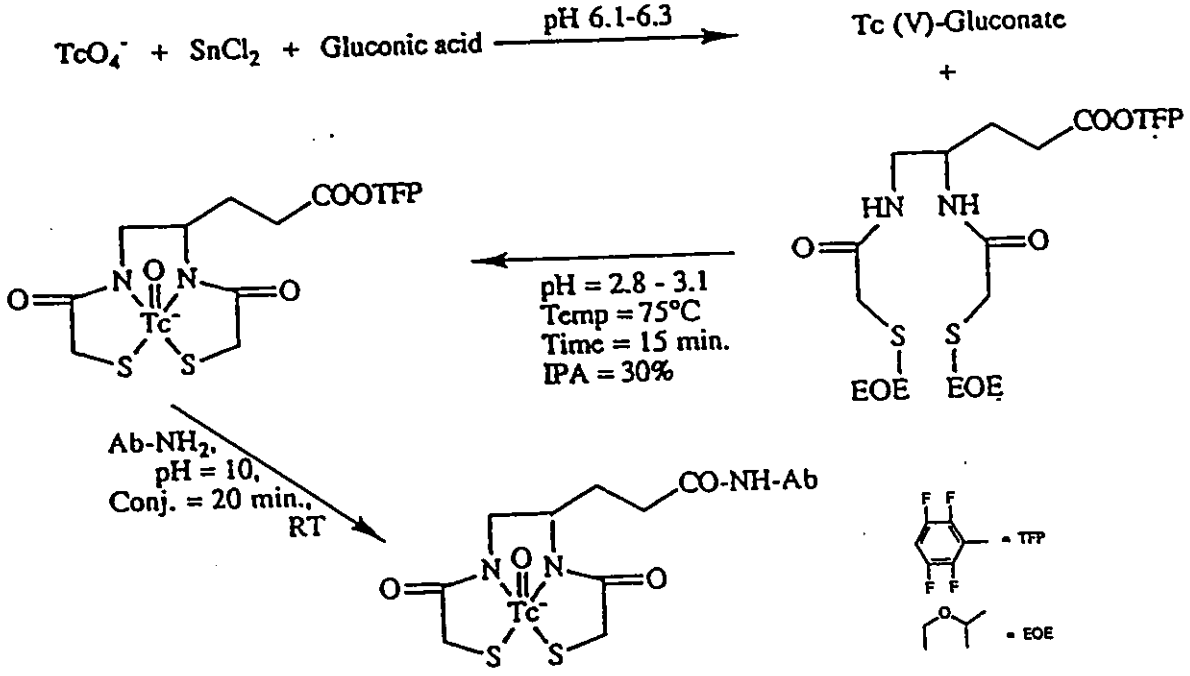

Figure 1.10. ^{99m}Tc kit labelling procedure for antibodies, IPA = isopropyl alcohol

An alternative approach for making the DADS ligands more clinically

useful is to add biologically significant fragments to the ligand framework to make it more organ specific. The presence of an amino or a carboxylate group in the ligand backbone allows for conjugation with biological molecules, such as antibodies (Ab) [56, 57] and fatty acids (FA) [58]. It is known that the heart uses fatty acids as a source of energy through metabolism, hence fatty acids, when bound to ^{99m}TcO(DADS), might be used to carry ^{99m}Tc to the heart, allowing for both imaging and studying the heart's metabolic activities. Kasina *et al.* [57] developed a kit for ^{99m}Tc antibody radiolabeling which used an N2S2 (DADS) bifunctional chelating agent, figure **1.10**. Stable ^{99m}Tc antibody fragments with retained immunoreactivity and tumor-targeting properties were obtained.

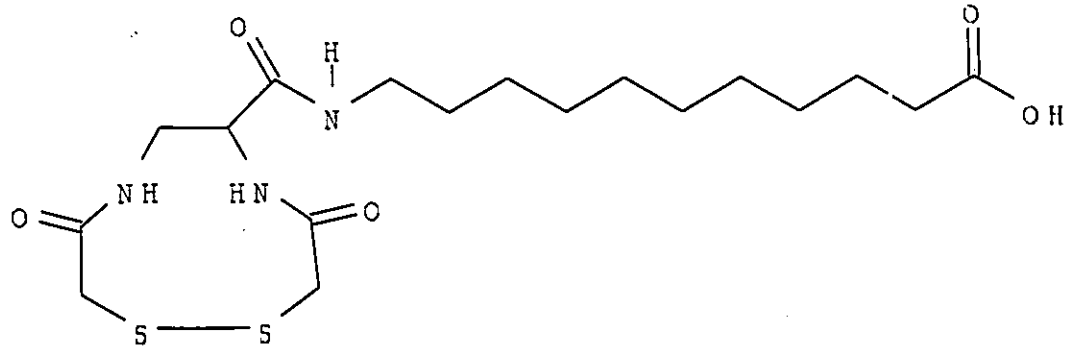

Figure 1.11. N2S2 (DADS) ligand conjugated with a fatty acid

The bifunctional N2S2 fatty acid ligand [58], shown in figure **1.11**, was prepared and characterized by NMR spectroscopy. The disulfide was reacted with $^{99m}TcO_4^-$ in the presence of stannous chloride. When the complex was injected into a rabbit, it was apparent that the complex was taken up by the lungs rather than the heart.

1.6.2. N2S2 (BAT):

Bis-aminoethanethiols (BAT) are a second class of N2S2 ligands that have been found to form stable complexes with TcO^{3+}. They differ from the (DADS) N2S2 ligands by having amino-nitrogen donor atoms as opposed to amido-nitrogen atoms. The first (BAT) N2S2 ligand was synthesized by Corbin *et al.* [59] in 1976. Burns *et al.* [60] showed that the ^{99m}TcO(BAT) complex was neutral and lipid soluble. It was latter demonstrated by Kung *et al.* [45] that the ^{99m}TcO(BAT) complex, shown in figure **1.12**, is capable of crossing the blood-brain barrier (BBB)

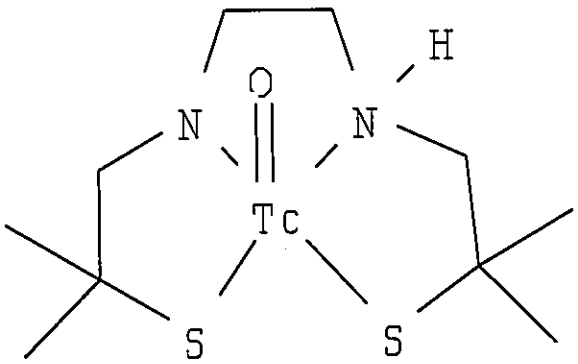

Figure 1.12. TcO(BAT)

and hence has the potential for use as a brain perfusion imaging agent.

Biological evaluation in rats [45] revealed that alkyl-substituted ^{99m}TcO(BAT) were initially taken up by the brain in significant amounts with a

distribution that reflected the cerebral blood flow. The redistribution of these compounds in the brain occurred within 15-min, thereby resulting in a homogenous distribution of radioactivity. This short retention time was a major drawback because current SPECT systems require 15-min to 1-hr imaging time. Kung *et al.* [61] attributed this rapid redistribution to the lack of a trapping mechanism to prevent facile two-way transport across the cell membrane. Therefore, based on this information, efforts were aimed at the development of ^{99m}TcO(BAT) complexes that have similar stability and lipid solubility but would be trapped intracellularly in the brain [61]. One proposed mechanism is the so called pH-trapping mechanism [62]. According to this mechanism, a neutral lipid soluble molecule containing an amine group would be trapped intracellularly as a positively charged ammonium species following entry into the brain. This hypothesis prompted some research groups [61, 63-66] to bind amino groups to their N2S2 frame, however, no significant increase in the brain retention time was achieved.

The emphasis of current research groups is now on modifying the N2S2 ligand frame to make the technetium radiopharmaceutical target a specific organ of the body. This is achieved by binding the N2S2 ligand to molecules or fragments, such as, antibodies [56], and fatty acids [67, 68], that can be recognized by certain receptors in that organ. Jones *et al.* [69] reported the TcO(N2S2)(FA) complex shown in figure **1.13**. It was found to display an inferior myocardial

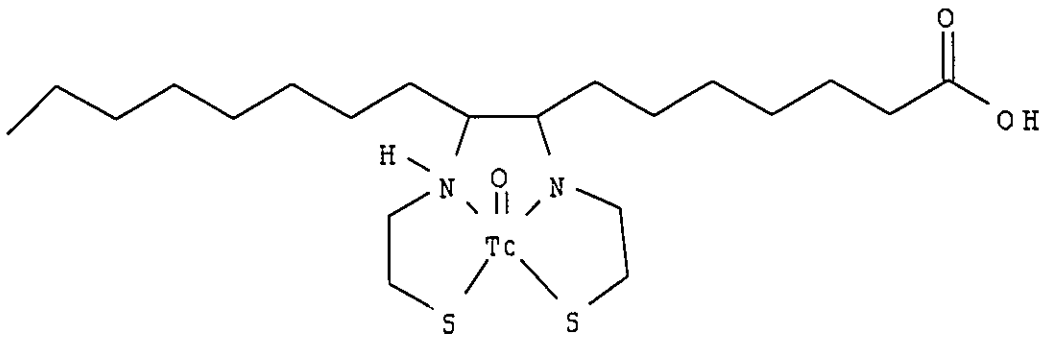

Figure 1.13. TcO(BAT-FA)

uptake and retention when coinjected with [^{125}I][p-iodophenyl pentadecanoic acid], (IPPA). Also, three fatty acid analogs as potential ^{99m}Tc tracers for myocardial metabolism were prepared [70]; each analog contained the N2S2 (BAT) ligand for coordination with ^{99m}Tc and varied the length of the fatty acid side chain (n= 13, 14, 15), figure **1.14.** Biodistribution studies were conducted in rats using IPPA as an internal standard. The initial heart uptake was significantly lower than that of IPPA (0.2, 0.32 and 0.46 dose/organ *vs* 2.0, 2.3 and 1.95 dose/organ for IPPA) but did increase with increasing alkyl chain lengths.

All of the above results seem discouraging in regards to the use of (^{99m}TcO)(N2S2)(FA) complexes as heart imaging agents. One reason for this might be that the N2S2 backbone alters the biological behaviour of the fatty acid when bound to it. This would then mean that the potential of this class of compounds as heart imaging agents is not as great as previously believed. On the other hand, the length of the alkyl chain fatty acid is one major factor that determines

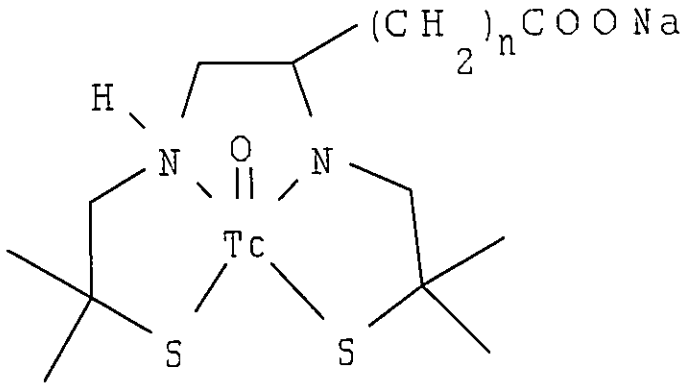

Figure 1.14. TcO(BAT-FA), n = 13, 14, and 15

whether it would be taken up by the heart. Investigation of N2S2 systems bound to fatty acids with longer chains is therefore still worth while.

1.7. Outline:

In addition to this introductory chapter, this thesis comprises six additional chapters. Chapter 2 provides a general description of the experimental methods and techniques that were used throughout this work. The results and details of the experiments carried out in this project are presented in chapters 3-6. Chapter 7 gives a brief summary of this thesis. Throughout this thesis, compounds, which were synthesized in the present work, are frequently referred to by Arabic numerals. The reader is advised to refer to the appendix for the numbering scheme used here.

1.8. Summary and objectives:

A rather different approach was taken here in the study of N2S2 systems. Instead of focusing on the modification of these ligands by adding biologically important fragments to the ligand framework, we attempted to extend the N2S2 systems into N2S3 and N2S4 systems. In other words, the focus in the present work was on the conversion of the N2S2 tetradentate ligands into N2S3 pentadentate and N2S4 hexadentate ligands. The interaction of these diaminopolythiol ligands with technetium and rhenium was then investigated.

We initially became interested in the study of N2S3 ligands when a technetium sample was submitted to us, by A. V. Kramer of the Department of Environmental Health Sciences at Johns Hopkins University [71], for single crystal X-ray structure determination. The crystal structure showed that the work of the Johns Hopkins group, which has not been published [71], had led to the isolation of the technetium complex, oxo(2-(1'-methyl-1'-mercaptoethyl)-3-(5''-methyl-5''-mercapto-3''-dehydroazahexyl)-thiazolidinato-N^{3},$N^{3''}$,$S^{1'}$,$S^{5''}$)technetium(V) **(7)**, which contains a thiazolidine ring. The formation of this complex was unexpected because A. V. Kramer [71] believed that the ligand used to make this complex was an N2S3 pentadentate ligand in which three sulfur and two nitrogen atoms are available for chelation with the metal. The X-ray structure determination of the technetium complex; however, showed that only two nitrogen and two sulfur atoms were bound to the metal. The third sulfur atom was, instead, bound to a

carbon atom in the ligand to give a thiazolidine ring. The contention by the Johns Hopkins group that they had made the correct pentadentate ligand, but the thiazolidine ring formation had taken place during the reaction with technetium seemed unlikely. It was decided to re-examine the ligand synthesis and it was established that the thiazolidine ring formation did occur during the ligand synthesis. This work is reported in chapter 3 and is the major contribution to the knowledge of this thesis.

Subsequently, steps were taken to prepare the correct N2S3 pentadentate ligand. This work, which is described in chapter 4, led to the isolation of N10-(thioethanoyl)-2,2,5,5-tetramethyl-3,4-dithia-7,10-diazabicyclo[5.3.0]decane **(10)**. In this ligand, all three sulfur atoms were available for metal chelation. Reaction of **(10)** with $ReO(P(Ph)_3)_2Cl_3$, however, produced the unexpected asymmetric ReON2S2 complex, oxo(1,1-dimethyl-3-aza-6-amidooctane-1,8-dithiolato)rhenium(V) **(11)**. It was found that the pendant ethylenethiol group was removed from the ligand **(10)** during the reaction with rhenium.

The conversion of N2S2 ligands into N2S4 ligands was also examined. Chapter 5 describes the synthesis of two closely related N2S4 hexadentate systems. Although the syntheses of the ligands were successful, their reactions with technetium and rhenium led to mixtures of products which could not be separated and hence were not characterized.

One interesting side-light of this work was the preparation of a particularly

stable borane containing N2S2 ligand, 3,3,11,11-tetramethyl-1,2-dithia-5,9-diazacycloundecane-5-borane **(16)**. The stability of this ligand was surprising, and the compound is one of the most stable borane-amine complexes known. This work is described in chapter **6**.

Although the major objective of this work was to synthesize N2S3 and N2S4 technetium and rhenium complexes, it will become apparent from the following chapters that much of the effort had to be invested in sorting out the chemistry of the ligand syntheses. Syntheses and full characterization of various N2S2, N2S3 and N2S4 ligands comprise the major part of this thesis. Methods of characterization included ^{1}H NMR, ^{13}C NMR, IR, Raman and mass spectroscopy. Double resonance NMR experiments were carried out for confirmation of the NMR assignments. Single crystal X-ray diffraction was used in cases where suitable crystals could be isolated.

Chapter 2

Experimental Methods

2.1. Chemical Reagents:

All commercially available chemicals were purchased and used without any further purifications, except in few cases where solvents were dried by distillation. All solvents were stored over molecular sieves.

2.2. Handling of Radioactive Material

The long half-life (2.12×10^5 yr) and the weak ß-emission (0.292 MeV) of ^{99}Tc mean that quantities less than 20mg of technetium can be handled without special precautions, other than those normally required for contamination control and compliance with the legislation relating to radioactive materials. The walls of laboratory glassware, rubber gloves, laboratory coat and safety glasses provide adequate radiation shielding. The major potential hazards relate to the spread of contamination, especially from dusty or volatile compounds and the consequent risk of ingestion [72].

All work involving ^{99}Tc was performed according to the regulations and recommendations of the Canadian Atomic Energy Control Board. Transfers of radioactive materials, syntheses, and glassware washing were carried out in a fume hood with a high flow rate. The floor of this fume hood was lined with

plastic sheeting which was replaced regularly. All contaminated waste was carried to the McMaster nuclear research building for appropriate disposal. All laboratory areas where technetium was used were monitored routinely, once every two weeks, by the McMaster Health Physics Department.

2.3. Compound Preparation and Analysis:

Details of compound preparation and analysis will be given in subsequent chapters. Technetium and rhenium starting materials were prepared as needed according to procedures in the literature. These include NH_4ReO_4, $ReO(PPh_3)_2Cl_3$ [73, 74], NH_4TcO_4 [75], $(n\text{-}Bu_4N)(TcOCl_4)$ [25] and $Tc(tu)_6Cl_3$ [32].

2.4. X-ray Crystallography:

Single X-ray diffraction was frequently used as a method of characterization throughout this work. The theoretical aspects of X-ray crystallography have been treated extensively by Burger [76], Luger [77], Stout and Jensen [78], and Glusker and Trueblood [79]. The following brief discussion will be limited to the methods used in the structure determination of compounds presented in this thesis.

2.4.1. Single Crystals:

The preparation of single crystals used in this work will be discussed in the appropriate chapters. Small crystals, 0.2mm, with well developed faces were examined under a polarizing microscope for homogeneity and the best of these crystals were chosen for data collection. Crystals which were too large were cut

with a razor blade. The crystals were mounted on a thin glass fibre or inside glass capillaries. Crystal densities were determined by suspension in an appropriate solvent mixture (detailed in the particular chapter). The measured density was then compared with the calculated density that is given by the following equation:

$$\rho = (M \times Z) / (0.6022 \times V) \text{ g cm}^{-3} \qquad 2.1$$

where M is the molecular weight, Z is the number of molecules in the unit cell and V is the volume of the unit cell in cubic angstroms.

2.4.2. Data Collection:

Syntex $P2_1$, a Nicolet P3, a Rigaku AFC6R or a Siemens P4 diffractometers were used for data collection and unit cell determination. When Syntex or Nicolet diffractometers were used, a full ϕ-rotation polaroid photograph of the crystal was taken with the other diffractometer angles set at zero, generating vertical and horizontal 2-fold symmetry on the film. Horizontal and vertical distances between symmetry related spots were measured and converted to χ and 2θ values for the reflection. A centering routine was used to determine the location of each reflection more accurately. A set of reflections, 15 - 20, with 2θ values that ranged between 18 to 40° were selected from the photograph and entered into a least-squares program to determine the unit cell parameters and orientation matrix which relates the crystal axes to the unit cell axes and diffractometer angles. The orientation matrix was used by the computer to drive

the diffractometer to the appropriate angles for hkl data collection.

When the Siemens or Rigaku diffractometers were used the polaroid photograph routine was not used. Fifteen to twenty five reflections were found through a random search routine. These reflections were used in the determination of the unit cell and the orientation matrix. High angle reflections were then measured for accurate unit cell determination.

Intensities were measured with use of graphite monochromatized CuKα (λ = 1.5405Å) and MoKα radiation (λ = 0.71073Å) with a coupled ω(crystal)-2θ(counter) scan. The range of θ-values depended upon the size and content (scattering power) of the crystal. The range of h, k and l was determined by crystal symmetry and the lengths of the cell edges such that $2\theta_{max}$ was the restricting value. The crystal system dictated what fraction of the available reciprocal space was required to make up a full set of unique $|F|$ data. At least two octants were collected in all cases. Three standard reflections, chosen either manually or automatically, were measured after each hundred reflections to monitor the crystal and instrument stability.

Intensities (I) and standard deviations σ_I were calculated according to equations 2.2 and 2.3, respectively:

$$I = N_p - N_b \qquad 2.2$$

$$\sigma_I = (N_p + N_b)^{1/2} \qquad 2.3$$

where N_p is the peak count and N_b is the background count.

2.4.3. Data Reduction:

The method of French and Wilson [80] was used in the treatment of the data set. Intensities and standard deviations were reduced to observed structure factors, $|F_o|$, and errors in F_o, $\sigma(F_o)$.

$$|F_o| = (I.A/Lp)^{1/2} \qquad 2.4.$$

$$\sigma = \sigma(I).A/2F_o.Lp \qquad 2.5.$$

where A is the absorption factor and Lp is the Lorentz polarization factor. The effect of absorption on the intensity of X-rays is

$$I = I_o\exp(-\mu\tau) \qquad 2.6$$

where I_o is the incident beam intensity, τ is the thickness of the crystal and μ is the linear absorption coefficient which depends on the absorber at a given radiation wavelength. The absorption problem is compounded with crystals of irregular shape. This introduces systematic errors into observed intensities. A ψ-scan was carried out at the end of most data collections [81]. It involves monitoring the intensity variation of a given reflection of moderate intensity as the crystal is rotated 360° in 10° increments. In all cases, however, a numerical absorption correction was applied by use of the program DIFFABS [82].

Symmetry equivalent reflections were averaged and $R_{internal}$ (R_{int}) was calculated to evaluate the consistency of the data set, see equation 2.7.

$$R_{int} = \{\Sigma N[\Sigma w(<F>-F)^2]/\Sigma(N-1)\Sigma w.F^2\}^{1/2} \qquad 2.7$$

where the inner summations are over N equivalent reflections averaged to give

<F> and the outer summations are over all unique reflections. <F> is the averaged mean, N is the number of equivalent reflections averaged and w is the weighting factor.

$$w = 1/[\sigma(F)]^2. \qquad 2.8$$

2.4.4. Structure Solution and Refinment

The structure factor, Fc, is a quantity that can be calculated for each hkl reflection on the basis of the model of electron density within the crystal.

$$Fc_{hkl} = \Sigma\, f_j \exp[2\pi i(hx_j + ky_j + lz_j)] \qquad 2.9$$

where x_j, y_j, z_j are the positional parameters of the j^{th} atom and f_j is the scattering factor of that atom. It is given by equation 2.10.

$$f = f_0 \exp[-B(\sin^2\theta)/\lambda^2] \qquad 2.10$$

where f_0 is the scattering factor of a spherical atom. Scattering factors are supplied by Cromer and Waber in Table 2.2A of the International Tables for X-ray Crystallography [83]. B is the temperature factor.

$$B = 8\pi^2 u^2 \qquad 2.11$$

where u is the mean square amplitude of atomic vibration and is described in three dimensions at the final stages of refinement.

The electron density, ρ_{xyz}, at any point (x,y,z) inside the unit cell can be calculated by a Fourier synthesis.

$$\rho_{xyz} = (1/V)\, \Sigma\Sigma\Sigma\, |F_{hkl}|\, \exp[-2\pi i(hx + ky + lz - \delta_{hkl})] \qquad 2.12$$

where V is the volume of the unit cell and the summations are over all h, k and

l. Measured intensities contain only the amplitudes of the structure factors $|Fo|$, thus the phase (δ_{hkl}) must be determined. The direct phasing method of SHELX [84] was employed in the phase determination of all structures presented in this thesis. It uses probability arguments to assign phases directly to some structure factors. These phased factors are then used in a Fourier synthesis to build a model and all the Fc's are calculated according to this model. The phases of Fc's are assigned to the corresponding Fc's. A complete structure solution is obtained after difference Fourier syntheses, which are carried out after least square refinement.

$$\Delta\rho = (1/V)\Sigma\Sigma\Sigma(|Fo| - |Fc|)\exp[-2\pi i(hx + ky + lz - \delta_c)] \qquad 2.13$$

where δ_c is the phase of Fc. Any electron density that is not accounted for shows up as a peak in the difference map.

Refinement of atomic positional and thermal parameters were carried out by the method of least-squares which minimized the quantity $\Sigma w(|Fo| - |Fc|)^2$. Structure solution was considered complete when the difference map was flat and when a comparison of final $|Fo|$ and $|Fc|$ values yielded suitable figures of merit, R, wR and S.

$$R = \Sigma||Fo| - |Fc||/\Sigma|Fo| \qquad 2.14$$

$$wR = [\Sigma w(|Fo| - |Fc|)^2/\Sigma(Fo)^2]^{1/2} \qquad 2.15$$

$$S = [\Sigma w(|Fo| - |Fc|)^2/(M - N)]^{1/2} \qquad 2.16$$

where w is the weight, M is the number of observed reflections and N is the number of refined parameters. The sums are over all reflections. Hydrogen atom

positions were either found in the difference map or calculated and fixed. In all cases, the whole data set was used, in other words, weak reflections or negative reflections, where $I > -3\sigma_I$, were not omitted.

2.5 Infrared Spectroscopy

Infrared spectra were recorded on a Perkin Elmer 283 or a Bio Rad FTS-40 spectrometer and reported in wavenumbers (cm^{-1}). Most samples were ground with dry KBr (1 - 5% w/w) and pressed into pellets. Liquid samples and Nujol mulls were held between NaCl or KBr discs. Spectra were calibrated against a polystyrene calibrant.

2.6 Raman Spectroscopy

Raman spectra were recorded on a SPEX Industries Model 14018 double monochrometer equipped with 1800 grooves/mm Holographic gratings. A Coherent Radiation Argon Laser Model 52 generated the green (λ = 514.5nm) exciting line. Spectra were calibrated against $HgCl_2$. Powder samples were contained in thin capillary tubes. A Jobin Yuon Mole S-3000 1-meter spectrometer was also used. It is equipped with 1800 grooves/mm Holographic gratings and a LEXEL 3500 Krypton Laser that generated the red (λ = 647.1nm) exciting line or a Stabilite 2016 Laser that generated the green (λ = 514.5nm) exciting line. The spectrometer is also equipped with a one-inch CCD detector

2.7 Nuclear Magnetic Resonance Spectroscopy

^{1}H and ^{13}C NMR spectra were obtained on Bruker AC-200, AC-300, and

AM-500 Fourier spectrometers equipped with 5mm dual frequency ^{1}H-^{13}C probes. Samples were dissolved in appropriate deuterated solvents and sealed in 507-PP thin wall 5mm NMR tubes. Tetramethylsilane (TMS) was used as an internal reference. Spectra were deuterium-locked by use of the deuterated solvent. ^{1}H NMR spectra were acquired at 500.14MHz on the AC-500, 300.13MHz on the AC-300 or 200.13MHz on the AC-200. Spectra were typically obtained in 8 scans in 16K data points. The free induction decays were processed by use of exponential multiplication (line broadening = 0.3Hz) and was zero-filled to 32K before Fourier transformation. ^{13}C spectra were acquired at 50.324MHz on the AC-200 or 125.76MHz on the AM-500. Sweep widths were 2500.00Hz for ^{1}H and 12195.122Hz for ^{13}C. Chemical shifts were recorded in δ values (ppm) relative to TMS and coupling constants were reported in Hz.

2.8 Mass Spectroscopy

Chemical ionization, (CI), and electron impact, (EI), mass spectra were recorded on a VG Analytical ZAB-E double focusing mass spectrometer. Low resolution spectra were recorded for routine sample analysis. Typical experimental conditions were as follows: resolution = 1000, electron energy = 70eV, source temperature 200°C, and source pressure = 2×10^{-6} mbar for EI and 4×10^{-5} mbar for CI. Elemental composition determination were made with a resolution of 5000. Mass spectra were recorded in mass-to-charge (m/z) ratio and relative intensity.

2.9 Chromatography

Analytical thin layer chromatography (TLC) was conducted by using DC-Alufolien Kiesselgel 60 F_{254} aluminium sheets with a stationary phase layer thickness of 0.2mm. Compounds were visualized with the use of I_2 vapour. The R_f value was calculated according to equation 2.17:

R_f = [distance travelled by substance]/[distance travelled by solvent front] 2.17

Preparative chromatographic separations were carried out with the use of columns packed with chromatographic silica gel (100 - 200 mesh).

Chapter 3

3.1. Introduction:

The reactivity of the nitrogen atoms of ligands derived from 3,6-diazaoctane-1,8-dithiol, suggested a way of synthesizing the ligand A, with five possible coordination sites. It was expected that a complex of type B would be obtained by reaction with the TcO^{3+} core:

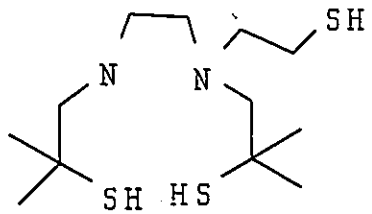

A

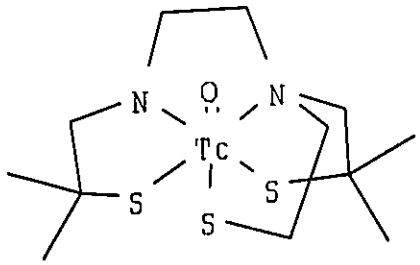

B

An attempt was made by the Johns Hopkins group [71] to synthesize the ligand, and subsequently a technetium compound was prepared, but, much to our surprise, an X-ray structure determination of the technetium complex showed that the expected product was not obtained; instead the additional ethylenethiol group had reacted with a CH_2 group proximal to the nitrogen atom to give a thiazolidine ring. The ligand yielded a normal, square pyramidal, technetium complex. As a result we have attempted to repeat the synthesis of the thiazolidine

containing ligand and characterize it fully, in order to explain how it was formed.

3.2. Experiments

3.2.1. Preparation of 2,2-dithio-bis(2-methylpropanal) (1):

This compound was prepared as described previously [85]:

Yield: 85%, IR: 1710, 1725cm^{-1}, $\nu_{C=O}$; ^1H NMR: ($CDCl_3$) δ 1.40 (S, 12H, 2 x $C(CH_3)_2$), 9.09 (S, 2H, CHO); EIMS: 206m/z (20, $M^{\cdot+}$), 177 (26, $M^{\cdot+}$ - $HC{=}O^{\cdot}$), 149 (11, $M^{\cdot+}$ - $HC.O.CHCH_3$), 113 (12), 107 (40), 72 (100, $HC.O.CH(CH_3)_2^{\cdot+}$), 71 (86, $HC.O.C(CH_3)_2^{+}$)

3.2.2. Preparation of 3,3,10,10-tetramethyl-1,2-dithia-5,8-diazacyclodeca-4,8-diene (2):

This compound was prepared according to the reported procedure [45], with a slight modification. To a solution of the dialdehyde **(1)** (10.00g, 48mmoL) in heptane (400.0mL), ethylene diamine (3.2mL, 48mmoL) and p-toluene sulfonic acid (0.200g) were added. The mixture was heated gently to boiling for 2hr. It was then concentrated in *vacuo*, and the residue was collected by filtration. The product was first washed with cold heptane (20.0mL) then with water (50.0mL). Finally, it was recrystallized from ethyl acetate. Yield: 8.37g (36mmoL, 75%); melting point: 162 - 164°C (lit. mp. [45]) 162 - 163°C) ; IR (KBr): 1655cm^{-1} $\nu_{C=N}$; CIMS: 231m/z (100, $M^{\cdot+}$+1); EIMS: 231m/z (6, $M^{\cdot+}$ + 1), 166 (44, $M^{\cdot+}$ - $S_2^{\cdot}$), 156 (39, $M^{\cdot+}$ - $SC(CH_2)_2$), 151 (20, 166 -CH_3), 124 (70, $M^{\cdot+}$ - $S_2C(CH_3)_2$), 98 (44), 84 (100, $C_4H_8N_2^{+}$), 82 (99, $C_4H_6N_2^{+}$), 68 (57); ^1H NMR ($CDCl_3$): δ 1.33 (s, 6H, 2 x CH_3), 1.41

(s, 6H, 2 x CH_3), 3.20 (d, J = 6.4Hz, 2H, (H6a, H7a)), 4.12 (d, J = 6.2Hz, 2H, (H6b, H7b)), 6.83 (s, 2H, (H4,H9)) ; ^{13}C NMR ($CDCl_3$): (5 signals were observed) δ (21.24, 2 x CH_3), (24.41, 2 x CH_3), (52.73, C3,10), (61.17, C6,7), (167.56, C4,9).

3.2.3. Preparation of 2,2,5,5-tetramethyl-3,4-dithia-7,10-diazabicyclo[5.3.0]decane (3) and 3,3,10,10-tetramethyl-1,2-dithia-5,8-diazacyclodecane (4):

The reduction of **(2)** was carried out according to the procedure reported by Joshua *et al.* [86], with slight modifications. To a suspension of the diimine **2** (2.02g, 8.78mmoL) in absolute ethanol (50.0mL), sodium borohydride (2.00g, 52.6mmoL) was added. The mixture was stirred at 25°C for 24hr, and then concentrated in *vacuo*. The residue was partitioned between water (50.0mL) and methylene chloride (50.0mL). The aqueous layer was washed with methylene chloride (3 x 10.0mL). The combined organic extracts were washed with water (15mL), dried over sodium sulfate and concentrated *in vacuo*. The residue was chromatographed on silica gel. Elution with methylene chloride-methanol (95:5) gave 2,2,5,5-tetramethyl-3,4-dithia-7,10-diazabicyclo[5.3.0]decane **(3)**: Yield: 1.18g (10.2mmoL, 58%); TLC: R_f = 0.60 CH_2Cl_2, CH_3OH (80 : 20); melting point: 66 - 67°C (lit.[86]) mp. 65°C); IR (KBr): 3298 cm^{-1} ν_{N-H}; CIMS: 233 (100, M^{+}+1), 158 (20, M^{+} - $SC(CH_3)_2$), 125 (18, 158 - SH); EIMS: 233 (2, M^{+} +1), 158 (62, M^{+} - $SC(CH_3)_2$), 143 (3, 158 - CH_3), 125 (47, 158 - SH), 84 (100, M^{+} - $(SC(CH_3)_2)_2$, $C_4H_8N_2^{+}$), 69 (24), 55 (22); ^1H NMR ($CDCl_3$): δ 1.23 (s, 3H, 1 x CH_3), 1.24 (s, 3H, 1 x CH_3), 1.30 (s, 3H, 1 x CH_3), 1.36 (s, 3H, 1 x CH_3), 2.27 (s, 1H, exchangeable N-H), 2.61 (d, $^2J_{H6AH6B}$ =

14.8Hz, 1H, H6A), 2.76 (m, 1H, H8A), 2.98 (m, 2H, H9A, H9B), 3.24 (m, 2H, H6B, H8B), 3.55 (s, 1H, H1); ^{13}C NMR ($CDCl_3$): (10 signals were observed) : δ (18.56, CH_3), (24.65, CH_3), (26.59, CH_3), (28.37, CH_3), (66.37, C6), (51.90 C5), (53.01, C2), (46.29, C9), (58.34, C8), (91.34, C1). A second elution with methylene chloride-methanol-ammonium hydroxide (5:4:1) gave 3,3,10,10-tetramethyl-1,2-dithia-5,8-diazacyclodecane **(4)**: Yield: 0.72g (3.08mmoL, 35%); TLC: R_f = 0.01 CH_2Cl_2, CH_3OH (80: 20); melting point: 56 - 58°C (lit. [86]) 255 - 256 °C for the HCl salt); IR (KBr): 3290 cm^{-1} ν_{N-H}; EIMS: 234 (21, $M^{\cdot+}$), 169 (6, M^+ - S_2H), 158 (100, M^+ - $HSCH(CH_3)_2$), 143 (8, 158 - CH_3), 125 (60, 158 - SH), 84 (70, $C_4H_8N_2$); ^1H NMR ($CDCL_3$): δ 1.22 (s, 6H, 2 x CH_3), 1.35 (s, 6H, 2 x CH_3), 1.96 (s, 2H, 2 exchangeable NH protons), 2.54 (d, ^2J = 12.5Hz, 2H, (H4A, H9A)), 2.78 (s, 4H, (2 x H6, 2 x H7)), 2.98 (d, ^2J = 12.5Hz, 2H, (H4B, H9B)), ^{13}C NMR ($CDCl_3$): (5 signals were observed) δ (25.87, 2 x CH_3), (28.31, 2 x CH_3), (46.53, C6,7), (51.69, C3,10), (58.60, C4,9).

As an alternative to the column separation, it was found that upon bubbling HCl gas through an ethanol solution of the mixture, **(4)** formed a precipitate while **(3)** did not [45, 86].

3.2.4. Conversion of 2,2,5,5-tetramethyl-3,4-dithia-7,10-diazabicyclo[5.3.0]decane (3) to 3,3,10,10-tetramethyl-1,2-dithia-5,8-diazacyclodecane (4):

A solution of 2,2,5,5-tetramethyl-3,4-dithia-7,10-diazabicyclo[5.3.0]decane **(3)** (1.00g, 4.3mmoL) in ethanol (20mL) was saturated with dry HCl gas. Sodium borohydride (0.50g, 13.2mmoL) was added to this solution in small portions. The

mixture was stirred under nitrogen for 18hr. The mixture was concentrated *in vacuo* and the product, 3,3,10,10-tetramethyl-1,2-dithia-5,8-diazacyclodecane **(4)**, was recovered with the use of a column following the procedure outlined in section **3.2.3.** Yield = 0.50g (2.14mmoL, 50%); characterization: see section **3.2.3.**

3.2.5. Preparation of 2,2,5,5,-tetramethyl-3,4,13-trithia-7,10-diazabicyclo[8.3.0]tridecane hydrochloride (5) and bis(2,2,5,5-tetramethyl-10-ethylenethiol-3,4-dithia-7,10-diazabicyclo[5.3.0]decane)disulfide (6):

A solution of ethylene sulfide (0.39mL, 6.47mmoL) in methylene chloride (5.0ml) was added slowly to a solution of **(3)** (1.00g, 4.31mmoL) in methylene chloride (10.0mL). The mixture was stirred at 25°C for 6 days under nitrogen atmosphere. The mixture was then chromatographed on silica gel. Elution with methylene chloride-methanol (90:10) gave the unreacted bicyclic **(3)** (0.2g, 20%), 2,2,5,5,-tetramethyl-3,4,13-trithia-7,10-diazabicyclo[8.3.0]tridecane **(5)**: Yield: 0.47g (1.3mmoL, 37%); melting point: 191-193°C decomposed; TLC: R_f = 0.30 CH_2Cl_2, CH_3OH (90:10); IR (KBr) 3390 $\upsilon_{N\text{-}H}$; EIMS: 292m/z (18, $M^{\cdot+}$), 227 (8, $M^{+1} - S_2H$), 218 (89, $M^+ - SC(CH_3)_2$), 185 (40, $M^+ - (CH_3)_2CHSS$), 158 (14, $M^+ - (CH_3)_2CSSCHCH_3$)), 144 (54, $M^+ - (CH_3)_2CSSC(CH_3)_2$), 131 (100, $M^+ - SC(CH_3)_2CHSCH_2CH_2N$), 116 (47, $SC(CH_3)_2CH_2NCH_2^+$), 98 (49), 84 (35, $C_4H_8N_2^+$), 70 (22, $C(CH_3)CH_2N^+$); CIMS: 293 (100, $M^{\cdot+} + 1$), 261 (8, $M^+ + 1 - S$), 259 (6, $M^+ - SH$), 233 (42, $M^+ + 1 - CH_2CH_2S$), 218 (20, $M^+ - SC(CH_3)_2$), 201 (7, $M^+ - S_2C(CH_3)$), 185 (11, $M^+ - HSSC(CH_3)_2$), 159 (9, $M^+ - (CH_3)_2CSSCCH_3$), 144 (11, $M^+ - (CH_3)_2CSSC(CH_3)_2$), 125 (8, 159 - SH_2); ^1H

NMR ($CDCl_3$): δ 1.27 (s, 3H, CH_3), 1.30 (s, 3H, CH_3), 1.33 (s, 3H, CH_3), 1.36 (s, 3H, CH_3), 2.20 (d, $^2J_{H6AH6B}$ = 11.4Hz, 1H, H6A), 2.44-3.23 (complex poorly resolved multiplet, 8H), 3.03 (d, $^2J_{H6BH6A}$ = 11.3Hz, 1H, H6B), 3.50 (s, 1H, H1); ^{13}C NMR ($CDCl_3$): (12 signals were observed) δ (21.77, CH_3), (24.40, CH_3), (28.07, CH_3), (30.24, CH_3), (30.94, C12), (45.27, C8), (49.87, C9), (51.72, C5), (52.90, C2), (55.12, C11), (57.72, C6), (90.79, C1); and the dimer bis(2,2,5,5-tetramethyl-10-ethylenethiol-3,4-dithia-7,10-diazabicyclo[5.3.0]decane)disulfide **(6)**: Yield: 0.63g (1.1mmoL, 25%), melting point: 97-100°C; TLC: R_f = 0.70 CH_2Cl_2, CH_3OH (90:10); IR (KBr): confirmed the absence of any NH group; Raman: no peak was observed at ≈ 2700 cm^{-1}, which confirmed the absence of SH group; DCIMS: 583 (6, $M^{+\cdot}$ + 1), 293 (100, monomer + 1), 259 (49, monomer - S), 218 (18), 185 (6); DEIMS: no parent ion peak ($M^{+\cdot}$) was observed, 83 (100, $C_4H_7N_2^+$); ^1H NMR ($CDCl_3$): δ 1.21 (s, 6H, 2 x CH_3), 1.26 (s, 3H, CH_3), 1.32 (s, 3H, CH_3), 2.85 (broad poorly resolved multiplet, 10H), 3.50 (s, 1H, H1); ^{13}C NMR ($CDCl_3$): 11 signals were observed, δ (19.15, CH_3), (24.51, CH_3), (26.67, CH_3), (28.37, CH_3), (39.04, C12), (52.09, C11), (53.11, C2,5), (54.28, C9), (57.79, C8), (66.39, C6), (98.90, C1). Single crystals of **(5)** were obtained by the slow evaporation (at -15°C) of a 50:50 methylene chloride and tetrahydrofuran solution. The structure solution showed that those crystals were those of the chloride salt of **(5)**. Methylene chloride which was used as a solvent in both the reaction and growing crystals is believed to be the primary source of hydrochloric acid. The presence of chlorine in the sample was confirmed

by qualitative scanning electron spectroscopy.

3.2.6. Preparation of Oxo(2-(1'-methyl-1'-mercaptoethyl)-3-(5"-methyl-5"-mercapto-3"-dehydroazahexyl)-thiazolidinato-N^3,$N^{3"}$,$S^{1'}$,$S^{5"}$)technetium(V) (7):

The technetium complex [71] was prepared by adding $Na_2S_2O_4$ (0.226g, 1.3mmoL) dissolved in 2N NaOH (8mL) to a stirred solution containing NH_4TcO_4 (0.180g, 1.0mmoL) and the ligand (0.39, 1.2mmoL) in 3:1 water/ethanol (25mL). The reaction mixture was stirred at room temperature for three hours then allowed to evaporate slowly overnight. The resulting yellow brown needles were filtered, washed with petroleum ether and air dried. Additional product was obtained by extraction of the filtrate with an equal volume of $CHCl_3$. The organic layer was washed with water (2 x 40mL), separated and dried over anhydrous sodium sulfate. Trituration with petroleum ether (100mL) yielded additional product which was collected by filtration, washed with petroleum ether and air dried. The products were combined and recrystallized from 2:1 acetonitrile/water (30mL). The yield, based on technetium, was 70%. ^{1}H NMR ($CDCl_3$): δ 1.41 (s, 3H, CH_3), 1.52 (s, 3H, CH_3), 1.68 (s, 3H, CH_3), 1.79 (s, 3H, CH_3), 2.09 (m, $^4J_{H3AH22B}$ = 1.8Hz, $^3J_{H3AH4A}$ = 5.8Hz, $^3J_{H3AH4B}$ = 11.7Hz, $^2J_{H3AH3B}$ = 11.7Hz, 1H, H3A), 3.22 (m, $^3J_{H3BH4A}$ = 1.3Hz, $^3J_{H3BH4B}$ = 4.1Hz, $^2J_{H3BH3A}$ = 11.8Hz, 1H, H3B), 3.35 (m, $^2J_{H4AH4B}$ = 13.2Hz, 1H, H4B), 3.39 (m, 1H, H21A), 3.40 (m, 1H, H21B), 3.81 (d, $^2J_{H5AH5B}$ = 11.5Hz, 1H, H5A), 3.92(d, $^2J_{H5BH5A}$ = 11.4Hz, 1H, H5B), 3.95 (s, 1H, H2), 3.97 (m, 1H, H22B), 4.32 (m, 1H, H4B), 4.33 (1H, H22A, m); ^{13}C NMR ($CDCl_3$) (12 signals

were observed): δ (26.26, CH_3), (27.98, CH_3), (30.20, CH_3), (30.91, CH_3), (30.91, C21), (56.44, C6), (57.65, C1), (58.04, C22), (61.97, C4), (64.33, C3), (81.56, C5), (92.48, C2); the numbering scheme used for this NMR assignment is the same as that shown in figure 3.7, Raman 928 $\nu_{Tc=O}$; IR (nujol), 929cm^{-1}, $\nu_{Tc=O}$.

3.3. Results and Discussion

3.3.1. Syntheses:

The original purpose of this work [71] was to attempt to make a six-coordinate technetium complex containing an oxo-group and N-(2-mercaptoethyl)-N,N'-di(2-methyl-2-mercaptopropyl)ethylenediamine, which would be bound through the nitrogen and thiol atoms to give an N2S3 system. The technetium complex, which was prepared was examined by single crystal X-ray diffraction and is illustrated in figure 3.7. The complex clearly does not contain the expected ligand. Instead, the expected pendant ethylenethiol group attached to the nitrogen atom has undergone an internal condensation to form a thiazolidine ring. The suggestion that the thiol group had attacked the CH_2 group proximal to the nitrogen atom directly, even in the presence of the technetium atom, was rejected. The synthetic pathway used to prepare the ligand was examined carefully, in order to see where cyclization might have occurred.

Reaction scheme 3.1 and 3.4 outline the synthesis of the thiazolidine ring containing ligand. The dithiadialdehyde **(1)** was prepared by the reaction of isobutyraldehyde with sulfur monochloride [84]. Condensation of the dialdehyde

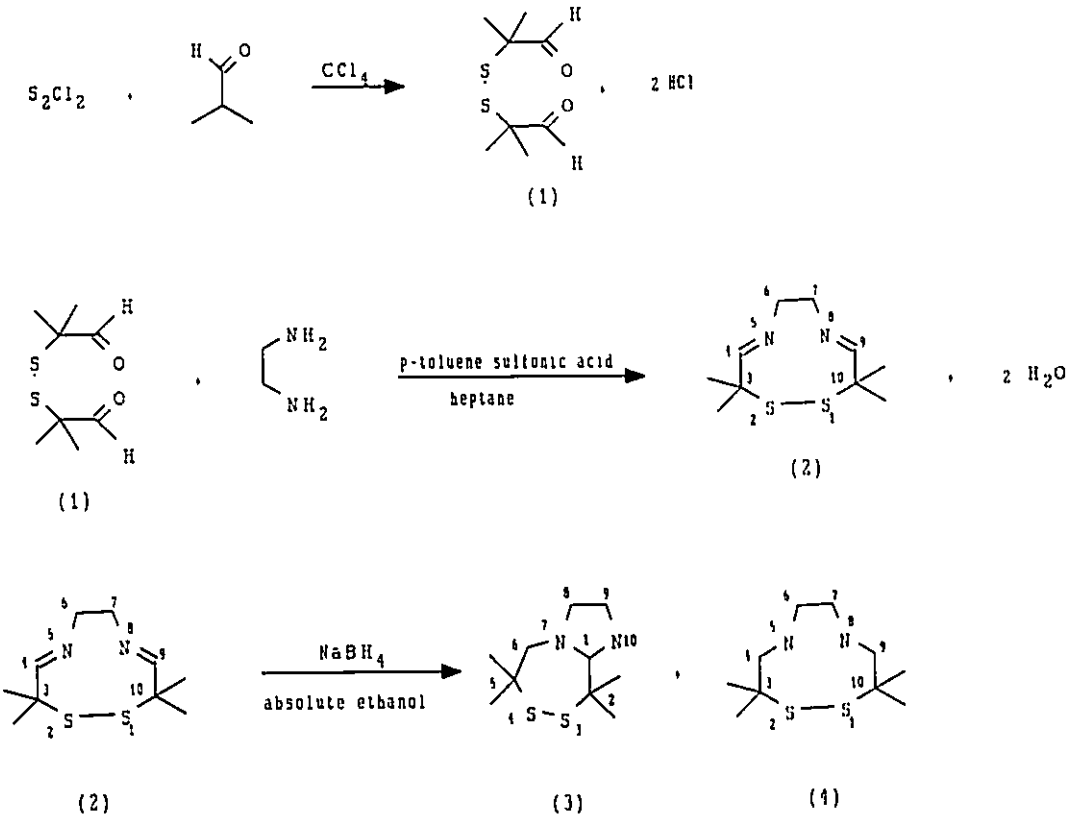

Figure 3.1. Reaction Scheme 3.1.

with ethylene diamine leads to the isolation of 3,3.10,10-tetramethyl-1,2-dithia-5,8-diazacyclodeca-4,8-diene **(2)**. Subsequent reduction of the dithiadiimine **(2)** with $NaBH_4$ was first reported by Kung [45] to give 3,310,10-tetramethyl-1,2-dithia-5,8-diazacyclodecane **(4)** in 76% yield. It was shown latter on by Lown [86, 87] that

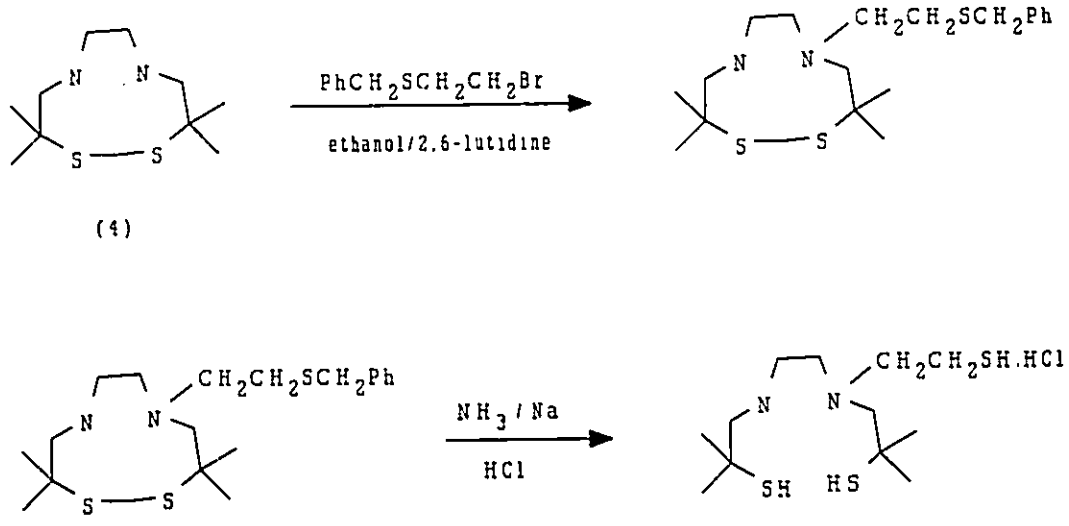

Figure 3.2. Reaction Scheme 3.2.

(4) was only a minor product in this $NaBH_4$ reduction reaction. The major product was in fact the bicyclic (3). Our observations were consistent with Lown's results. We have also found that compound (3) can, in turn, be converted to (4) by sodium borohydride reduction in acidic ethanol solution, reaction 3.3. In addition, it has been shown recently that a considerably higher yield of (4) can be achieved if $NaBH_4$ was replaced by $NaBCNH_3$ [88] in the reduction of (2). It became clear to us at this point that the Johns Hopkins group were actually using (3) to make a ligand of type A, shown in section 3.1, when they thought that they were using (4). Reaction scheme 3.2. outlines the synthetic sequence that the Johns Hopkins

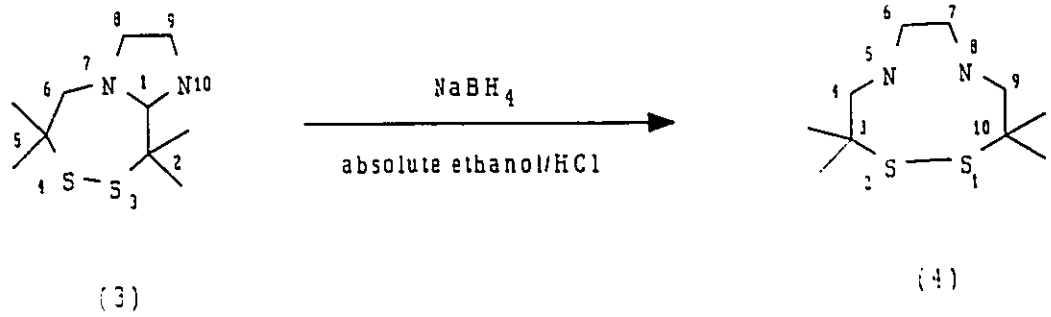

(3) (4)

Figure 3.3 Reaction 3.3

group believed it had followed [71]. Explaining the formation of the thiazolidine ring containing technetium complex is not easy if ligand **(4)** was indeed used as the starting material in the preparation.

We believed that the formation of the thiazolidine ring is easier to envision if compound **(3)** was used. Carbon # 1 in **(3)** is highly electrophilic and hence can be susceptible to nucleophilic attack by the sulfur atom of the additional ethylenethiol group. It was, therefore, decided to investigate this hypothesis by examining the reaction of **(3)** with ethylene sulfide (reaction scheme **3.4**). This reaction was extremely slow in aromatic solvents, such as, benzene and toluene [89, 90]. In halogenated solvents, chloroform and dichloromethane, the reaction seemed to proceed at a slow rate. Dichloromethane was the solvent of choice for the reaction. A mixture of **(3)** and ethylene sulfide was stirred in CH_2Cl_2 under

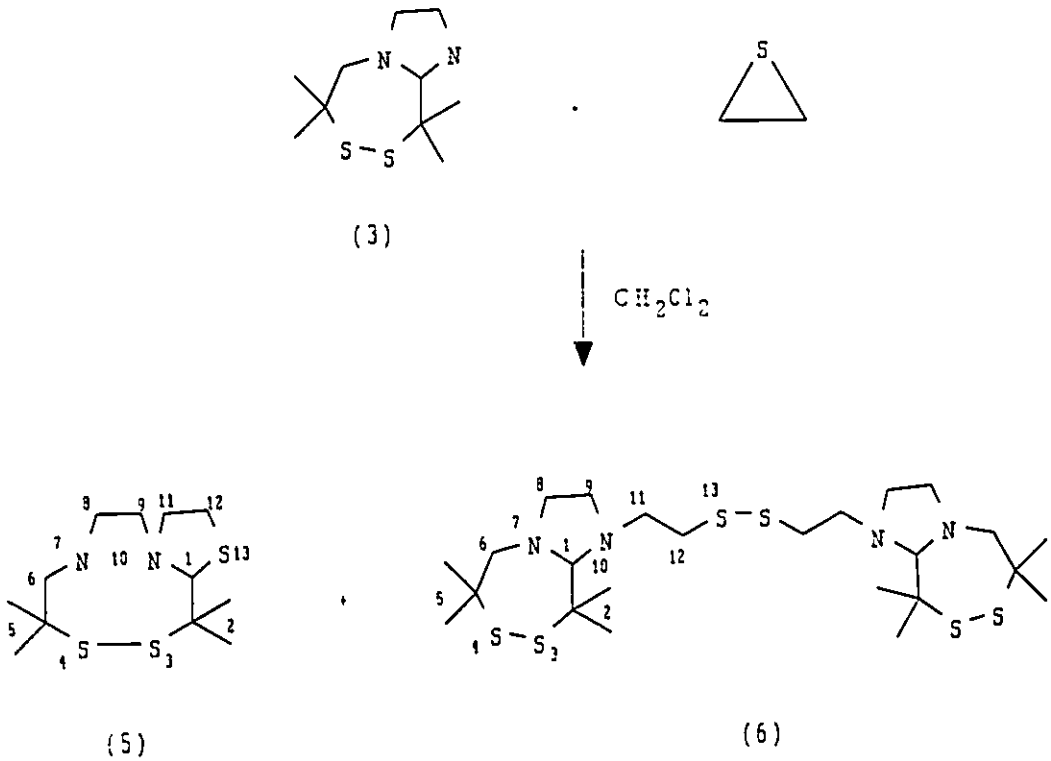

Figure 3.4. Reaction Scheme 3.4.

nitrogen atmosphere for six days. Subsequent chromatographic separation led to the isolation of the target molecule, the thiazilidine containing ligand **(5)**, and the dimer **(6)**. Although the ^{13}C NMR spectra were consistent with the structural assignments, the ^{1}H NMR spectra were not very informative because of the overlap of signals corresponding to the methylene protons. Fortunately, it was possible to isolate single crystals of **(5)**. The crystal structure shown in figure 3.5 provided a conclusive evidence for the formation of the thiazolidine ring before

the addition of the metal. The assignment of a dimeric structure to compound **(6)** was based on the evidence provided by ^{13}C NMR and mass spectra. Also, the absence of any SH stretch in both the infra red and Raman spectra ruled out the monomer thiol.

NMR spectroscopy was used in the characterization of each of the intermediates involved in this synthesis. The ^{1}H and ^{13}C NMR for compound **(2)** were easily assigned. The singlet at 2.78ppm in the ^{1}H NMR spectrum of compound **(4)** was assigned to the four protons on carbons 6 and 7 because it split into a pattern corresponding to an A_2B_2 system when dimethylsulfoxide (DMSO) was used as a solvent instead of $CDCl_3$. Once the proton NMR was assigned for compound **(4)**, a $^{13}C/^{1}H$ correlation spectrum was obtained and used in the assignment of the ^{13}C spectrum. In the case of compound **(3)** the ^{1}H NMR spectrum was more complex. $^{1}H/^{1}H$ and $^{1}H/^{13}C$ correlation spectra were needed for the assignment. The ^{13}C NMR spectra of compounds **(5)** and **(6)** were assigned by comparison with those of compounds **(3)** and **(4)**. The ^{1}H and ^{13}C NMR spectra of the technetium complex **(7)** were assigned with the aid of $^{1}H/^{1}H$ and $^{1}H/^{13}C$ correlation NMR spectra and nuclear Overhauser effect (NOE) experiments. It should be noted that the chemical shifts of the carbon atoms have shifted considerably upon chelation with technetium. Table 3.1 shows the ^{13}C chemical shifts for the ligand **(5)** and the corresponding technetium complex **(7)**; the difference in chemical shifts is also listed.

Table 3.1. Comparison Between ^{13}C Chemical Shifts of 2,2,5,5,-tetramethyl-3,4,13-trithia-7,10-diazabicyclo[8.3.0]tridecane hydrochloride **(5)** and Oxo(2-(1'-methyl-1'-mercaptoethyl)-3-(5''-methyl-5''-mercapto-3''-dehydroazahexyl)-thiazolidinato-N^3,$N^{3''}$,$S^{1'}$,$S^{5''}$)technetium(V) **(7)**:

carbon Atom#	5	7	Δ
CH_3	21.77	26.26	4.49
CH_3	24.40	27.98	3.58
CH_3	28.07	30.20	2.13
CH_3	30.24	30.91	0.67
12	30.94	30.91	-0.03
8	45.27	61.97	16.70
9	49.87	64.33	14.46
5	51.72	56.44	4.72
2	52.90	57.65	4.75
11	55.12	58.04	2.92
6	57.72	81.56	23.84
1	90.79	92.48	1.69

The numbering of the carbon atoms in the above table is the same as that used for compound **(5)** in figure **3.4.** Table **3.1** shows that carbon atoms 8, 9 and 6 are the atoms most affected by technetium chelation in terms of NMR chemical shifts. C(6) and C(8) are bound to N(7) which undergoes deprotonation upon reaction with metal and forms a strong Tc-N bond.

3.3.2. X-ray Structures:

The structures of 2,2,5,5,-tetramethyl-3,4,13-trithia-7,10-diazabicyclo[8.3.0]tridecane hydrochloride **(5)** and Oxo(2-(1'-methyl-1'-

mercaptoethyl)-3-(5''-methyl-5''-mercapto-3''-dehydroazahexyl)-thiazolidinato-N^3,$N^{3''}$,$S^{1''}$,$S^{5''}$)technetium(V) (7) have been determined by single crystal X-ray diffraction. Tables 3.2 - 3.10 list the results of the X-ray work and figures 3.5 and 3.7 show crystal structures. The numbering scheme in these figures will be used in the following discussion. There are a number of interesting structural features, particularly when the ligand (5) is compared with the technetium complex. Much of the general conformation of (5) is retained in the complex; torsional angles in the framework bonds are generally within about 10° in the two molecules. Only the torsional angles about N(2)-C(4) and N(2)-C(5) differ by much more than 20° in the two molecules. The new steric requirements of the coordination of N(2) to the technetium atom cause the change. N(2) goes from a substituted ammonium ion to a coordinated amido-group in the complex.

In (5) S(1),N(1),N(2),S(2) are not planar; they are twisted towards a very distorted tetrahedron, with the atoms laying 0.446(8)Å, S(1); -0.285(6)Å, N(1); 0.319(8)Å, N(2); and -0.480(6)Å, S(2); out of the best plane through the atoms. The requirement of square pyramidal geometry in the complex forces the four atoms towards a plane, but does not suppress the distortion completely since the atoms are still 0.096(7)Å, S(1); -0.119(8)Å, N(1); 0.130(8)Å, N(2); and -0.106(7)Å, S(2); out of the best plane through the four atoms. The technetium atom lies -0.735(5)Å out of this plane.

The deprotonation of N(2) means that the atom is a much better base and

binds more strongly to the technetium atom. The Tc-N(2) distance is 0.300Å shorter than the Tc-N(1) distance, which lies in the normal range for Tc-N distances in this type of compound. The Tc-O distance of 1.665(5)Å lies in the normal range as do the Tc-S distances [91]. Equivalent bond distances in **(5)** and **(7)** generally do not differ significantly, but coordination of N(1) results in longer N(1)-C(2), N(1)-C(3) and N(1)-C(22) bonds in the complex by 0.026Å, 4.4σ, 0.054Å, 5.1σ and 0.048Å, 4.2σ, respectively[1]. The longer (weaker) N(1) bond results in a stronger C(2)-S(3) bond in the complex, which is shorter by 0.050Å, 5.9σ.

In thiazolidine rings the C-S bonds are rarely the same length. In compounds studied previously [92], it was found that the lengths of the C-S bonds proximal to the nitrogen atom have varied from 1.816(5)Å to 1.885(6)Å, whereas the distal C-S bonds have varied from 1.784(5)Å to 1.869(6)Å. It was noted that steric repulsion caused by bulky groups attached to the α and/or β carbon atoms causes long C-S bonds with consequent shortening of the C-S bond to the less sterically crowded carbon atom. Clearly the same effect is present here. In both **(5)** and **(7)**, the S(3)-C(2) bond, which involves a carbon atom bound to nitrogen, carbon and hydrogen atoms, and which is adjacent to the bulky dimethylated C(1) system, is longer than S(3)-C(21), where the carbon atom is bound only to a carbon and hydrogen atoms and which is adjacent to a CH_2 group. The S(3)-C(2) distance lies at the upper end of the previous range of

---

[1] $\sigma = (\sigma_1^2 + \sigma_2^2)^{1/2}$

equivalent distances and consequently the S(3)-C(21) distance lies at the lower end of its range. It should be noted that the steric effects are completely taken up in the bond lengths; the C(2)-S(3)-C(21) angles (94.2(3), 92.3(3)°) lie within the small range of C-S-C angles observed previously (92.4(2)-95.4(3)°).

The changes in the torsional angles N(1)C(2)S(3)C(21) and C(2)S(3)C(21)C(22) from 15.1(4), 9.7(5)° in (7) to 2.5(4), 20.8(5)° in (5) means that while the conformation of the thiazolidine ring in (5) is an open envelope, with C(22) 0.564Å out of the plane through the other four atoms, the conformation of the ring in (7) is roughly a C_2 system with C(2) 0.372Å and N(1) - 0.244Å out of the plane of the other three atoms. The former conformation has been observed in2*R*,4*S*-2-(2'-methyl-3'hydroxymethylenepyridine-C4')-5,5-dimethylthiazolidine-4-carboxylic acid [93] and the latter in *S*-2,2,5,5-tetramethylthiazolidine-4-carboxylic acid [92].

In the solid state each cation in 2,2,5,5,-tetramethyl-3,4,13-trithia-7,10-diazabicyclo[8.3.0]tridecane hydrochloride (5) is hydrogen bonded to two chloride ions, which are related by an inversion centre. These chloride ions are, in turn, hydrogen bonded to another cation related to the first by the same inversion centre, giving $(cation)_2Cl_2$ units. one of the hydrogen bonds is quite strong (N(2)...Cl, 3.0417(7) Å), but the other is weaker (N(2)...Cl, 3.2234(7) Å). All other interactions are van der Waals, as is the case for the packing of the corresponding technetium complex (7).

Table 3.2. Crystal data.

Compound	(7)	(5)
formula	$C_{12}H_{23}N_2OS_3Tc$	$C_{12}H_{25}ClN_2S_3$
formula weight	406.4	329.0
crystal colour, habit	orange needle	colourless needle
size (mm)	0.10 x 0.13 x 0.30	0.15 x 0.20 x 0.40
systematic absences	h00, h=2n+1; 0k0, k=2n+1; 00ℓ, ℓ=2n+1	none
crystal system, space group	orthorhombic, $P2_12_12_1$	triclinic, P-1
unit cell (Å and deg.)	a = 7.679(2) b = 11.993(4) c = 18.268(4)	a = 6.921(1) b = 9.650(1) c = 13.712(2) α = 106.88(1) β = 101.04(1) γ = 97.93(1)
Volume ($Å^3$)	1682.4(7)	841.7(3)
Z	4	2
density (calc.), g cm^{-3}	1.604	1.298
T (K)	295	296
absorp. coeff., mm^{-1}	1.185	0.586
absorption correction	analyt.,A^*_{min}=1.10,A^*_{max}=1.20	DIFABS, T_{min}= 0.831, T_{max}=1.158
standard reflctns. (e.s.d.)	102 (0.011), 0-5-6 (0.014)	-103 (0.014), 1-11 (0.014), 222 (0.017)
max 2θ (deg)	50	45
reflctns. meas.	-8≤h≤9, 0≤k≤14, 0≤ℓ≤21	0≤h≤7, -10≤k≤10, -14≤ℓ≤14
no. of reflctns. meas.	3390	2515
no. of unique reflctns.	2841	2222
R_{int}	0.0201	0.0359

	(7)	(5)
no. of reflctns, I>0, used	2841	2222
F(000)	832	352
final R, R_w	0.0533, 0.0425	0.0948, 0.0676
final Δ/σ max, ave.	0.114, 0.020	0.982,0.033
final diff. map, eÅ^{-3}	0.87, -0.82	0.60,-0.54
no. of variables	173	263
secondary extinction, x	N/A	N/A
wtg. function	$w^{-1}=\sigma_F^2+0.000336F^2$	$w^{-1}=\sigma_F^2+0.0009F^2$
goodness of fit	1.06	1.08
data-to-parameter ratio	16.4:1	8.4:1
diffractometer	Nicolet P2	Siemens P4
radiation	MoKα, λ=0.71073Å	MoKα, λ=0.71073Å
scan type	θ-2θ	θ-2θ
scan range	1° each side of Kα	0.6° each side of Kα
program package used	SHELX	SHELXTL
quantity minimized	$\Sigma w(\|F_o\|-\|F_c\|)^2$	$\Sigma w(\|F_o\|-\|F_c\|)^2$
absolute structure	yes	not applicable
H atoms	included and refined	calculated position

Table 3.3. Atomic positional parameters ($x10^4$) and equivalent isotropic temperature factors ($A^2 \times 10^3$) for $C_{12}H_{23}N_2OS_3Tc$.

Atom	x	y	z	U_{eq}
Tc	1886 (1)	5973.3 (5)	8759.0 (3)	30.3
S(1)	511 (2)	7683 (2)	8842 (1)	41
S(2)	23 (2)	5302 (2)	9623 (1)	42
S(3)	5523 (3)	8867 (2)	7925 (1)	53
O	1528 (7)	5309 (5)	7976 (3)	54
N(1)	4173 (7)	7020 (5)	8510 (3)	31
N(2)	3594 (7)	5275 (6)	9363 (4)	43
C(1)	1945 (12)	8530 (6)	8233 (4)	40
C(2)	3788 (9)	8235 (6)	8481 (4)	30
C(3)	5511 (10)	6785 (7)	9103 (4)	41
C(4)	5428 (10)	5563 (7)	9278 (5)	55
C(5)	3195 (12)	4572 (6)	9996 (4)	48
C(6)	1345 (9)	4113 (7)	9952 (4)	40
C(11)	1469 (11)	8246 (8)	7420 (5)	60
C(12)	1570 (12)	9771 (7)	8394 (5)	57
C(21)	6258 (12)	7555 (8)	7556 (4)	53
C(22)	4922 (10)	6687 (6)	7777 (4)	43
C(61)	692 (13)	3727 (8)	10696 (4)	56
C(62)	1208 (13)	3163 (7)	9408 (5)	65

U_{eq} defined as one third of the trace of the orthogonalized U_{ij} tensor.

Table 3.4. Atomic coordinates ($x10^4$) and equivalent isotropic displacement coefficients ($Å^2x10^3$) for $C_{12}H_{25}ClN_2S_3$:

	x	y	z	U^{eq}
Cl	3543 (2)	1978 (2)	129 (1)	56 (1)
S(1)	6793 (2)	4066 (2)	4162 (1)	49 (1)
S(2)	4672 (2)	2378 (2)	3056 (1)	49 (1)
S(3)	10101 (3)	7157 (2)	2844 (1)	59 (1)
N(1)	8552 (6)	4229 (4)	2050 (3)	35 (2)
N(2)	7337 (6)	1137 (5)	1432 (3)	41 (2)
C(1)	7323 (8)	5593 (5)	3605 (4)	37 (2)
C(2)	9045 (8)	5387 (5)	3053 (4)	36 (2)
C(3)	10085 (8)	3346 (6)	1910 (4)	47 (2)
C(4)	9159 (8)	1789 (6)	1161 (5)	52 (3)
C(5)	7693 (8)	929 (6)	2476 (4)	46 (2)
C(6)	5776 (9)	721 (6)	2846 (4)	48 (3)
C(11)	8029 (9)	6916 (6)	4618 (5)	56 (3)
C(12)	5396 (8)	5716 (6)	2905 (5)	55 (3)
C(21)	9704 (10)	6258 (7)	1458 (5)	62 (3)
C(22)	8116 (9)	4863 (6)	1203 (4)	54 (3)
C(61)	6312 (11)	389 (7)	3881 (5)	76 (4)
C(62)	4116 (9)	-499 (6)	2044 (5)	63 (3)

U_{eq} defined as one third of the trace of the orthogonalized U_{ij} tensor

Table 3.5. Selected interatomic distances (Å) and angles (°) for $C_{12}H_{23}N_2OS_3Tc$, **(7)**, and $C_{12}H_{25}ClN_2S_3$ **(5)**.

	(7)	(5)		(7)	(5)
Tc-S(1)	2.311(2)	-	Tc-S(2)	2.278(2)	-
Tc-O	1.665(5)	-	Tc-N(1)	2.207(5)	-
Tc-N(2)	1.907(5)	-	S(1)-S(2)	-	2.040(2)
S(1)-C(1)	1.860(7)	1.871(6)	S(2)-C(6)	1.850(7)	1.838(6)
S(3)-C(2)	1.835(6)	1.885(6)	S(3)-C(21)	1.792(8)	1.794(6)
N(1)-C(2)	1.486(8)	1.442(6)	N(1)-C(3)	1.510(8)	1.456(7)
N(1)-C(22)	1.513(8)	1.465(8)	N(2)-C(4)	1.458(9)	1.491(8)
N(2)-C(5)	1.469(8)	1.481(8)	C(1)-C(2)	1.53(1)	1.535(8)
C(1)-C(11)	1.56(1)	1.527(7)	C(1)-C(12)	1.54(1)	1.528(8)
C(3)-C(4)	1.51(1)	1.519(7)	C(5)-C(6)	1.52(1)	1.518(9)
C(6)-C(61)	1.528(9)	1.53(1)	C(6)-C(62)	1.51(1)	1.519(7)
C(21)-C(22)	1.52(1)	1.520(8)			

Bond angles:

	(7)	(5)
S(1)-Tc-S(2)	89.0(1)	-
S(1)-Tc-N(1)	82.7(1)	-
S(1)-Tc-N(2)	131.7(2)	-
S(2)-Tc-N(1)	147.6(1)	-

	(7)	(5)
S(2)-Tc-N(2)	82.9(2)	-
O-Tc-S(1)	114.0(2)	-
O-Tc-S(2)	108.8(2)	-
O-Tc-N(1)	103.2(2)	-
O-Tc-N(2)	113.7(3)	-
N(1)-Tc-N(2)	79.6(2)	-
Tc-S(1)-C(1)	100.1(2)	-
S(2)-S(1)-C(1)	-	108.7(2)
S(1)-S(2)-C(6)	-	106.6(2)
C(6)-S(2)-Tc	98.7(2)	-
C(2)-S(3)-C(21)	94.2(3)	92.3(3)
Tc-N(1)-C(3)	106.7(4)	-
C(2)-N(1)-Tc	114.0(4)	-
C(2)-N(1)-C(3)	110.1(5)	113.7(4)
C(2)-N(1)-C(22)	106.9(5)	109.6(4)
C(22)-N(1)-Tc	109.4(4)	-
C(22)-N(1)-C(3)	109.8(5)	111.2(5)
Tc-N(2)-C(5)	124.3(5)	-
C(4)-N(2)-Tc	119.6(5)	-
C(4)-N(2)-C(5)	115.6(6)	115.4(4)

	(7)	(5)
S(1)-C(1)-C(2)	104.3(4)	110.3(4)
S(1)-C(1)-C(11)	108.6(5)	100.1(4)
S(1)-C(1)-C(12)	107.7(5)	110.3(4)
C(2)-C(1)-C(11)	116.0(6)	110.1(4)
C(2)-C(1)-C(12)	110.2(7)	113.8(4)
C(11)-C(1)-C(12)	109.5(6)	111.5(5)
N(1)-C(2)-S(3)	106.4(4)	107.3(4)
C(1)-C(2)-S(3)	114.5(4)	110.6(4)
C(1)-C(2)-N(1)	114.9(5)	116.0(4)
N(1)-C(3)-C(4)	107.4(6)	110.9(4)
C(3)-C(4)-N(2)	106.9(6)	111.4(5)
N(2)-C(5)-C(6)	111.0(6)	112.6(4)
S(2)-C(6)-C(61)	110.1(5)	109.7(4)
S(2)-C(6)-C(62)	109.5(5)	104.1(4)
C(5)-C(6)-S(2)	104.6(5)	111.8(4)
C(5)-C(6)-C(61)	111.7(6)	107.5(5)
C(5)-C(6)-C(62)	112.0(6)	112.9(5)
C(61)-C(6)-C(62)	108.9(6)	110.9(4)
S(3)-C(21)-C(22)	106.7(5)	105.0(5)
C(21)-C(22)-N(1)	107.9(5)	108.5(4)

Table 3.6. Anisotropic temperature factors ($A^2 \times 10^3$) for $C_{12}H_{23}N_2OS_3Tc$

Atom	U_{11}	U_{22}	U_{33}	U_{12}	U_{13}	U_{23}
Tc	22.9 (2)	35.8 (3)	21.2 (3)	-4.2 (3)	-1.5 (3)	-1.6 (3)
S(1)	28.5 (9)	46 (1)	49 (1)	7.5 (8)	5.0 (9)	8 (1)
S(2)	29 (1)	47 (1)	50 (1)	0.7 (9)	8.8 (8)	9 (1)
S(3)	49 (1)	41 (1)	70 (1)	-10 (1)	17 (1)	8 (1)
O	53 (4)	59 (4)	51 (3)	-23 (3)	-2 (3)	-10 (3)
N(1)	28 (3)	33 (3)	33 (3)	-3 (3)	1 (2)	-2 (3)
N(2)	27 (3)	48 (4)	53 (4)	-4 (3)	-1 (3)	13 (3)
C(1)	33 (4)	46 (4)	42 (4)	6 (4)	5 (5)	17 (3)
C(2)	39 (4)	25 (4)	26 (4)	-4 (3)	8 (3)	-4 (3)
C(3)	29 (4)	51 (5)	43 (4)	-9 (4)	-9 (4)	-1 (4)
C(4)	24 (4)	60 (6)	80 (6)	-6 (4)	-13 (4)	42 (5)
C(5)	43 (4)	38 (4)	62 (5)	2 (5)	-5 (5)	26 (4)
C(6)	38 (4)	33 (4)	48 (4)	0 (4)	10 (3)	12 (4)
C(11)	49 (6)	79 (7)	52 (5)	-4 (5)	-4 (4)	32 (5)
C(12)	48 (6)	51 (5)	73 (6)	9 (5)	4 (5)	18 (5)
C(21)	61 (6)	55 (5)	44 (5)	-10 (4)	23 (4)	-8 (4)
C(22)	47 (5)	46 (5)	37 (4)	-4 (4)	17 (4)	-11 (4)
C(61)	64 (6)	73 (7)	32 (4)	-2 (5)	9 (4)	16 (4)
C(62)	81 (7)	41 (5)	73 (7)	-14 (5)	7 (6)	-7 (5)

The anisotropic displacement exponent takes the form $-2\pi^2(h^2a^{*2}U_{11} + ... + 2hka^*b^*U_{12} + ...)$ where a^*, b^* and c^* are the reciprocal lattice vectors

Table 3.7. Anisotropic displacement coefficients ($Å^2x10^3$) for $C_{12}H_{25}ClN_2S_3$

	U_{11}	U_{22}	U_{33}	U_{12}	U_{13}	U_{23}
Cl	52 (1)	55 (1)	52 (1)	15 (1)	2 (1)	9 (1)
S(1)	63 (1)	49 (1)	39 (1)	15 (1)	18 (1)	14 (1)
S(2)	41 (1)	52 (1)	61 (1)	13 (1)	20 (1)	20 (1)
S(3)	57 (1)	50 (1)	65 (1)	-1 (1)	17 (1)	18 (1)
N(1)	27 (2)	42 (3)	35 (3)	9 (2)	5 (2)	10 (2)
N(2)	33 (3)	46 (3)	40 (3)	8 (2)	7 (2)	9 (2)
C(1)	38 (3)	38 (3)	38 (3)	15 (3)	8 (3)	12 (3)
C(2)	34 (3)	37 (3)	37 (3)	11 (2)	6 (3)	11 (3)
C(3)	32 (3)	47 (4)	49 (4)	4 (3)	10 (3)	1 (3)
C(4)	38 (3)	57 (4)	60 (4)	12 (3)	22 (3)	12 (3)
C(5)	45 (4)	47 (3)	47 (4)	18 (3)	7 (3)	17 (3)
C(6)	61 (4)	41 (3)	46 (4)	11 (3)	9 (3)	24 (3)
C(11)	64 (4)	48 (4)	63 (4)	20 (3)	28 (4)	18 (3)
C(12)	43 (4)	56 (4)	81 (5)	25 (3)	20 (4)	36 (4)
C(21)	65 (4)	63 (4)	59 (4)	-3 (3)	12 (4)	32 (4)
C(22)	53 (4)	68 (4)	35 (4)	3 (3)	1 (3)	19 (3)
C(61)	111 (6)	65 (4)	67 (5)	25 (4)	25 (5)	39 (4)
C(62)	66 (5)	53 (4)	65 (4)	-5 (3)	22 (4)	14 (3)

The anisotropic displacement exponent takes the form:

$-2\pi^2(h^2a^{*2}U_{11} + ... + 2hka^*b^*U_{12} + ...)$, where a*, b* and c* are the reciprocal lattice vectors.

Table 3.8. Hydrogen atom positions ($x10^3$) and temperature factors ($A^2 \times 10^3$) for $C_{12}H_{23}N_2O_3Tc$

Atom	x	y	z	U
H(2)	394 (9)	857 (5)	888 (4)	10 (17)
H(3A)	650 (10)	714 (6)	888 (4)	33 (21)
H(3B)	496 (12)	736 (8)	948 (5)	63 (27)
H(4A)	586 (15)	529 (10)	945 (7)	50 (43)
H(4B)	635 (13)	620 (10)	984 (7)	80 (44)
H(5A)	391 (13)	405 (10)	1003 (7)	20 (31)
H(5B)	334 (11)	510 (7)	1058 (5)	55 (24)
H(11A)	40 (16)	856 (10)	728 (7)	64 (39)
H(11B)	126 (21)	731 (14)	731 (8)	101 (66)
H(11C)	220 (10)	863 (7)	727 (5)	9 (44)
H(12A)	214 (10)	979 (7)	876 (4)	18 (22)
H(12B)	256 (15)	1002 (11)	791 (6)	96 (39)
H(12C)	46 (17)	999 (11)	826 (7)	82 (44)
H(21A)	623 (12)	777 (8)	711 (6)	35 (24)
H(21B)	761 (16)	707 (10)	772 (6)	68 (40)
H(22A)	411 (11)	663 (7)	738 (4)	76 (25)
H(22B)	537 (14)	571 (10)	779 (6)	106 (33)
H(61A)	155 (15)	294 (11)	1096 (7)	53 (41)

H(61B)	131 (26)	390 (17)	1149 (10)	136 (91)
H(61C)	-34 (34)	350 (24)	1121 (14)	80 (124)
H(62A)	147 (11)	341 (7)	898 (4)	23 (25)
H(62B)	28 (13)	284 (10)	922 (6)	75 (39)
H(62C)	169 (15)	232 (10)	956 (6)	85 (32)

Table 3.9. Hydrogen atom coordinates ($x10^3$) for $C_{12}H_{25}ClN_2S_3$

	x	y	z
H(C2)	1010	516	351
H(N2A)	644	170	134
H(N2B)	681	28	90
H(3A)	1075	330	258
H(3B)	1107	381	164
H(4A)	879	182	46
H(4B)	1013	117	118
H(5A)	862	178	298
H(5B)	830	9	245
H(11A)	836	780	445
H(11B)	697	700	498
H(11C)	920	678	506
H(12A)	569	650	263
H(12B)	487	480	234
H(12C)	441	592	331
H(21A)	1092	601	129
H(21B)	925	688	107
H(22A)	681	511	115
H(22B)	812	416	54

H(61A)	689	-48	377
H(61B)	726	122	440
H(61C)	512	22	412
H(62A)	458	-142	189
H(62B)	296	-60	233
H(62C)	376	-25	141

Hydrogen atoms were given fixed isotropic temperature factors, U = 0.080 $Å^2$

Table 3.10. Best Planes and torsional angles for **(7)** and **(5)**

Plane	Distance of atom from plane, Å
(7):	
S(1),N(1),N(2),S(2)	S(1), 0.096; N(1), -0.119; N(2), 0.130; S(2), -
1.837x + 5.577y + 15.571z = 18.0515	0.106; Tc, -0.735; O, -2.391;
C(22),C(21),S(3),C(2)	S(3), -0.059; N(1), 0.541; C(2), 0.043; C(21),
4.723X - 2.276Y + 13.981 = 11.7293	0.071; C(22), -0.510
C(21), S(3), C(2),N(1)	S(3), 0.091; N(1), 0.083; C(2), -0.109; C(21),
5.263X + 0.404Y + 13.289 = 13.7055	0.066; C(22), -0.510.
C(2),S(3),C(21)	N(1), 0.372; C(22), -0.244.
4.900X - 1.179Y + 13.951 = 12.7170	
(5):	
S(1),N(1),N(2),S(2)	S(1), 0.446; N(1), -0.285; N(2), 0.319; S(2),
4.864x - 5.285y + 7.107z = 3.6674	0.480
C(21),S(3),C(2),N(1)	S(3), 0.015; N(1), 0.014; C(2), -0.018; C(21),
6.602x - 3.676y + 0.677z = 4.2162	-0.011; C(22), -0.564.

Torsional angles (°)

	(7)	**(5)**
OTcS(1)C(1)	-75.5(2)	-
OTcS(2)C(6)	87.0(2)	-

	(7)	(5)
OTcN(1)C(2)	110.7(4)	-
OTcN(1)C(3)	-127.8(4)	-
OTcN(2)C(4)	88.7(5)	-
OTcN(2)C(5)	-100.9(5)	-
TcS(1)C(1)C(2)	-47.0(4)	-
TcS(1)C(1)C(11)	77.5(5)	-
TcS(1)C(1)C(12)	-163.5(5)	-
S(2)S(1)C(1)C(2)	-	-90.3(3)
S(2)S(1)C(1)C(11)	-	153.8(3)
S(2)S(1)C(1)C(12)	-	36.2(4)
TcS(2)C(6)C(5)	41.7(5)	-
TcS(2)C(6)C(61)	161.8(5)	-
TcS(2)C(6)C(62)	-77.9(5)	-
C(6)S(2)S(1)C(1)	-	123.4(3)
C(2)S(3)C(21)C(22)	9.7 (5)	20.8(5)
TcN(1)C(2)S(3)	-157.7(4)	-
TcN(1)C(2)C(1)	-30.2(5)	-
TcN(1)C(3)C(4)	37.9(6)	-
TcN(1)C(22)C(21)	169.3(5)	-
C(2)N(1)C(3)C(4)	162.0(6)	152.5(5)

	(7)	(5)
C(22)N(1)C(3)C(4)	-80.3(6)	-83.5(6)
TcN(2)C(4)C(3)	36.1(6)	-
TcN(2)C(5)C(6)	21.2(6)	-
C(4)N(2)C(5)C(6)	-167.9(6)	162.4(4)
S(1)C(1)C(2)S(3)	175.4(4)	-163.4(2)
S(1)C(1)C(2)N(1)	52.1(5)	74.1(5)
C(11)C(1)C(2)S(3)	56.6(6)	-53.9(5)
C(11)C(1)C(2)N(1)	-66.7(6)	-176.4(5)
C(12)C(1)C(2)S(3)	-69.7(7)	72.1(4)
C(12)C(1)C(2)N(1)	167.0(7)	-50.4(6)
S(3)C(2)N(1)C(3)	82.7(5)	98.4(5)
S(3)C(2)N(1)C(22)	-35.9(5)	-26.7(4)
N(1)C(2)S(3)C(21)	15.1(4)	2.5(4)
C(1)C(2)S(3)C(21)	-112.7(4)	-124.9(4)
C(1)C(2)N(1)C(3)	-149.8(5)	-137.4(5)
C(1)C(2)N(1)C(22)	91.5(5)	97.5(6)
N(1)C(3)C(4)N(2)	-46.8(6)	-47.4(7)
C(3)C(4)N(2)C(5)	-135.2(6)	-63.1(6)
N(2)C(5)C(6)C(61)	-160.5(6)	175.3(4)
N(2)C(5)C(6)C(62)	76.4(6)	52.8(7)

	(7)	(5)
C(5)C(6)S(2)S(1)	-	-59.4(4)
C(61)C(6)S(2)S(1)	-	59.8(4)
C(62)C(6)S(2)S(1)	-	178.4(4)
S(3)C(21)C(22)N(1)	-32.1(5)	-40.3(6)
C(21)C(22)N(1)C(2)	44.8(5)	44.4(6)
C(21)C(22)N(1)C(3)	-74.4(5)	-82.1(5)

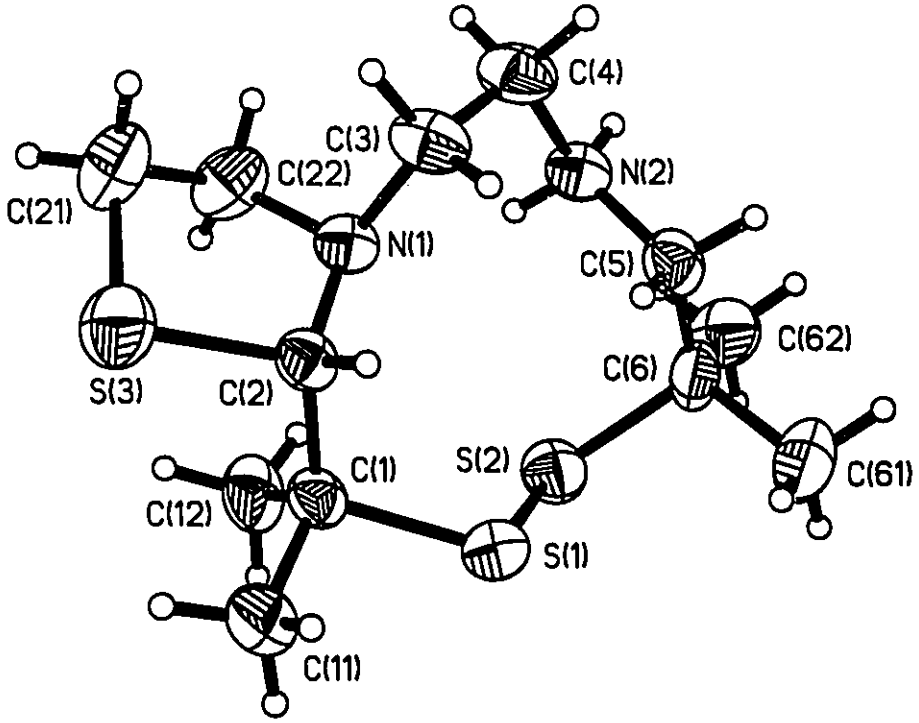

Figure 3.5. The structure of the cation in 2,2,5,5-tetramethyl-3,4,13-trithia-7,10-diaza*bicyclo*[8.3.0]tridecane hydrochloride **(5)**

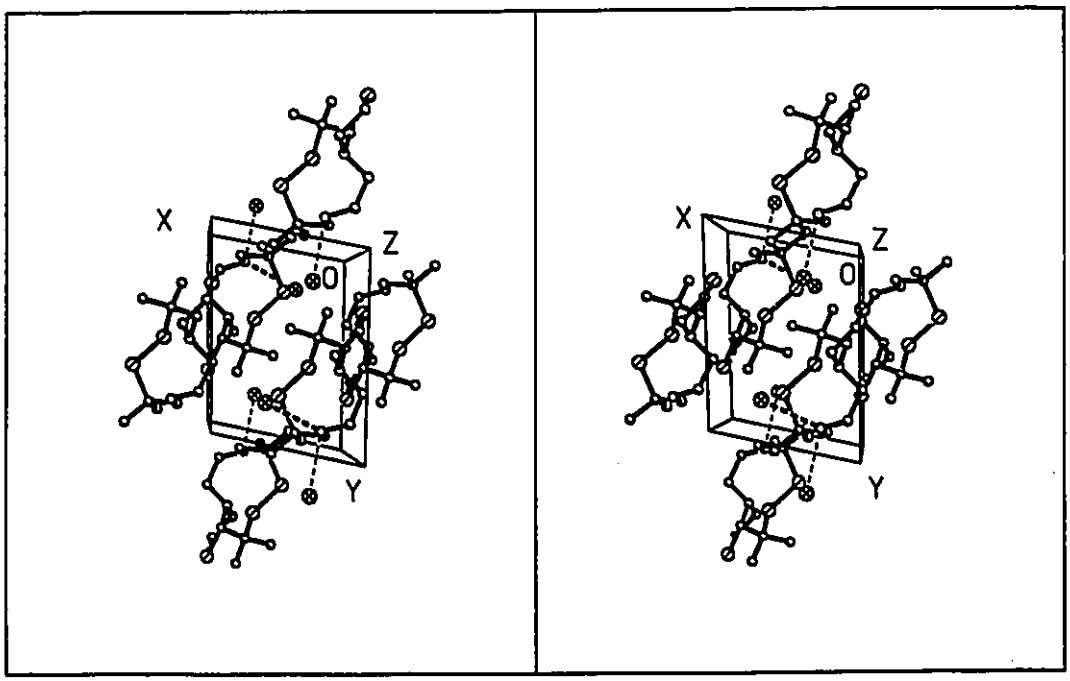

Figure 3.6. The Packing diagram for 2,2,5,5-tetramethyl-3,4,13-trithia-7,10-diaza*bicyclo*[8.3.0]tridecane hydrochloride **(5)**

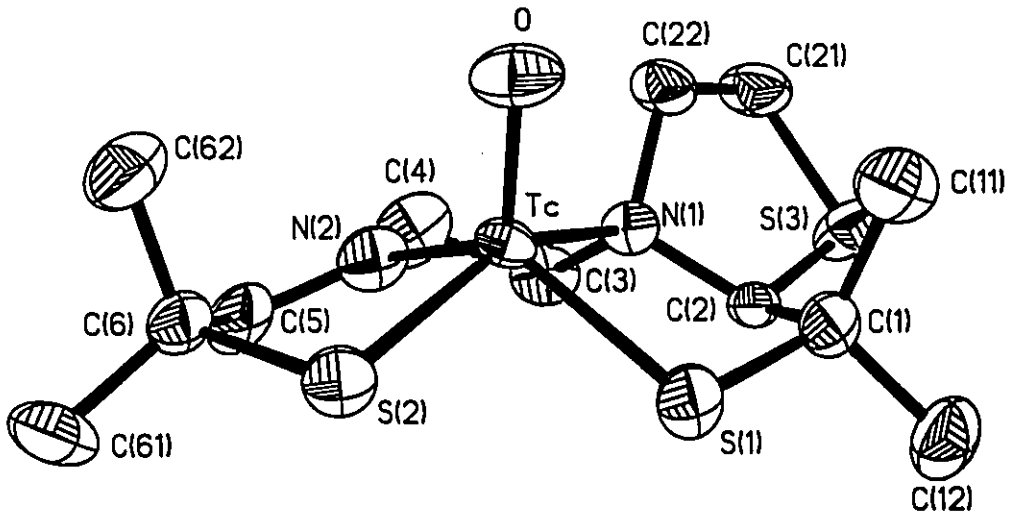

Figure 3.7. Oxo(2-(1'-methyl-1'-mercaptoethyl)-3-(5"-methyl-5"-mercapto-3"-dehydroazahexyl)-thiazolidinato-N^3,$N^{3"}$,$S^{1'}$,$S^{5"}$)technetium(V) **(7)**.

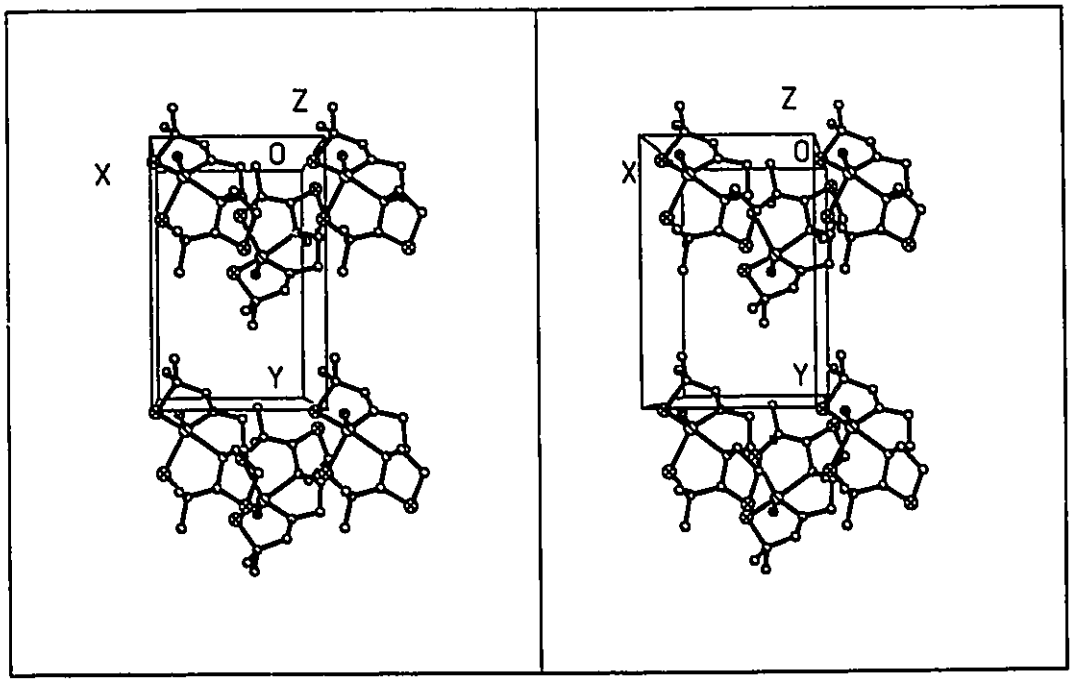

Figure 3.8 The packing diagram for the complex **(7)**

Chapter 4

4.1. Introduction

In the previous chapter, it was demonstrated that 2,2,5,5-tetramethyl-3,4-dithia-7,10-diazabicyclo[5.3.0]decane (3) is the major product in the reduction of

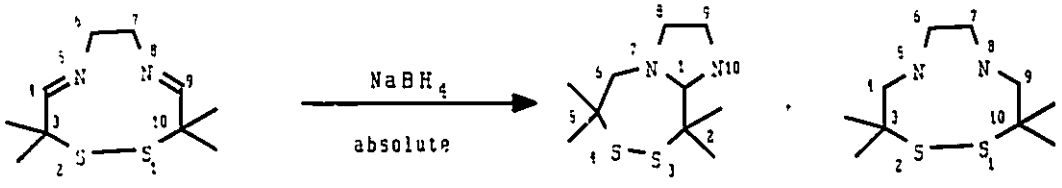

(2) (3) (4)

3,3,10,10-tetramethyl-1,2-dithia-5,8-diazacyclodeca-4,8-diene (2). It was also shown that the reaction of compound (3) with ethylene sulfide is extremely slow and leads to the formation of the thiazolidine ring containing ligand (5) in which the third sulfur atom is bound to carbon # 1. This prevented the added ethylenethiol group from chelation with the metal.

This chapter describes further investigation of the addition of a third ethylenethiol group to (3). Compound (8), 2-(triphenyl)ethanoic acid, in which the sulfur atom, protected with a trityl group, was used instead of ethylene sulfide.

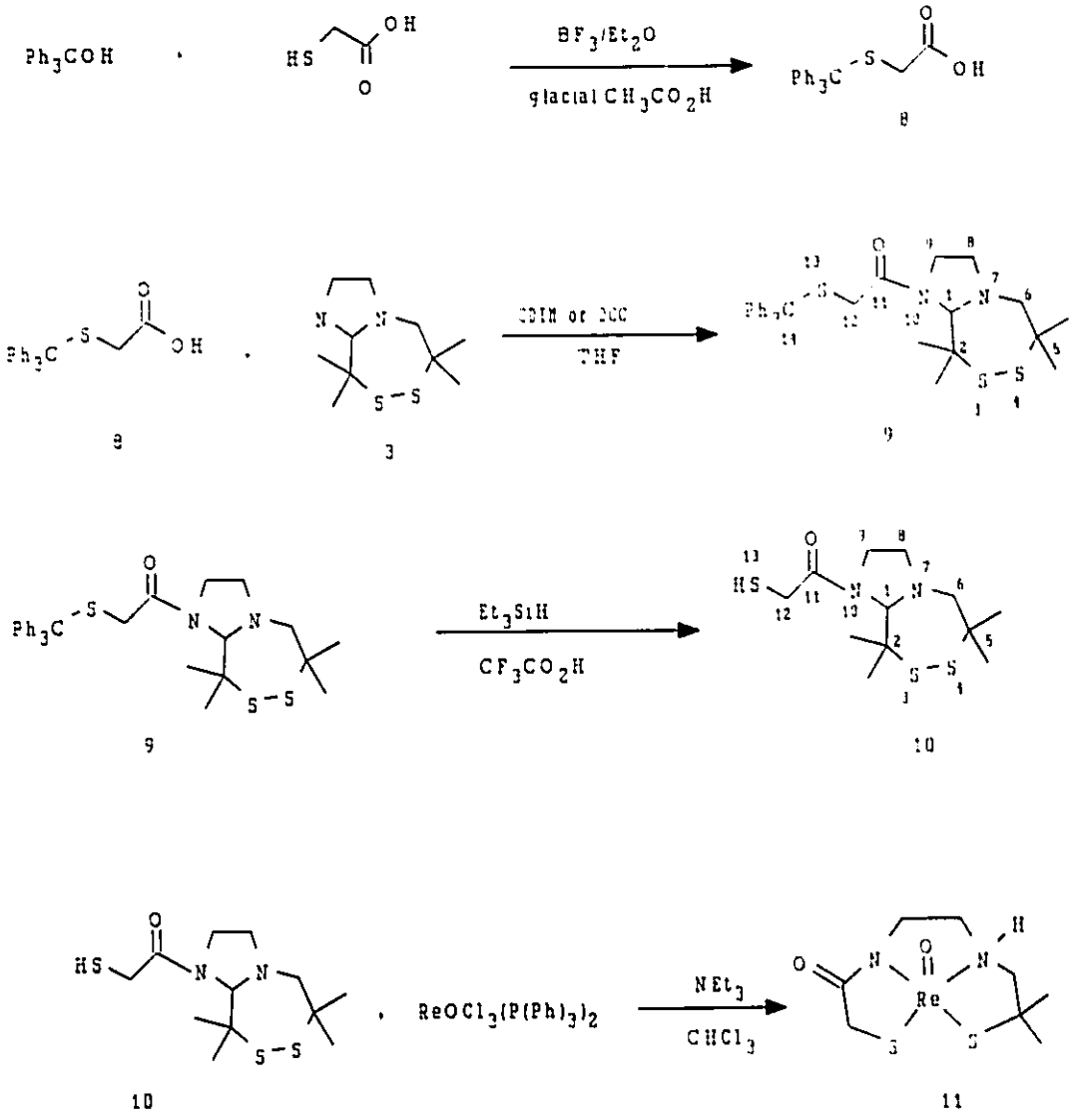

Figure 4.1. Reaction Scheme 4.1.

Compound **(8)** was combined with **(3)** through an amide linkage and the protecting trityl group was removed. The interaction of the deprotected ligand

(10) with rhenium was studied subsequently. Reaction scheme 4.1 outlines the reactions carried out in this chapter.

4.2. Experiments

4.2.1. Preparation of 2-(Triphenylmethyl)thioethanoic acid (8)

Compound (8) was synthesised according to the reported procedure [42]. Glacial acetic acid (20.0mL), mercaptoacetic acid (2.09g, 1.6mL, 22.7mmoL) and triphenylmethanol (6.00g, 23.0mmoL) were mixed and kept warm at 70 °C until the reactants dissolved (≈ 5min). Boron trifluoride etherate (5.0mL) was added and the heat source was removed. The resulting yellow solution was stirred magnetically at room temperature until a white precipitate had formed (≈ 45min). The reaction mixture was poured into 50.0mL of ice-cold distilled water, and deposited a white solid that was filtered and washed thoroughly with water. The product was then recrystallized from toluene; yield: (5.38g, 16.1mmoL, 71%); mp: 159 - 161 °C (lit. [42] 158.5 - 160.0 °C); TLC:R_f = 0.33 ($C_2H_2Cl_2/CH_3OH$, 9:1); IR (KBr pellet): ν_{max} cm^{-1}, (RI): 3000 broad (62, ν_{OH}), 2540-2990 (55, ν_{CH}), 1709 (82, $\nu_{C=O}$), 1595 (32), 1487 (54), 1445 (51), 1410 (43), 1385 (33), 1292 (67), 1227 (21), 1180 (21), 1152 (48), 1082 (30), 1030 (32), 995 (18), 905 broad (34), 843 (20), 768 (44), 745 (95), 709 (74), 699 (100), 625 (19), 618 (50); MS (DEI): 243 (100, CPh_3^+), 215 (9), 165 (88, $CPh_3^+ - C_6H_6^{\cdot}$), 115 (7); MS (DCI): 352 (4, $M^{\cdot} + NH_4^+$), 243 (100, CPh_3^+), 165 (6, $CPh_3^+ - C_6H_6^{\cdot}$); ^1H NMR ($CDCl_3$): δ 2.95 (s, 2H, S-CH_2), 7.30 (m, 15H, aryl), 10.20 (s, 1H, CO_2H); ^{13}C NMR ($CDCl_3$): δ (34.68, S-CH_2), (67.46, C-Ph_3), (128.10, 144.11,

aryl), (175.79, CO_2H).

4.2.2 Preparation of N10-(triphenylmethylthioethanoyl)-2,2,5,5-tetramethyl-3,4-dithia-7,10-diazabicyclo[5.3.0]decane (9):

Two methods were used in the synthesis of compound (9). Method a involved the use of N,N'-carbonyldiimidazole (CDIM) [94, 95] and method b involved the use of 1,3-dicyclohexylcarbodiimide (DCC).

4.2.2.1. Method a

2-(Triphenylmethyl)thioethanoic acid (8) (3.60g, 10.8mmoL) was dissolved in tetrahydrofuran (THF), (15.0mL). To this solution, N,N'-carbonyldiimidazole (1.77g, 10.9mmoL) was added and the mixture was stirred for three hours under a nitrogen atmosphere. The bicyclic 2,2,5,5-tetramethyl-3,4-dithia-7,10-diazabicyclo[5.3.0]decane (3) (2.50g, 10.8mmoL) was then added to the solution and the mixture was stirred under nitrogen for another 24 hours. The THF was evaporated under reduced pressure and the remaining residue was partitioned between methylene chloride (25.0mL) and 0.1M HCl solution (25.0mL). The aqueous layer was washed with methylene chloride (3 x 15.0mL). The methylene chloride portions were combined, washed with 0.1M HCl solution (15.0mL), 5% sodium bicarbonate solution (15.0mL), and water (3 x 15.0mL). The combined portions were then dried over anhydrous sodium sulphate. The methylene chloride was evaporated under reduced pressure. This resulted in the isolation of a colourless oil, which solidified to give a white solid, (9), upon addition of

methanol (10.0mL). The solid was collected by vacuum filtration and washed with methanol (3 x 10.0mL). Yield = 4.16g (7.6mmoL, 70%).

4.2.2.2. Method b

2-(Triphenylmethyl)thioethanoic acid **(8)**, (4.00g, 12.0mmoL), was dissolved in methylene chloride (25.0mL) and 1,3-dicyclohexylcarbodiimide (DCC) (2.52g, 12.2mmoL) was added to the resulting solution. The mixture was stirred at room temperature for one hour under a nitrogen atmosphere. 2,2,5,5-tetramethyl-3,4-dithia-7,10-diazabicyclo[5.3.0]decane **(3)**, (2.79g, 12.0mmoL) was added, and the mixture was stirred for another 18 hours. The white precipitate that formed, dicyclohexylurea (DCU), was filtered off and washed with methylene chloride (2 x 20.0mL). The filtrate was extracted with 0.5M HCl solution (20.0mL), 5% sodium bicarbonate solution (20.0mL) and water (3 x 20.0mL). An additional precipitate that formed in the methylene chloride layer, DCU, was removed by filtration. The solution was dried with anhydrous sodium sulphate and the methylene chloride was removed by evaporation under reduced pressure. Methanol (10.0mL) was added to the remaining oil. This resulted in the formation of a white precipitate, **(9)**, that was collected by filtration and washed with methanol (3 x 10.0mL). Yield = 4.93g (9.0mmoL, 75%).

Single crystals of **(9)** were obtained by dissolving the compound (100mg) in chloroform (5.0mL). Methanol (2.0mL) was added to the solution, which was left to evaporate slowly at -15 °C .

Compound (9) showed the following: mp: 166 - 168 °C; TLC: R_f = 0.68 (pure chloroform); IR (KBr): 1661 cm^{-1}, $\nu_{C=O}$; MS (DCI): 549 (1, $M^{\cdot+}$ + 1), 307 (47, $M^{\cdot+}$ - $C(Ph)_3^{\cdot}$ + 2H), 275 (9, $M^{\cdot+}$ - $SC(Ph)_3$ + 2H), 243 (100, $C(Ph)_3^{+}$), 231 (14, $M^{\cdot+}$ - $C.O.CH_2SC(Ph)_3$), 199 (10, 231 - S), 157 (14, 231 - $SC(CH_3)_2$), 125(10, 231 - $SSC(CH_3)_2$); MS (DEI): 549 (1, $M^{\cdot+}$ + 1), 474 (12, $M^{\cdot+}$ - $SC(CH_3)_2$), 243 (78, $C(Ph)_3^{+}$), 231 (100, $M^{\cdot+}$ - $C.O.CH_2SC(Ph)_3$), 165 (19, $C(Ph)_3^{+}$ - $C_6H_6^{\cdot}$); ^1H NMR ($CDCL_3$): δ 1.22 (s, 6H, 2 x $-CH_3$), 1.24 (s, 3H, CH_3), 1.27 (s, 3H, CH_3), 2.51 (d, $^2J_{H6AH6B}$ = 14.7 Hz, 1H, H6A), 2.67 (m, 1H, H8A), 2.97, 2.84 (AB quartet, $^2J_{H12AH12B}$ = 11.9 Hz, 2H, (H12A, H12B)), 2.97 - 3.32 (complex multiplet, 4H, (H6B, H8B, H9A, H9B)), 4.65 (s, 1H, H1), 7.27 (m, 9H, aryl), 7.44 (m, 6H, aryl); ^{13}C NMR ($CDCl_3$): 16 signals were observed: δ (20.03, CH_3), (25.00, CH_3), (26.72, CH_3), (28.14, CH_3), (36.50, C12), (47.92, C9), (53.74, C2, C5), (54.75, C8), (66.05, C6), (67.21, C14), (86.23, C1), (126.90, aryl), (128.06, aryl), (129.42, aryl), (143.91, aryl), (167.70, C11).

4.2.3 Preparation of N10-(thioethanoyl)-2,2,5,5-tetramethyl-3,4-dithia-7,10-diazabicyclo[5.3.0]decane (10):

The use of trifluoroacetic acid in the removal of trityl groups was reported by Brenner *et al.* [42]. The trityl protected compound (9) (1.00g, 1.8mmoL) was dissolved in 5.0mL of trifluoroacetic acid. Triethylsilane (0.31mL, 2.0mmoL) was added to the resulting orange solution. The solution turned colourless and a white precipitate formed immediately. The mixture was transferred into a separatory funnel and partitioned between hexanes (10mL) and water (10mL). The aqueous

phase was filtered through celite and washed with hexanes (3 x 10mL) and the water was removed under reduced pressure. The product, **(10)**, was recovered from the aqueous phase as a colourless oil. Yield = 0.28g (0.91mmoL, 51%); TLC: R_f = 0.60, CH_2Cl_2, CH_3OH (80:20), MS (DEI): 307 (15, $M^{\cdot+}$ + 1), 232 (100, $M^{\cdot+}$ - $COCH_2SH$), 217 (4, $M^{\cdot+}$ - $HSCH_2C.O.N$), 199 (42, 231 - S), 157 (63, 231 - $SC(CH_3)_2$), 125 (14, 231 - $SSC(CH_3)_2$), 83 (6, $C_4H_7N_2^{\cdot+}$); MS (DCI): 307 (100, $M^{\cdot+}$ + 1), 275 (6, $M^{\cdot+}$ + 1 - S), 233 (25, $M^{\cdot+}$ + 1 - $COCH_2SH$), 199 (6, 231 - S), 157 (7, 231 - $SC(CH_3)_2$); ^1H NMR ($CDCl_3$): δ 1.24 (s, 6H, 2 x CH_3), 1.28 (s, 3H, CH_3), 1.35 (s, 3H, CH_3), 2.07 (t, $^3J_{H13H12(A,B)}$ = 6.0Hz, 1H, exchangeable SH), 2.58 (d, $^2J_{H6AH6B}$ = 15.1Hz, 1H, H6A), 3.00 (m, 1H, H8A), 3.21-3.50 (m, 3H, (H6B, H9A, H9B)), 3.29 (d, $^3J_{H12(A,B)H13}$ = 5.8, 2H, (H12A, H12B)), 3.69 (m, 1H, H8B), 4.72 (s, 1H, H1).

4.2.4. Preparation of Oxo(1,1-dimethyl-3-aza-6-amidooctane-1,8-dithiolato)rhenium(V) (11):

$ReO(P(Ph)_3)_2Cl_3$ (150.0mg, 0.18mmoL) was dissolved in chloroform (100mL) to give a light green solution. Upon addition of **(10)** (80mg, 0.26mmoL), the solution turned dark red. Triethylamine (0.5mL) was added to the mixture and the solution was stirred for 24 hours. The chloroform was removed under reduced pressure. The remaining residue was washed with diethyl ether (3 x 15mL), dried, redissolved in chloroform (3.0mL) and passed through a chromatography silica gel column. Elution with a chloroform/methanol mixture (80:20) led to the isolation of the product **(11)**. Yield 27mg (0.064mmoL, 36%). A

dark green band remained at the top of the column and was not recovered.

Single crystals of **(11)** were obtained by dissolving the compound in dimethylformamide (DMF) and letting the solvent evaporate at room temperature. The density was measured by suspending the crystals in a mixture of bromoform and carbon tetrachloride.

IR (KBr pellet): 3433 cm^{-1}, ν_{N-H}; 1607 cm^{-1}, $\nu_{C=O}$; 973, $\nu_{Re=O}$; Raman: 972 $\nu_{Re=O}$

4.3. Results and Discussion:

4.3.1. Synthesis:

Reaction scheme **4.1** summarises the syntheses described in this chapter. Unlike the reaction of **(3)** with ethylene sulfide, which required a period of one week and a large excess of ethylene sulfide before any appreciable product could be recovered, the coupling of 2-(Triphenylmethyl)thioethanoic acid **(8)** with 2,2,5,5-tetramethyl-3,4-dithia-7,10-diazabicyclo[5.3.0]decane **(3)** in the presence of N,N'-carbonyldiimidazole (CDIM) or 1,3-dicyclohexylcarbodiimide (DCC) required only 24 hours of stirring at room temperature and resulted in a high yield (75%). The product of this reaction, **(9)**, was recovered in high purity as a colourless solid. It was characterized by electron impact and chemical ionization mass spectroscopy, ^{1}H and ^{13}C NMR spectroscopy and X-ray crystallography. The mass and NMR spectra were presented in the experimental section and the X-ray structure will be discussed in the following section. The NMR spectrum was assigned by comparison with the NMR spectra of **(3)**. Further confirmation of this

assignment was achieved with the use of a $^{13}C/^{1}H$ correlation NMR spectrum.

The next step in the synthesis involved the deprotection of the sulfur atom in compound **(9)** by removal of the trityl group with trifluoroacetic acid and triethylsilane. This led to the isolation of **(10)** in 51% yield. Compound **(10)** was a colourless oil that was characterized by mass and ^{1}H NMR spectroscopy. The presence of a thiol group in **(10)** was confirmed by the appearance of a triplet at 2.07ppm in the proton NMR spectrum, which was assigned to the SH proton. Upon addition of D_2O, this triplet disappeared and the splitting in the doublet at 3.29ppm, which was assigned to the CH_2 protons next to the SH group, was removed.

The reaction of the deprotected ligand **(10)** with $ReOCl_3(P(Ph)_3)_2$, led to the isolation of an unexpected rhenium complex **(11)**. This complex contained neither an N2S3 pentadentate ligand nor did it contain a thiazolidine ring containing ligand. Instead, the X-ray structure, which is presented in section **4.3.3**, showed that one ethylenethiol group was lost from the ligand in the process of the reaction. The resultant rhenium complex contained the unusual asymmetric monoaminemonoamidedithiol (MAMA) N2S2 ligand. Although this compound represents the first example of an Re or Tc asymmetric N2S2 complex that has been determined by X-ray crystallography, the synthesis of asymmetric (MAMA) N2S2 ligands [96] and their reactions with Tc [97] have been reported. In addition to X-ray structure determination, complex **(11)** was characterized by vibrational

spectroscopy. The Re=O stretching frequency dominates the Raman spectrum and occurs at 972 cm^{-1}. The IR spectrum shows a strong absorption ($\nu_{Re=O}$) at 973 cm^{-1}. It also shows the amide C=O absorption at 1606 cm^{-1}. The Re=O stretch is well within the range of several well-characterized Re(V) complexes containing the $(Re=O)^{3+}$ core [98].

4.3.2. The Crystal Structure of N10-(triphenylmethylthioethanoyl)-2,2,5,5-tetramethyl-3,4-dithia-7,10-diazabicyclo[5.3.0]decane (9):

The structure of compound (9) has been determined by single crystal X-ray diffraction. Single crystals were obtained by dissolving the compound (100mg) in chloroform (5.0mL). Methanol (2.0mL) was added to the solution, which was left to evaporate slowly at -15 °C. The crystals were unstable and were found to turn into powder when left dry for 3 hours. Consequently, the crystal chosen for the data collection was sealed into a capillary tube that was saturated with methanol vapour. Automatic unit cell determination and data collection were performed on a Rigaku AFC6R diffractometer with the use of CuKα (λ = 1.540598 Å) radiation. Unit cell parameters were refined by least-square fit of positional parameters for 21 reflections ($50.83° \leq 2\theta \leq 73.78°$). Temperature factors for nonhydrogen atoms were refined anisotropically. Details of crystal data and solution refinement are listed in table 4.1. Tables 4.2 - 4.6 list the atomic coordinates, bond distances, bond angles, anisotropic displacement coefficients, and H-Atom coordinates. Figure 4.2. shows the crystal structure and figure 4.3. shows the packing diagram for (9). It

should be noted that the unit cell contained at least one methanol molecule and probably a water molecule whose positions could not be clearly defined. It was highly disordered and it is likely that there was evaporation during the data collection. This caused the poor quality of the data set which is reflected in the relatively high residuals (R = 17.08%, R_w = 9.70%, S = 2.79).

As shown in figure 4.2., the molecule is bicyclic, comprising 5-membered and 7-membered rings fused together. All the bond distances and bond angles are within the expected range. The S(3)-S(4) disulfide bond is 2.006(4) Å which is slightly shorter than the disulfide bond in compound **(5)** described in chapter **(3)** (2.040(2) Å). The C(2)S(3)S(4)C(5) torsional angle is minus 84.1°. The amido nitrogen atom, N(10), has a shorter bond to C(11), 1.36(1)Å, compared to those to C(1) and C(9) which are 1.49(1)Å and 1.468(9)Å, respectively. This is expected because of the considerable π character of the N(10)-C(11) bond.

Table 4.1. Crystal Data for N10-(triphenylmethylthioethanoyl)-2,2,5,5-tetramethyl-3,4-dithia-7,10-diazabicyclo[5.3.0]decane (9):

Empirical Formula	$C_{32}H_{36}N_2O_3S_3$
Color; Habit	colorless plate
Crystal size (mm)	0.2 x 0.4 x 0.3
Crystal System	Triclinic
Space Group	P-1
Unit Cell Dimensions	a = 11.125(1) Å b = 11.986(1) Å c = 13.562(2) Å α = 103.54(1)° β = 90.29(1)° γ = 107.11(1)°
Volume	1675.1(8) $Å^3$
Z	2
Formula weight	592.8
Density(calc.)	1.175 Mg/m^3
Absorption Coefficient	2.277 mm^{-1}
F(000)	628
Diffractometer Used	Rigaku AFC6R
Radiation	CuKα (λ = 1.540598 Å)
Temperature (K)	296
Monochromator	Highly oriented graphite crystal
2θ Range	12.5 to 152.1°
Scan Type	2θ - θ

Scan Speed	32°/min. in ω, with up to 9 rescans
Scan Range (ω)	0.8° plus Kα-separation
Background Measurement	Stationary crystal and stationary counter at beginning and end of scan, each for 25% of total scan time
Standard Reflections	3 measured every 150 reflections
Index Ranges	$-12 \leq h \leq 12$, $0 \leq k \leq 13$, $-15 \leq l \leq 15$
Reflections Collected	5398
Independent Reflections	5000 (R_{int} = 3.75%)
Reflections used	5000
Absorption Correction	DIFABS
System Used	Siemens SHELXTL PLUS (PC Version)
Solution	Direct Methods
Refinement Method	Full-Matrix Least-Squares
Quantity Minimized	$\Sigma w(\|F_o\| - \|F_c\|)^2$
Hydrogen Atoms	Riding model, fixed isotropic U
Weighting Scheme	$w^{-1} = \sigma^2(F)$
Number of Parameters Refined	346
Final R Indices	R = 17.08 % , wR = 9.70 %
Goodness-of-Fit	S = 2.79
Largest and Mean Δ/σ	0.228, 0.030
Data-to-Parameter Ratio	14.5:1
Largest Difference Peak	1.15 eÅ^{-3}
Largest Difference Hole	-0.67 eÅ^{-3}

Table 4.2. Atomic coordinates ($x10^4$) and equivalent isotropic displacement coefficients ($Å^2x10^3$) for N10-(triphenylmethylthioethanoyl)-2,2,5,5-tetramethyl-3,4-dithia-7,10-diazabicyclo[5.3.0]decane **(9)**:

	x	y	z	U(eq)
S(3)	1688(3)	7650(3)	12810(2)	78(1)
S(4)	422(3)	6015(3)	12615(2)	81(1)
S(13)	2226(2)	8630(2)	8212(2)	59(1)
O(1)	1672(6)	10361(5)	10602(4)	64(3)
N(7)	-431(6)	7189(6)	11137(5)	54(3)
N(10)	724(6)	8362(7)	10123(5)	52(3)
C(1)	674(8)	8220(8)	11189(6)	57(4)
C(2)	1855(9)	7933(9)	11508(7)	68(5)
C(2')	3016(8)	9110(9)	11740(8)	92(6)
C(2'')	2094(9)	6885(9)	10770(7)	84(6)
C(5)	-1118(9)	6284(9)	12602(7)	67(5)
C(5')	-148(1)	6681(9)	13692(7)	106(7)
C(5'')	-206(1)	5042(9)	12028(8)	99(6)
C(6)	-1099(8)	7255(7)	12049(6)	64(4)
C(8)	-1189(8)	6948(8)	10182(6)	68(5)
C(9)	-195(8)	7303(8)	9462(6)	67(5)
C(11)	1209(8)	9460(8)	9929(7)	52(4)
C(12)	1214(8)	9497(7)	8828(6)	58(4)

C(14)	2107(8)	8696(7)	6862(6)	51(4)
C(15)	2989(8)	9864(8)	6669(7)	58(4)
C(16)	3250(9)	9890(9)	5655(7)	73(5)
C(17)	402(1)	1090(1)	542(1)	98(7)
C(18)	455(1)	1193(1)	620(1)	111(9)
C(19)	428(1)	1195(1)	722(1)	104(7)
C(20)	3513(9)	10864(9)	7428(9)	79(5)
C(21)	731(8)	8530(8)	6562(6)	52(4)
C(22)	-192(9)	7489(8)	6672(7)	65(5)
C(23)	-145(1)	7366(9)	6511(8)	80(5)
C(24)	-1826(9)	826(1)	6217(7)	82(6)
C(25)	-908(9)	9295(9)	6092(7)	69(5)
C(26)	363(9)	9420(8)	6264(6)	61(4)
C(27)	2571(9)	7645(8)	6283(7)	57(4)
C(28)	3723(9)	7567(9)	6613(7)	67(5)
C(29)	420(1)	667(1)	6116(9)	83(6)
C(30)	357(1)	586(1)	5261(9)	85(6)
C(31)	244(1)	5946(9)	4896(8)	91(6)
C(32)	194(1)	6817(9)	5424(7)	72(5)
C(100)	482(1)	200(1)	600(11)	150(6)
O(100)	386(1)	234(1)	104(1)	238(6)
O(101)	387(1)	461(1)	207(1)	272(6)

* Equivalent isotropic U defined as one third of the trace of the orthogonalized U_{ij} tensor

Table 4.3. Bond lengths (Å) for N10-(triphenylmethylthioethanoyl)-2,2,5,5-tetramethyl-3,4-dithia-7,10-diazabicyclo[5.3.0]decane (9)

S(3)-S(4)	2.006 (4)	S(3)-C(2)	1.88 (1)
S(4)-C(5)	1.84 (1)	S(13)-C(12)	1.83 (1)
S(13)-C(14)	1.858 (9)	O(1)-C(11)	1.213 (9)
N(7)-C(1)	1.45 (1)	N(7)-C(6)	1.44 (1)
N(7)-C(8)	1.46 (1)	N(10)-C(1)	1.49 (1)
N(10)-C(9)	1.468 (9)	N(10)-C(11)	1.36 (1)
C(1)-C(2)	1.54 (2)	C(2)-C(2')	1.57 (1)
C(2)-C(2")	1.50 (1)	C(5)-C(5')	1.54 (1)
C(5)-C(5")	1.56 (1)	C(5)-C(6)	1.52 (2)
C(8)-C(9)	1.51 (1)	C(11)-C(12)	1.50 (1)
C(14)-C(15)	1.54 (1)	C(14)-C(21)	1.53 (1)
C(14)-C(27)	1.55 (1)	C(15)-C(16)	1.41 (1)
C(15)-C(20)	1.36 (1)	C(16)-C(17)	1.37 (2)
C(17)-C(18)	1.40 (2)	C(18)-C(19)	1.41 (2)
C(19)-C(20)	1.421 (2)	C(21)-C(22)	1.40 (1)
C(21)-C(26)	1.39 (2)	C(22)-C(23)	1.37 (1)
C(23)-C(24)	1.40 (2)	C(24)-C(25)	1.40 (1)
C(25)-C(26)	1.39 (1)	C(27)-C(28)	1.39(2)
C(27)-C(32)	1.37 (1)	C(28)-C(29)	1.37 (2)
C(29)-C(30)	1.36 (1)	C(30)-C(31)	1.38 (2)
C(31)-C(32)	1.39 (2)	C(100)-O(100)	1.35 (2)

Table 4.4. Bond angles (°) for N10-(triphenylmethylthioethanoyl)-2,2,5,5-tetramethyl-3,4-dithia-7,10-diazabicyclo[5.3.0]decane (9)

S(4)-S(3)-C(2)	105.6(3)	S(3)-S(4)-C(5)	104.8(3)
C(14)-S(13)-C(12)	103.9(4)	C(1)-N(7)-C(8)	108.9(7)
C(1)-N(7)-C(6)	114.1(6)	C(8)-N(7)-C(6)	116.2(7)
C(1)-N(10)-C(9)	108.5(6)	C(11)-N(10)-C(1)	121.1(6)
C(11)-N(10)-C(9)	126.7(8)	N(10)-C(1)-C(2)	110.3(7)
N(10)-C(1)-N(7)	103.9(6)	C(2)-C(1)-N(7)	109.5(8)
S(3)-C(2)-C(1)	108.5(6)	S(3)-C(2)-C(2')	100.3(6)
S(3)-C(2)-C(2'')	110.7(8)	C(1)-C(2)-C(2')	109.6(9)
C(1)-C(2)-C(2'')	113.2(7)	C(2'')-C(2)-C(2')	113.6(8)
S(4)-C(5)-C(5')	110.6(7)	S(4)-C(5)-C(5'')	104.4(7)
S(4)-C(5)-C(6)	110.8(6)	C(5'')-C(5)-C(5')	111.1(8)
C(5'')-C(5)-C(6)	111.1(8)	C(6)-C(5)-C(5')	108.8(8)
N(7)-C(6)-C(5)	114.9(8)	N(7)-C(8)-C(9)	102.4(7)
N(10)-C(9)-C(8)	101.8(6)	O(1)-C(11)-C(12)	121.3(9)
N(10)-C(11)-O(1)	122.0(9)	N(10)-C(11)-C(12)	116.6(7)
S(13)-C(12)-C(11)	108.0(7)	S(13)-C(14)-C(15)	112.8(5)
S(13)-C(14)-C(21)	107.8(6)	S(13)-C(14)-C(27)	103.8(7)
C(15)-C(14)-C(21)	111.7(8)	C(15)-C(14)-C(27)	107.6(7)
C(21)-C(14)-C(27)	112.9(6)	C(14)-C(15)-C(16)	118.0(7)

C(14)-C(15)-C(20)	122.7(9)	C(20)-C(15)-C(16)	119.2(9)
C(15)-C(16)-C(17)	121.7(9)	C(18)-C(17)-C(16)	119 (1)
C(17)-C(18)-C(19)	120 (1)	C(20)-C(19)-C(18)	118 (1)
C(15)-C(20)-C(19)	121 (1)	C(14)-C(21)-C(22)	118.6(9)
C(14)-C(21)-C(26)	121.8(7)	C(26)-C(21)-C(22)	119.4(9)
C(21)-C(22)-C(23)	120 (1)	C(24)-C(23)-C(22)	120.6(9)
C(25)-C(24)-C(23)	119 (1)	C(26)-C(25)-C(24)	120 (1)
C(21)-C(26)-C(25)	120.5(8)	C(14)-C(27)-C(28)	118.8(7)
C(14)-C(27)-C(32)	123.3(9)	C(32)-C(27)-C(28)	117.8(9)
C(29)-C(28)-C(27)	121.4(8)	C(28)-C(29)-C(30)	120 (1)
C(29)-C(30)-C(31)	120 (1)	C(32)-C(31)-C(30)	120.1(9)
C(27)-C(32)-C(31)	121 (1)		

Table 4.5. Anisotropic displacement coefficients ($Å^2$ x 10^3) for N10-(triphenylmethylthioethanoyl)-2,2,5,5-tetramethyl-3,4-dithia-7,10-diazabicyclo[5.3.0]decane **(9)**

	U_{11}	U_{22}	U_{33}	U_{12}	U_{13}	U_{23}
S(3)	81(2)	82(2)	68(2)	22(2)	-6(2)	19(2)
S(4)	96(2)	70(2)	83(2)	29(2)	6(2)	28(2)
S(13)	60(2)	69(2)	57(1)	31(1)	13(1)	21(1)
O(1)	67(5)	46(4)	68(4)	9(4)	1(4)	0(3)
N(7)	50(5)	50(5)	54(5)	5(4)	9(4)	8(4)
N(10)	47(5)	62(5)	40(4)	8(4)	-2(3)	7(4)
C(1)	47(6)	59(6)	61(6)	14(5)	4(5)	10(5)
C(2)	63(7)	63(7)	68(7)	8(6)	7(5)	15(6)
C(2')	63(7)	11 (1)	107(9)	17(7)	1(7)	37(8)
C(2")	87(8)	88(8)	90(8)	53(7)	19(7)	12(7)
C(5)	80(8)	60(7)	57(6)	13(6)	13(5)	17(5)
C(5')	14 (1)	98(9)	78(8)	36(8)	61(8)	27(7)
C(5")	11 (1)	73(9)	11 (1)	22(8)	15(8)	31(8)
C(6)	71(7)	48(6)	70(7)	15(5)	18(5)	13(5)
C(8)	69(7)	57(6)	67(7)	8(6)	4(6)	7(5)
C(9)	78(7)	58(7)	56(6)	14(6)	-2(5)	3(5)
C(11)	41(6)	53(6)	64(6)	16(5)	11(5)	15(5)
C(12)	56(6)	58(6)	64(6)	21(5)	21(5)	17(5)

C(14)	55(6)	50(6)	53(5)	18(5)	11(5)	17(5)
C(15)	55(6)	52(6)	69(7)	15(5)	7(5)	20(5)
C(16)	81(8)	69(7)	80(7)	27(6)	23(6)	36(6)
C(17)	9 (1)	12 (1)	13(1)	51(9)	44(9)	7 (1)
C(18)	64(9)	12 (1)	18 (2)	27(9)	4 (1)	91 (1)
C(19)	55(8)	9 (1)	15 (1)	-5(7)	-7(8)	31(9)
C(20)	46(7)	72(8)	108(9)	-1(6)	1(6)	25(7)
C(21)	53(6)	60(6)	40(5)	19(5)	2(4)	6(5)
C(22)	60(7)	57(7)	69(6)	11(6)	9(5)	8(5)
C(23)	60(7)	61(7)	100(9)	5(6)	13(6)	-1(6)
C(24)	52(7)	10 (1)	74(7)	24(7)	-1(6)	-13(7)
C(25)	61(7)	67(7)	83(7)	31(6)	5(6)	13(6)
C(26)	60(7)	59(7)	59(6)	23(6)	4(5)	-1(5)
C(27)	58(6)	56(6)	64(6)	21(5)	21(5)	23(5)
C(28)	58(7)	80(8)	65(6)	23(6)	9(5)	17(6)
C(29)	71(8)	85(9)	11 (1)	40(7)	35(7)	38(8)
C(30)	10 (1)	69(8)	97(9)	45(8)	45(8)	26(7)
C(31)	12 (1)	75(8)	81(8)	50(8)	18(8)	7(7)
C(32)	88(8)	67(7)	65(7)	36(7)	16(6)	9(6)

The anisotropic displacement exponent takes the form: $-2\pi^2(h^2a^{*2}U_{11} + ... + 2hka^*b^*U_{12} + ...)$

Table 4.6. H-Atom coordinates ($x10^4$) and isotropic displacement coefficients ($Å^2$ x 10^3) for N10-(triphenylmethylthioethanoyl)-2,2,5,5-tetramethyl-3,4-dithia-7,10-diazabicyclo[5.3.0]decane **(9)**

	x	y	z	U
H(1)	584	8929	11645	80
H(2A')	3715	8938	12021	139
H(2B')	2795	9723	12231	139
H(2C')	3247	9388	11138	139
H(2A'')	1398	6170	10725	125
H(2B'')	2850	6770	11012	125
H(2C'')	2197	7046	10109	125
H(5A')	-835	7404	14034	156
H(5B')	-1514	6059	14038	156
H(5C')	-2278	6832	13695	156
H(5A'')	-2034	4443	12384	150
H(5B'')	-1802	4819	11352	150
H(5C'')	-2896	5099	11990	150
H(6A)	-676	8019	12505	80
H(6B)	-1945	7246	11894	80
H(8A)	-1659	6108	9973	80
H(8B)	-1758	7422	10237	80

H(9A)	-520	7512	8896	80
H(9B)	172	6669	9213	80
H(12A)	1512	10309	8758	80
H(12B)	370	9134	8515	80
H(16)	2872	9183	5120	80
H(17)	4235	10948	4743	148
H(18)	5080	12644	6038	172
H(19)	4669	12676	7726	155
H(20)	3328	10884	8122	118
H(22)	77	6866	6851	80
H(23)	-2080	6674	6623	120
H(24)	-2702	8176	6089	122
H(25)	-1154	9897	5858	80
H(26)	993	10143	6209	80
H(28)	4194	8165	7196	80
H(29)	4980	6606	6360	124
H(30)	3887	5232	4904	127
H(31)	2007	5385	4282	140
H(32)	1133	6846	5192	80

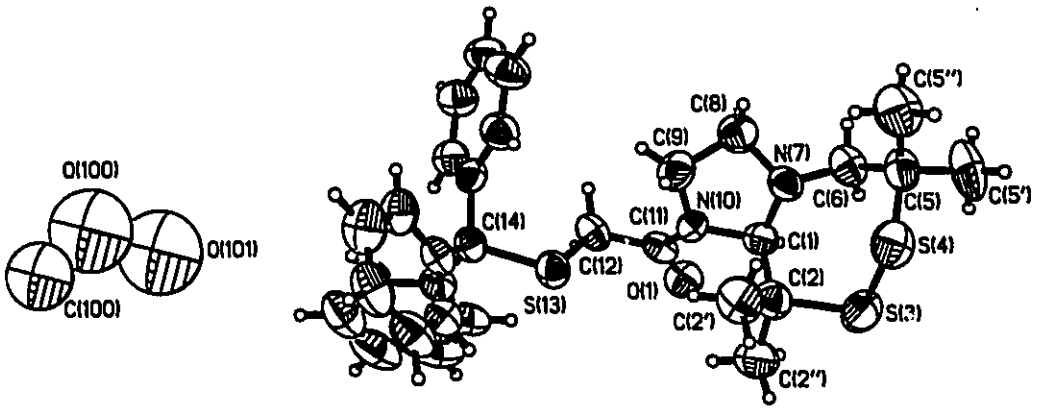

Figure 4.2(a). The Crystal Structure of (9); the numbering of the aromatic carbon atoms is shown on the next page.

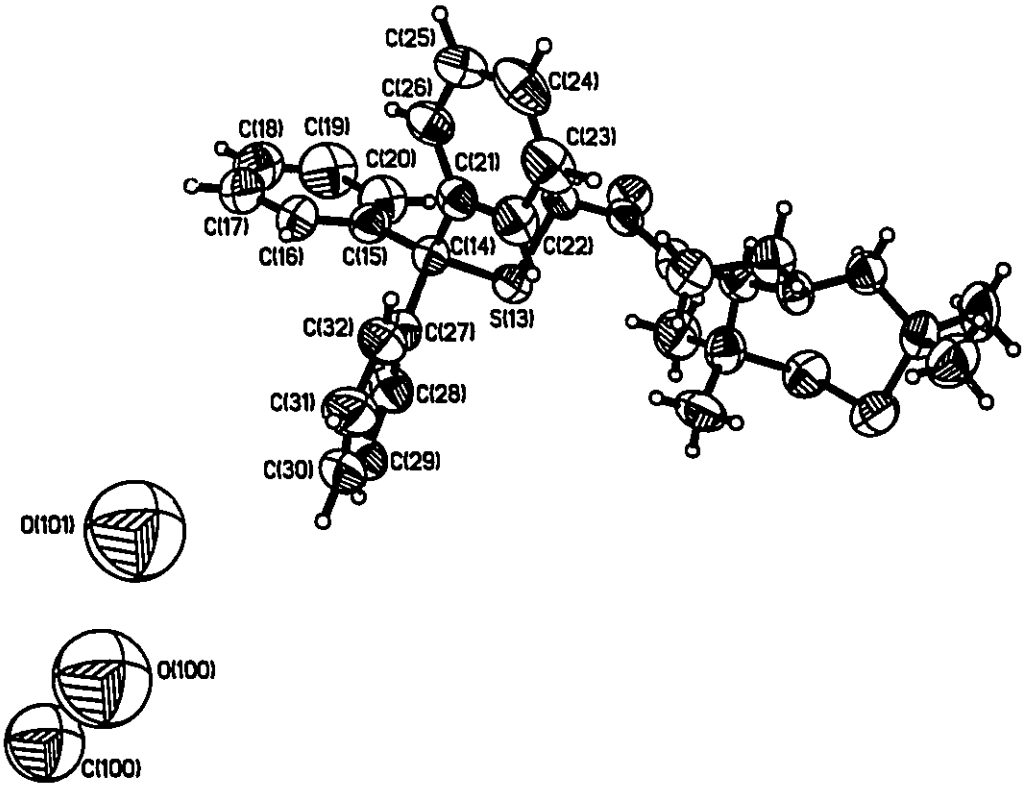

Figure 4.2(b): The crystal structure of **(9)** with the numbering scheme for the aromatic carbon atoms

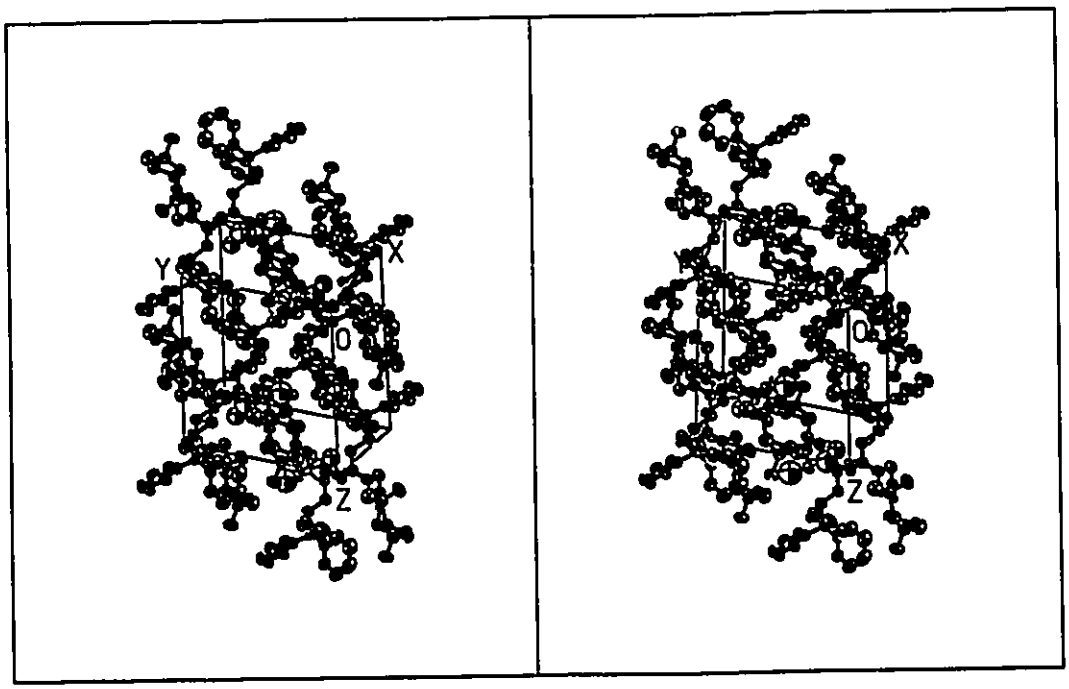

Figure 4.3. The packing diagram of N10-(triphenylmethylthioethanoyl)-2,2,5,5-tetramethyl-3,4-dithia-7,10-diazabicyclo[5.3.0]decane **(9)**

4.3.3. The Crystal Structure of The Asymmetric ReON2S2 Complex (11):

The structure of the asymmetric ReON2S2 complex, $ReC_8H_{15}N_2O_2S_2$, has been determined by single crystal X-ray diffraction. The crystal was mounted by gluing to the end of a glass fibre. Automatic unit cell determination and data collection were performed on a Siemens P4 diffractometer with the use of MoKα (λ = 0.71073 Å) radiation. Unit cell parameters were refined by least-squares fit of positional parameters for 23 reflections ($7.28° \leq 2\theta \leq 24.73°$). Temperature factors of non-hydrogen atoms were refined anisotropically. Details of crystal data and solution refinement are listed in table 4.7.

Table 4.7. Crystal Data and solution refinement for $ReC_8H_{15}N_2O_2S_2$ **(11)**:

Empirical Formula	$C_8H_{15}N_2O_2ReS_2$
Color; Habit	red rod
Crystal size (mm)	0.2 x 0.2 x 0.4
Crystal System	Monoclinic
Space Group	$P2_1/n$
Unit Cell Dimensions	a = 10.633(2) Å b = 11.221(2) Å c = 11.6780(10) Å β = 116.100(0)°
Volume	1251.3(4) Å^3
Z	4
Formula weight	421.5
Density(calc.)	2.238 g cm^{-3}
Density (Measured)	2.21(2) g cm^{-3}
Absorption Coefficient	10.0 mm^{-1}
F(000)	800
Diffractometer Used	Siemens P4
Radiation	MoKα (λ = 0.71073 Å)
Temperature (K)	23° C
Monochromator	Highly oriented graphite crystal
2θ Range	7.0 to 45.0°
Scan Type	θ - 2θ
Scan Speed	Variable; 3.00 to 60.00°/min. in ω
Scan Range (ω)	0.80° plus Kα-separation

Background Measurement	Stationary crystal and stationary counter at beginning and end of scan, each for 25% of total scan time
Standard Reflections	3 measured every 97 reflections
Index Ranges	$-1 \leq h \leq 13, -1 \leq k \leq 14, -15 \leq l \leq 14$
Reflections Collected	3660
Independent Reflections	2866 (R_{int} = 2.64%)
Reflections used	2866
Absorption Correction	DIFABS
System Used	Siemens SHELXTL PLUS (PC Version)
Solution	Direct Methods
Refinement Method	Full-Matrix Least-Squares
Quantity Minimized	$\Sigma w(\|F_o\|-\|F_c\|)^2$
Extinction Correction	not applied
Hydrogen Atoms	Riding model, fixed isotropic U
Weighting Scheme	$w^{-1} = \sigma^2(F)$
Parameters Refined	136
Final R Indices	R = 4.71 %, wR = 3.40 %
Goodness-of-Fit	S = 1.13
Largest and Mean Δ/σ	0.002, 0.001
Data-to-Parameter Ratio	21.1:1
Largest Difference Peak	1.03 eÅ^{-3}
Largest Difference Hole	-0.98 eÅ^{-3}

Atomic coordinates for non-hydrogen atoms, bond distances and bond angles for $ReC_8H_{15}N_2O_2S_2$ are listed in tables 4.8, 4.9 and 4.10, respectively. Figure 4.4 shows the crystal structure and figure 4.5 illustrates the packing diagram for this complex. The ligand atoms bound to Re form a rough square pyramid such that the Re atom lies 0.747 Å above the best S1, N1, N2, S2 plane. The Re=O bond (1.681 (5) Å) is comparable to distances in similar compounds. The Re=O bond distance is 1.662 (5) Å in the rhenium complex of 2,3-bis(mercaptoacetamido)propionic acid [52]. Oxo(1,1,8,8-tetraethyl-3,6-diazaoctane-1,8-dithiolato)rhenium [99] which exists as a hydrogen bonded dimer in which the intermolecular $N\text{-}O_{oxo\ ligand}$ distance is 2.877(4) Å, has a longer Re=O bond distance of 1.709(2) Å. The present complex also shows hydrogen bonding. In this case, however, the hydrogen bonding is between the amino nitrogen atom and the amido oxygen atom on the ligand backbone. The oxo ligand is not involved in hydrogen bonding. The two Re-N bonds are significantly different. The Re(1)-N(2) bond distance is 1.997 (6) Å compared to 2.151 (4) Å for the Re(1)-N(1) bond distance. This is in accordance with the observation that N(2), the amido nitrogen atom, becomes deprotonated upon chelation with Re(1), whereas, N(1), the amino nitrogen atom couples to the rhenium atom only through its lone-pair electrons. This is consistent with the fact that diamidodithiol (DADT) N2S2 ligands form anionic complexes with ReO^{+3} and TcO^{+3}, whereas, bis(aminothiol) (BAT) N2S2 ligands tend to form the corresponding neutral complexes. In the DADT case both

nitrogen atoms become deprotonated upon chelation whereas in the BAT case only one nitrogen atom is deprotonated.

Table 4.8. Atomic coordinates ($x10^4$) and equivalent isotropic displacement coefficients ($Å^2x10^3$) for $ReC_8H_{15}N_2O_2S_2$ **(11)**:

	x	y	z	U(eq)
Re(1)	53(1)	701(1)	2356(1)	27(1)
S(1)	-983(2)	1578(2)	3480(2)	31(1)
S(2)	-1697(2)	-657(2)	1607(2)	41(1)
O(1)	-73(5)	1580(5)	1145(4)	46(2)
O(2)	1501(6)	-2639(4)	1987(6)	59(3)
N(1)	1929(5)	1155(5)	4031(5)	30(2)
N(2)	1238(6)	-736(5)	2547(5)	36(2)
C(1)	453(7)	2547(5)	4569(6)	31(2)
C(2)	1751(7)	1769(6)	5092(6)	35(2)
C(3)	2897(7)	103(6)	4496(7)	40(3)
C(4)	2765(6)	-611(6)	3365(7)	45(3)
C(5)	734(8)	-1791(6)	1935(7)	45(3)
C(6)	-812(8)	-1867(6)	1194(7)	46(3)
C(11)	142(8)	2934(7)	5670(6)	46(3)
C(12)	610(9)	3632(6)	3833(7)	48(3)

* Equivalent isotropic U defined as one third of the trace of the orthogonalized U_{ij} tensor

Table 4.9. Bond lengths (Å) for $ReC_8H_{15}N_2O_2S_2$ **(11):**

Re(1)-S(1)	2.276 (2)	Re(1)-S(2)	2.262 (2)
Re(1)-O(1)	1.681 (5)	Re(1)-N(1)	2.151 (4)
Re(1)-N(2)	1.997 (6)	S(1)-C(1)	1.850 (6)
S(2)-C(6)	1.833 (9)	O(2)-C(5)	1.24 (1)
N(1)-C(2)	1.50 (1)	N(1)-C(3)	1.502 (8)
N(2)-C(4)	1.485 (8)	N(2)-C(5)	1.364 (9)
C(1)-C(2)	1.516 (9)	C(1)-C(11)	1.53 (1)
C(1)-C(12)	1.54 (1)	C(3)-C(4)	1.50 (1)
C(5)-C(6)	1.49 (1)		

Table 4.10. Bond angles (°) for $ReC_8H_{15}N_2O_2S_2$ **(11)**:

S(1)-Re(1)-O(1)	110.6(2)	S(1)-Re(1)-N(1)	82.2(2)
S(1)-Re(1)-N(2)	136.6(2)	S(2)-Re(1)-S(1)	89.4(1)
S(2)-Re(1)-O(1)	108.8(2)	S(2)-Re(1)-N(1)	141.9(2)
S(2)-Re(1)-N(2)	82.6(2)	O(1)-Re(1)-N(1)	108.9(2)
N(2)-Re(1)-O(1)	112.4(3)	N(2)-Re(1)-N(1)	78.6(2)
Re(1)-S(1)-C(1)	100.8(3)	Re(1)-S(2)-C(6)	99.8(3)
Re(1)-N(1)-C(2)	117.1(4)	Re(1)-N(1)-C(3)	110.9(4)
C(3)-N(1)-C(2)	112.2(5)	Re(1)-N(2)-C(4)	117.0(4)
Re(1)-N(2)-C(5)	124.0(5)	C(5)-N(2)-C(4)	119.0(6)
S(1)-C(1)-C(2)	105.6(4)	S(1)-C(1)-C(11)	109.1(5)
S(1)-C(1)-C(12)	109.9(4)	C(2)-C(1)-C(11)	108.7(5)
C(2)-C(1)-C(12)	112.2(7)	C(12)-C(1)-C(11)	111.2(6)
N(1)-C(2)-C(1)	110.8(5)	N(1)-C(3)-C(4)	108.5(5)
N(2)-C(4)-C(3)	105.6(6)	O(2)-C(5)-C(6)	121.4(6)
N(2)-C(5)-O(2)	122.9(7)	N(2)-C(5)-C(6)	115.7(7)
S(2)-C(6)-C(5)	111.6(5)		

Table 4.11. Anisotropic displacement coefficients ($Å^2 \times 10^3$) for $ReC_8H_{15}N_2O_2S_2$ **(11)**:

	U_{11}	U_{22}	U_{33}	U_{12}	U_{23}	U_{13}
Re(1)	27(1)	28(1)	27(1)	4(1)	12(1)	4(1)
S(1)	24(1)	34(1)	35(1)	1(1)	13(1)	-3(1)
S(2)	32(1)	42(1)	41(1)	-5(1)	10(1)	-11(1)
O(1)	57(3)	49(3)	37(2)	6(3)	26(3)	14(2)
O(2)	76(4)	35(3)	91(4)	11(3)	60(4)	-4(3)
N(1)	25(3)	30(3)	36(3)	2(2)	13(2)	3(2)
N(2)	35(3)	34(3)	45(3)	8(3)	22(3)	0(3)
C(1)	29(3)	27(3)	35(3)	-4(3)	12(3)	-3(3)
C(2)	26(3)	33(4)	39(3)	-5(3)	8(3)	-9(3)
C(3)	24(3)	40(4)	48(4)	13(3)	8(3)	4(3)
C(4)	33(4)	38(4)	70(5)	13(3)	29(4)	1(4)
C(5)	61(5)	36(4)	56(4)	4(4)	42(4)	-2(3)
C(6)	60(5)	42(4)	45(4)	-9(4)	30(4)	-14(3)
C(11)	47(4)	46(4)	39(4)	-4(4)	14(3)	-17(3)
C(12)	68(5)	25(4)	57(4)	5(4)	33(4)	3(3)

The anisotropic displacement exponent takes the form:

$-2\pi^2(h^2a^{*2}U_{11} + ..+ 2hka^*b^*U_{12} + ...)$

Table 4.12. H-Atom coordinates ($x10^4$) and isotropic displacement coefficients ($Å^2$ x 10^3) for $ReC_8H_{15}N_2O_2S_2$ **(11)**:

	x	y	z	U
H(1)	2358	1757	3455	50
H(2A)	1311	921	5151	50
H(2B)	2779	2185	5747	50
H(3A)	3634	380	5245	50
H(3B)	2772	-236	5354	50
H(4A)	3155	-1312	3445	50
H(4B)	3125	-116	2907	80
H(6A)	-981	-2606	1891	50
H(6B)	-1160	-2075	310	80
H(11A)	742	3508	6239	50
H(11B)	-420	2111	5661	50
H(11C)	-650	3441	5214	80
H(12A)	-250	4075	3477	80
H(12B)	825	3362	3160	80
H(12C)	1353	4133	4404	80

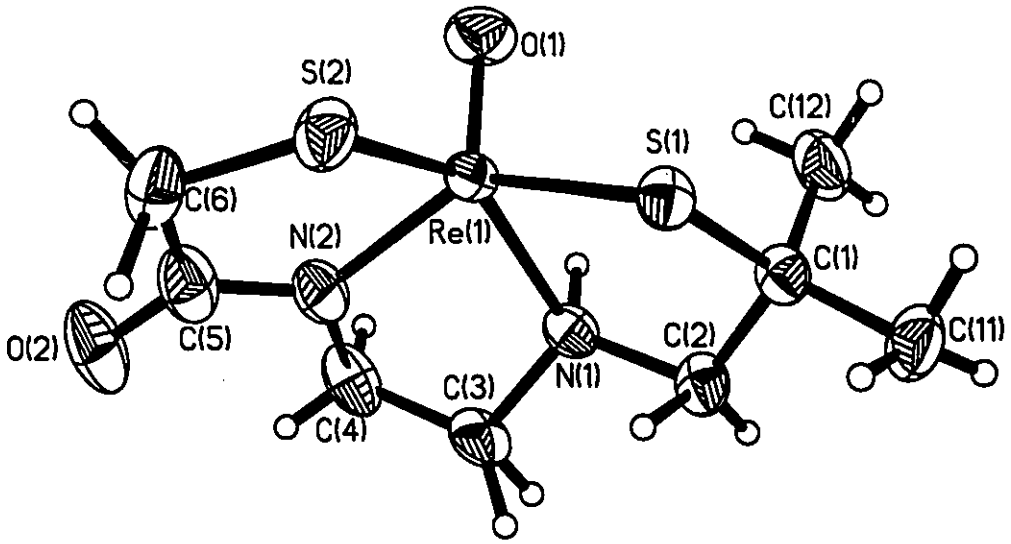

Figure 4.4. The crystal structure of $ReC_8H_{15}N_2O_2S_2$ **(11)**

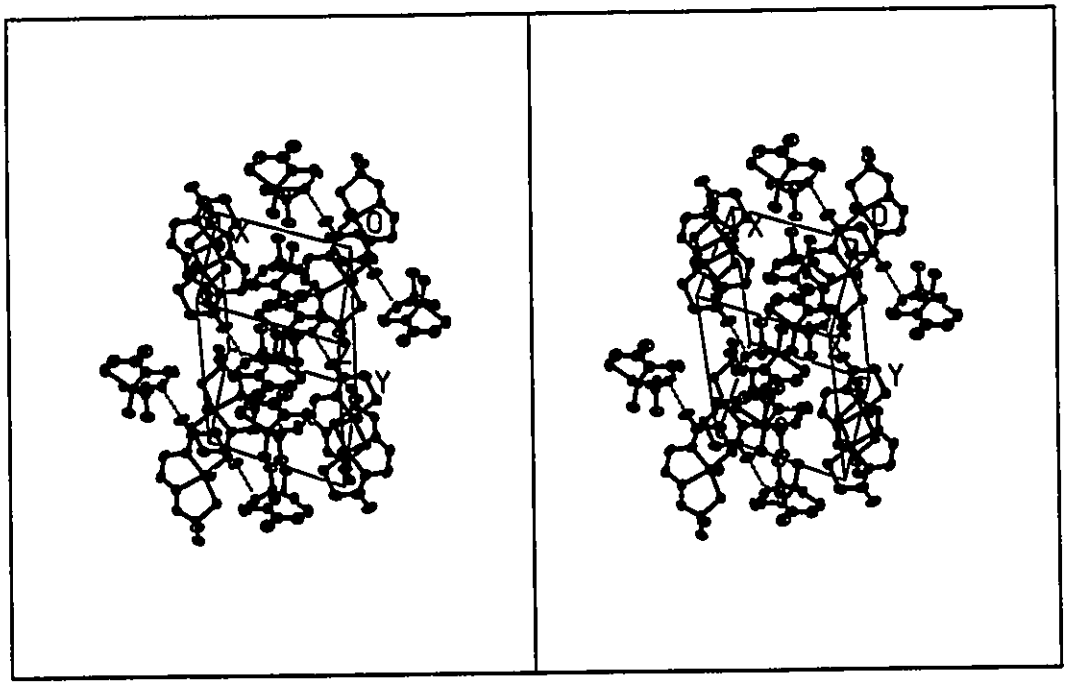

Figure 4.5. The packing diagram for $ReC_8H_{15}N_2O_2S_2$ **(11)**

Chapter 5

5.1. Introduction:

This chapter describes the investigation of the reaction of ethylene sulfide with 3,3,10,10-tetramethyl-dithia-5,8-diazacyclodecane **(4)** which led to the

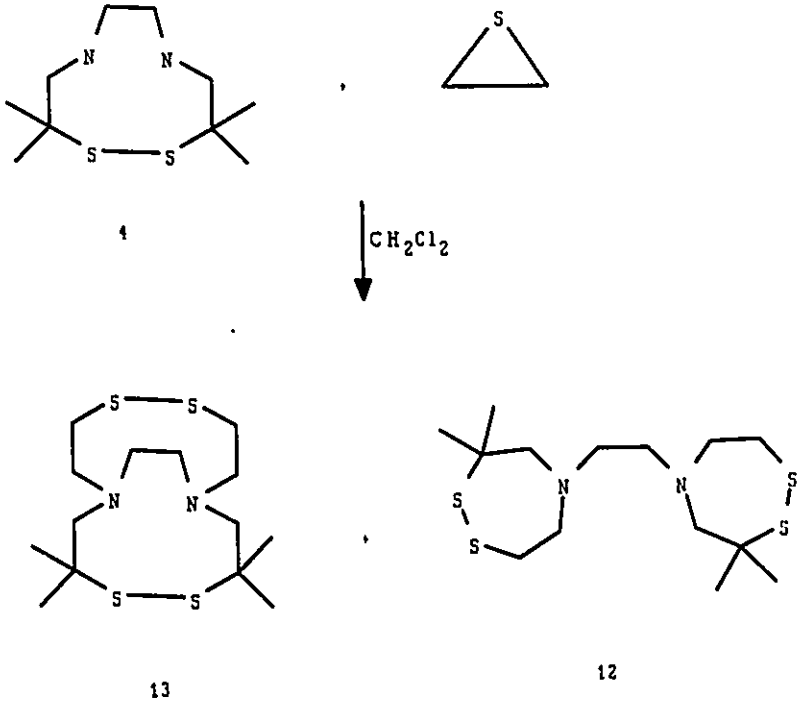

4 13 12

Figure 5.1. Reaction Scheme 5.1.

isolation of the N2S4 ligands **(12)** and **(13)**. This reaction is shown in figure **5.1.** The study of the interaction of these N2S4, **(12)** and **(13)**, ligands with technetium is worthwhile. These ligands are hexadentate and could form complexes with

Tc(III) in which all six donor atoms are bound to the metal. Conversely, interaction with TcO^{3+} would probably lead to the formation of a normal TcON2S2 complex in which the two extra thiol groups are not involved in the metal chelation. Najafi *et. al.* [100, 101] have recently reported a synthesis of an N2S4 ligand which uses an approach that is different from ours. They proposed that this ligand would interact with the metal as an N2S2 donor leaving the two extra sulfur atoms free to react with the disulfide linkages in antibodies. Therefore, these chelating agents could be used in labelling antibodies with ^{99m}Tc and ^{186}Re.

5.2. Experiments

5.2.1. Synthesis of 3,3,10,10-tetramethyl-dithia-5,8-diazacyclodecane (4):

The synthesis of compound **(4)** was described in section 3.2.3.

5.2.2. Reaction of ethylene sulfide with 3,3,10,10-tetramethyl-dithia-5,8-diazacyclodecane (4):

A solution of ethylene sulfide (0.8mL, 13mmoL) in methylene chloride (5.0mL) was added to a stirred solution of **(4)** (1.17g, 5mmoL) in methylene chloride (15.0mL). The mixture was heated under reflux and monitored daily by TLC (silica gel on aluminum, methylene chloride/methanol 95:5). After all the starting material was consumed (14 days), the solution was concentrated under a stream of dry nitrogen. The remaining residue was tested by TLC (silica gel on aluminum, methylene chloride/methanol 95:5) and was found to contain six

components. Two of these products, compounds **(12)** and **(13)**, were successfully separated by column chromatography (silica gel, 100-200 mesh, methylene chloride/methanol 98:2). Compound **(12)** showed the following; Yield: 0.69g (2mmoL, 39%); TLC: R_f = 0.52 (CH_2Cl_2/methanol 95:5); mp: 57-59 °C; IR (KBr): 2821-2930cm^{-1} ν_{C-H}, no ν_{N-H} was observed; Raman: 493cm^{-1} ν_{S-S}, 534, 569 and 642cm^{-1} ν_{C-S}, no ν_{S-H} was observed; CIMS: 353 (40, $M^{\cdot+}$ + 1); 335 (37); 247 (4, $M^{\cdot+}$ + 1 - $C(CH_3)_2S$-S); 190 (19, M^+ - $N(CH_2CH_2SSC(CH_3)_2CH_2)$); 176 (100, M^+ - $CH_2N(CH_2CH_2SSC(CH_3)_2CH_2)$); 158 (18, $C_7H_{14}N_2S^+$); 130 (14, $C_6H_{12}NS^+$); 102(13, $C_4H_8NS^+$); 84 (13, $C_4H_8N_2^+$); EIMS: 353 (3, $M^{\cdot+}$ + 1); 334 (4); 176 (100, M^+ - $CH_2N(CH_2CH_2SSC(CH_3)_2CH_2)$); 158 (85, $C_7H_{14}N_2S^+$); 149 (18, $C_5H_{11}S_2N^+$); 121 (55, $C_4H_9S_2^+$); 102 (64, $C_4H_8NS^+$); 100 (87); 84 (51, $C_4H_8N_2^+$); 71 (24); ^{1}H NMR ($CDCl_3$): δ 1.28 (s, 12H, 4 x CH_3); 2.79 (s, 4H, >N$\underline{C}H_2\underline{C}H_2$N<); 2.80 (s, 4H, 2 x (>N$\underline{C}H_2C(CH_3)_2$-)); 2.84 (t, J = 6.0Hz, 4H, 2 x (-S$\underline{C}H_2CH_2$N<)); 3.06 (t, J = 5.8Hz, 4H, 2 x (>N$\underline{C}H_2CH_2$S-)); ^{13}C NMR ($CDCl_3$): 6 signals were observed, δ (26.29, 4 x CH_3); (41.13, -S$\underline{C}H_2CH_2$N<); (51.72, -$\underline{C}(CH_3)_2$S); (57.04, >N$\underline{C}H_2CH_2$S-); (57.94, >N$\underline{C}$2$H_2\underline{C}H_2$N<); (70.31, >N$\underline{C}H_2C(CH_3)_2$S-).

Compound **(13)** showed the following: Yield: 0.43g (1.2mmoL, 24%); TLC: R_f = 0.22 (CH_2Cl_2/methanol 95:5); IR($CDCl_3$): 2811-2960cm^{-1} ν_{C-H}, no ν_{N-H} or ν_{S-H} were observed; ^{1}H NMR ($CDCl_3$): δ 1.28 (s, 6H); 1.49 (s, 6H); 2.74 (s, 2H); 2.77 (s, 2H); 2.84 (s, 2H); 2.86 (t, J = 6.0HZ, 2H); 2.88 (s, 2H); 3.06 (t, J = 6.0Hz, 2H); 3.98 (s, 2H); ^{13}C NMR ($CDCl_3$): 12 signals were observed; δ (26.27,2 x CH_3), (31.45, 2 x

CH_3), 41.06, (51.47, $\underline{C}(CH_3)_2$), (51.82, $\underline{C}(CH_3)_2$), 53.29, 53.65, 56.89, 58.84, 59.81, 70.33, 71.62.

5.3. Results and discussion:

5.3.1. Syntheses:

The reaction of ethylene sulfide with 3,3,10,10-tetramethyl-dithia-5,8-diazacyclodecane **(4)** was found to occur at a very slow rate. In benzene [89, 90], with the reaction mixture held at 50°C for 24 hours, no appreciable product was observed. With methylene chloride as the solvent, the reaction proceeded slowly. It took a period of two weeks for the reaction to go to completion. The reaction was also carried out in a methylene chloride /toluene mixture in a Carius-tube sealed under vacuum and kept at 110°C for one week. In the two cases where the reaction had gone to completion, six products were detected by thin layer chromatography (TLC). Only the two major products in this reaction mixture were successfully separated by column chromatography in a pure form. The first product (39% yield) was 1,2-di-(N-(3,3-dimethyl-1,2-dithia-5-aza-cycloheptyl) ethane **(12)** and the second product was tentatively formulated as **(13)**.

5.3.2. 1,2-Di-(N-(3,3-dimethyl-1,2-dithia-5-aza-cycloheptyl) ethane (12):

1,2-Di-(N-(3,3-dimethyl-1,2-dithia-5-aza-cycloheptyl) ethane **(12)** was characterized by NMR and mass spectroscopy and X-ray crystallography. The ^{13}C and ^{1}H NMR assignment, shown in figure **5.2**, was confirmed by $^{1}H/^{1}H$ and $^{1}H/^{13}C$ correlation experiments. The ligand has an inversion centre which makes

the NMR spectra relatively easy to interpret. The two seven-membered rings are equivalent and all four methyl groups give a singlet both in the carbon and proton NMR spectra.

The formation of **(12)** involves an attack by the two added ethylenethiol groups on the disulfide bond of the parent ligand **(4)**. This process opens the 10-membered ring and results in the formation of two 7-membered rings.

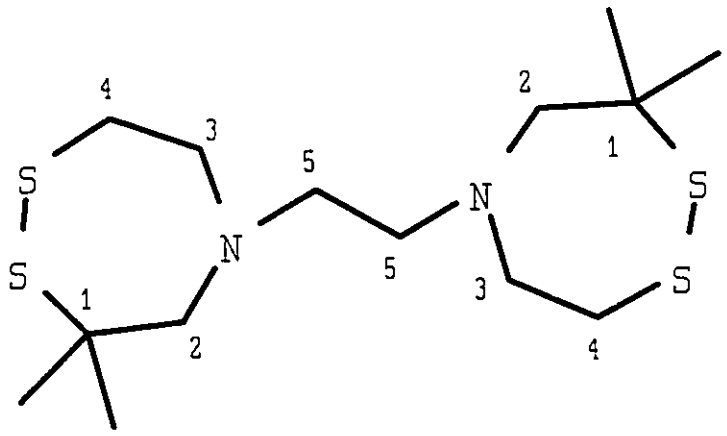

Atom	^{13}C (ppm)	^{1}H (ppm)	J (Hz)
4 x CH_3	26.29	1.26, s	
1	51.72		
2	70.31	2.81, s	
3	57.04	3.05, t	$J_{3\text{-}4}$ = 6Hz
4	41.13	2.85, t	$J_{4\text{-}3}$ = 6Hz
5	57.94	2.79, s	

Figure 5.2. ^{1}H and ^{13}C NMR assignment for **(12)**

5.3.3. X-ray structure of 1,2-di-(N-(3,3-dimethyl-1,2-dithia-5-aza-cycloheptyl) ethane (12):

The structure of **(12)** was determined by X-ray diffraction. Single crystals of **(12)** were obtained by the slow evaporation of a chloroform/methanol (8:2) mixture, containing **(12)**, at -15°C. The crystal density was measured by suspension in an aqueous solution of zinc chloride (2.00mL). The crystal was mounted by gluing it to the end of a glass fibre. Automatic unit cell determination and data collection were performed on a Siemens P4 diffractometer with the use of MoKα(λ = 0.71073 Å) radiation. Unit cell parameters were obtained from a least square fit of χ, ϕ and Θ for 25 reflections ($20.6°7 \leq 2\theta \leq 29.53°$). Temperature factors for non-hydrogen atoms were refined anisotropically. Details of crystal data and solution refinement are given in table 5.1.

The high residuals (R = 14.04%, wR = 6.67% and S = 2.23) are caused by the disorder in the position of the sulfur atoms. The compound crystallizes in a monoclinic space group. There are two independent molecules in the unit cell, both having sulfur atom disorder but to a different extent. In one molecule, each sulfur atom had two positions with 0.48/0.52 occupancy (for S1a, S1a' and S2a, S2a'). This model gave reasonable geometry, see table 5.3 and 5.4 for the bond distances and bond angles. In the second molecule, however, the disorder was not as easy to model. It was clear that the disorder was present because attempts to refine the structure without disorder produced high residuals (R = 19.69%, wR

= 13.07% and S = 3.54) with a large peak (2.5 e $Å^{-1}$) showing in the difference map. One set of the sulfur atoms (S1, S2) with an occupancy of 0.79, were clearly defined and these positions gave a reasonable geometry for the sulfur atoms. The other 21% of each of the sulfur atoms (S1', S2') was less clearly defined. This is reflected in the poor geometry of this position for a sulfur atom (S1', S2'), see table 5.3 and 5.4. It is interesting to note that the disorder in the sulfur positions did not cause disorder in the position of the methyl and methylene carbons bound to the carbon atoms next to the sulfur atoms. However, these atoms show considerably higher temperature factors, see tables 5.2 and 5.5, than the rest of the atoms in the molecule.

The disorder was refined as follows:

(a) the temperature factors for each of the sulfur atoms were fixed at 0.05 while the occupancies were refined.

(b) the occupancies were fixed and the temperature factors were refined independently and isotropically.

(c) while the occupancies were kept fixed for the rest of the refinement, the temperature factors were refined independently and anisotropically.

Table 5.1. Crystal Data and solution refinement for 1,2-di-(N-(3,3-dimethyl-1,2-dithia-5-aza-cycloheptyl) ethane (12):

Empirical Formula	$C_{14}H_{28}N_2S_4$
Color; Habit	colorless rod
Crystal size (mm)	0.2 x 0.3 x 0.4
Crystal System	Monoclinic
Space Group	C2/c
Unit Cell Dimensions	a = 18.825(4) Å b = 10.207(3) Å c = 20.573(5) Å β = 105.23(2)°
Volume	3814 (2) Å^3
Z	8
Formula weight	354.3
Density (calc.)	1.233 g cm^{-3}
Density (measured)	1.21(2) g cm^{-3}
Absorption Coefficient	0.491 mm^{-1}
F(000)	1488
Diffractometer Used	Siemens P4
Radiation	MoKα (λ = 0.71073 Å)
Temperature (K)	297
Monochromator	Highly oriented graphite crystal
2θ Range	5.0 to 50.0°
Scan Type	2θ-θ

Scan Speed	Variable; 1.54 to 14.65°/min. in ω
Scan Range (ω)	0.80° plus Kα-separation
Background Measurement	Stationary crystal and stationary counter at beginning and end of scan, each for 25.0% of total scan time
Standard Reflections	2 measured every 98 reflections
Index Ranges	$0 \le h \le 22$, $0 \le k \le 12$, $-24 \le l \le 23$
Reflections Collected	3489
Independent Reflections	3381 (R_{int} = 3.89%)
Reflections Used	3381
Absorption Correction	DIFABS
System Used	Siemens SHELXTL PLUS (PC Version)
Solution	Direct Methods
Refinement Method	Full-Matrix Least-Squares
Quantity Minimized	$\Sigma w(\|F_o\| - \|F_c\|)^2$
Extinction Correction	not applied
Hydrogen Atoms	Riding model, fixed isotropic U
Weighting Scheme	$w^{-1} = \sigma^2(F)$
N of Parameters Refined	199
Final R Indices	R = 14.04 %, wR = 6.67 %
Goodness-of-Fit	S = 2.23
Largest and Mean Δ/σ	0.379, 0.033
Data-to-Parameter Ratio	17.0:1
Largest Difference Peak	0.63 eÅ^{-3}
Largest Difference Hole	-0.49 eÅ^{-3}

Table 5.2. Atomic coordinates ($x10^4$) and equivalent isotropic displacement coefficients ($Å^2x10^3$) for 1,2-di-(N-(3,3-dimethyl-1,2-dithia-5-aza-cycloheptyl) ethane **(12)**:

	x	y	z	U(eq)	occupancy
S(1)	121(1)	2386(3)	4921(1)	99(1)	0.79
S(1')	-31(8)	1511(16)	5142(5)	153(11)	0.21
S(2)	24(1)	1925(2)	5847(1)	76(1)	0.79
S(2')	208(4)	3263(10)	5529(5)	64(4)	0.21
N(1)	-1516(2)	2973(4)	5077(2)	57(2)	1
C(1)	-450(2)	3342(5)	6095(2)	49(2)	1
C(2)	-1037(3)	3912(5)	5510(3)	66(2)	1
C(3)	-1369(3)	2811(7)	4410(2)	99(3)	1
C(4)	-772(3)	1883(8)	4380(3)	106(4)	1
C(5)	-2302(2)	3132(5)	5048(3)	69(3)	1
C(11)	70(3)	4412(6)	6467(3)	84(3)	1
C(12)	-820(3)	2697(7)	6587(3)	117(4)	1
S(1a)	1101(1)	1798(4)	2602(1)	89(2)	0.48
S(1a')	992(2)	2133(5)	2601(2)	109(2)	0.52
S(2a)	1602(2)	3558(5)	2689(2)	130(2)	0.48

S(2a')	1612(2)	3719(3)	2746(2)	69(1)	0.52
N(1a)	2206(2)	2140(4)	4071(2)	47(2)	1
C(1a)	2564(3)	3240(6)	3104(2)	52(2)	1
C(2a)	2625(2)	2039(5)	3566(2)	55(2)	1
C(3a)	1586(3)	1226(5)	3939(2)	67(2)	1
C(4a)	891(3)	1692(7)	3436(2)	81(3)	1
C(5a)	2665(2)	2099(5)	4775(2)	55(2)	1
C(11a)	2966(3)	2964(6)	2573(2)	82(3)	1
C(12a)	2874(3)	4449(5)	3512(3)	88(3)	1

* Equivalent isotropic U defined as one third of the trace of the orthogonalized U_{ij} tensor

Tables 5.3 and 5.4 present the bond distances and bond angles for one half of each of the two 1,2-di-(N-(3,3-dimethyl-1,2-dithia-5-aza-cycloheptyl) ethane **(12)** independent molecules. The other two halves are crystallographically equivalent to the ones listed. With the exception of S1' and S2', which are poorly defined as reflected by their geometries, all bond distance and bond angles fall within the expected range.

Table 5.3. Bond lengths (Å) for 1,2-di-(N-(3,3-dimethyl-1,2-dithia-5-aza-cycloheptyl) ethane **(12)**:

S(1)-S(2)	2.016 (3)	S(1)-C(4)	1.829 (6)
S(1')-S(2')	1.96 (2)	S(1')-C(4)	1.84 (1)
S(2)-C(1)	1.842 (6)	S(2')-C(1)	1.91 (1)
N(1)-C(2)	1.451 (6)	N(1)-C(3)	1.480 (7)
N(1)-C(5)	1.474 (6)	C(1)-C(2)	1.519 (6)
C(1)-C(11)	1.531 (7)	C(1)-C(12)	1.520 (8)
C(3)-C(4)	1.48 (1)	C(5)-C(5A)	1.48 (1)
S(1a)-S(2a)	2.015 (1)	S(1a)-C(4a)	1.863 (5)
S(1a')-S(2a')	1.972 (5)	S(1a')-C(4a)	1.833 (6)
S(2a)-C(1a)	1.818 (4)	S(2a')-C(1a)	1.817 (5)
N(1a)-C(2a)	1.464 (7)	N(1a)-C(3a)	1.464 (6)
N(1a)-C(5a)	1.480 (5)	C(1a)-C(2a)	1.536 (7)
C(1a)-C(11a)	1.510 (8)	C(1a)-C(12a)	1.520 (8)
C(3a)-C(4a)	1.516 (6)	C(5a)-C(5aA)	1.49 (1)
distances between disordered positions:			
S(1)...S(1')	1.08 (2)	S(1)...S(2')	1.51 (1)
S(1')...S(2)	1.49 (1)	S(2)...S(2')	1.59 (1)
S(1a)...S(1a')	0.400 (4)	S(1a)...S(2a')	2.170 (3)
S(1a')...S(2a)	1.833 (4)	S(2a)...S(2a')	0.199 (3)

Table 5.4. Bond angles (°) for 1,2-di-(N-(3,3-dimethyl-1,2-dithia-5-aza-cycloheptyl) ethane **(12)**:

S(1)-S(2)-C(1)	104.5(2)	S(1')-S(2')-C(1)	99.7(6)
S(2)-S(1)-C(4)	102.2(3)	S(2')-S(1')-C(4)	101.5(8)
C(2)-N(1)-C(5)	114.1(4)	C(3)-N(1)-C(2)	113.9(4)
C(3)-N(1)-C(5)	113.9(4)	S(2)-C(1)-C(2)	112.6(4)
S(2')-C(1)-C(2)	89.2(4)	S(2)-C(1)-C(11)	113.9(3)
S(2')-C(1)-C(11)	84.3(4)	S(2)-C(1)-C(12)	100.6(4)
S(2')-C(1)-C(12)	150.5(5)	C(2)-C(1)-C(11)	111.0(4)
C(2)-C(1)-C(12)	109.2(4)	C(11)-C(1)-C(12)	108.8(4)
N(1)-C(2)-C(1)	116.0(4)	N(1)-C(3)-C(4)	115.9(5)
S(1)-C(4)-C(3)	112.4(5)	S(1')-C(4)-C(3)	120.6(6)
N(1)-C(5)-C(5A)	112.0(5)	S(2a)-S(1a)-C(4a)	100.2(2)
S(2a')-S(1a')-C(4a)	105.3(3)	S(1a)-S(2a)-C(1a)	105.5(2)
S(1a')-S(2a')-C(1a)	108.8(3)	C(2a)-N(1a)-C(3a)	112.1(4)
C(2a)-N(1a)-C(5a)	114.1(3)	C(3a)-N(1a)-C(5a)	113.3(4)
S(2a)-C(1a)-C(2a)	109.6(3)	S(2a')-C(1a)-C(2a)	111.7(4)
S(2a)-C(1a)-C(11a)	108.7(3)	S(2a')-C(1a)-C(11a)	112.6(3)
S(2a)-C(1a)-C(12a)	107.7(4)	S(2a')-C(1a)-C(12a)	101.5(4)
C(2a)-C(1a)-C(11a)	109.2(4)	C(2a)-C(1a)-C(12a)	110.6(4)
C(11a)-C(1a)-C(12a)	111.0(5)	N(1a)-C(2a)-C(1a)	114.6(4)
N(1a)-C(3a)-C(4a)	115.5(4)	S(1a)-C(4a)-C(3a)	107.0(4)
S(1a')-C(4a)-C(3a)	115.7(4)	N(1a)-C(5a)-C(5aA)	111.2(4)

Table 5.5. Anisotropic displacement coefficients ($Å^2x10^3$) for 1,2-di-(N-(3,3-dimethyl-1,2-dithia-5-aza-cycloheptyl) ethane **(12)**:

	U_{11}	U_{22}	U_{33}	U_{12}	U_{13}	U_{23}
S(1)	64(1)	168(3)	78(2)	-11(2)	41(1)	-31(2)
S(1')	263(20)	94(14)	142(15)	43(13)	124(15)	-19(11)
S(2)	64(1)	80(2)	82(1)	17(1)	15(1)	-11(1)
S(2')	43(4)	77(8)	80(6)	-8(5)	30(4)	3(6)
N(1)	34(2)	71(4)	62(3)	-11(2)	6(2)	-1(3)
C(1)	43(3)	54(4)	52(3)	-9(3)	19(2)	-10(3)
C(2)	53(3)	66(5)	74(4)	-7(3)	7(3)	10(4)
C(3)	78(4)	184(8)	34(3)	-42(5)	15(3)	7(4)
C(4)	62(4)	171(8)	92(5)	-18(5)	34(3)	-68(5)
C(5)	48(3)	61(5)	98(4)	-6(3)	18(3)	0(4)
C(11)	75(4)	92(5)	84(4)	-23(4)	17(3)	-10(4)
C(12)	121(5)	159(8)	66(4)	-67(5)	16(4)	2(5)
S(1a)	58(2)	165(4)	37(2)	3(2)	2(1)	-19(2)
S(1a')	47(2)	193(5)	75(2)	-13(3)	-3(2)	-6(3)
S(2a)	106(3)	210(5)	68(2)	36(3)	10(2)	63(3)
S(2a')	51(2)	71(3)	92(2)	33(2)	33(2)	33(2)

N(1a)	48(2)	60(3)	32(2)	-8(2)	10(2)	3(2)
C(1a)	59(3)	57(4)	45(3)	8(3)	25(2)	7(3)
C(2a)	47(3)	59(4)	53(3)	4(3)	5(2)	-4(3)
C(3a)	73(4)	76(5)	59(4)	-27(4)	26(3)	-2(3)
C(4a)	49(3)	157(7)	33(3)	-16(4)	3(2)	12(4)
C(5a)	56(3)	59(5)	51(3)	11(3)	12(2)	6(3)
C(11a)	93(4)	106(6)	62(4)	3(4)	45(3)	-4(4)
C(12a)	124(5)	54(5)	97(5)	-6(4)	52(4)	-11(4)

The anisotropic displacement exponent takes the form:

$-2\pi^2(h^2a^{*2}U_{11} + ... + 2hka^*b^*U_{12} + ...)$

Table 5.6 lists the atomic coordinates for the hydrogen atoms. These positions were calculated at the end of the structure refinement. The hydrogen atoms on the methylene carbon atoms next to the disordered sulfur atoms were not included in the final solution. All hydrogen atoms were assigned the default temperature factors, except those which were bound to carbon atoms with U_{eq} > 0.7. The temperature factors of these hydrogen atoms were calculated to be equal to 1.5 x U_{eq} for the carbon atom to which they were bound.

Table 5.6. H-Atom coordinates ($x10^4$) and isotropic displacement coefficients ($Å^2x10^3$) for 1,2-di-(N-(3,3-dimethyl-1,2-dithia-5-aza-cycloheptyl) ethane **(12)**:

	x	y	z	U
H(2A)	-134	450	569	80
H(2B)	-794	442	524	80
H(3A)	-124	366	427	153
H(3B)	-182	255	410	153
H(5A)	-253	369	468	80
H(5B)	-236	352	546	80
H(11A)	-115	476	682	125
H(11B)	549	404	665	125
H(11C)	106	510	616	125
H(12A)	-114	330	734	170
H(12B)	-1104	197	637	170
H(12C)	-446	239	697	170
H(2aA)	245	129	329	80
H(2aB)	313	189	379	80
H(3aA)	147	106	436	80
H(3aB)	173	410	378	80

H(5aA)	314	245	479	80
H(5aB)	273	121	494	80
H(11aA)	348	281	278	122
H(11aB)	276	220	232	122
H(11aC)	2916	370	227	122
H(12aA)	339	432	373	135
H(12aB)	282	520	322	135
H(12aC)	261	459	385	135

Figure 5.3. shows the crystal structure of 1,2-di-(N-(3,3-dimethyl-1,2-dithia-5-aza-cycloheptyl) ethane **(12)**. The two seven-membered rings are crystallographically equivalent, related by an inversion centre. The ethylene group linking the two rings has a staggered confirmation, with the rings *anti* (or *trans*) with respect to each other. The NCCN torsional angle is 180°. The lone pairs on each of the nitrogen atoms also point in opposite directions. This is the most energetically favourable rotomer because it minimizes the steric interaction between the two bulky rings. The two methyl groups on each ring are on opposite sides. Figure 5.4 shows the packing diagram for the ligand. There are two independent molecules in the unit ceil each with an inversion centre. The shortest intermolecular interactions are between S1' and S1' (3.41 Å) and S1a' and S2a' (3.64 Å).

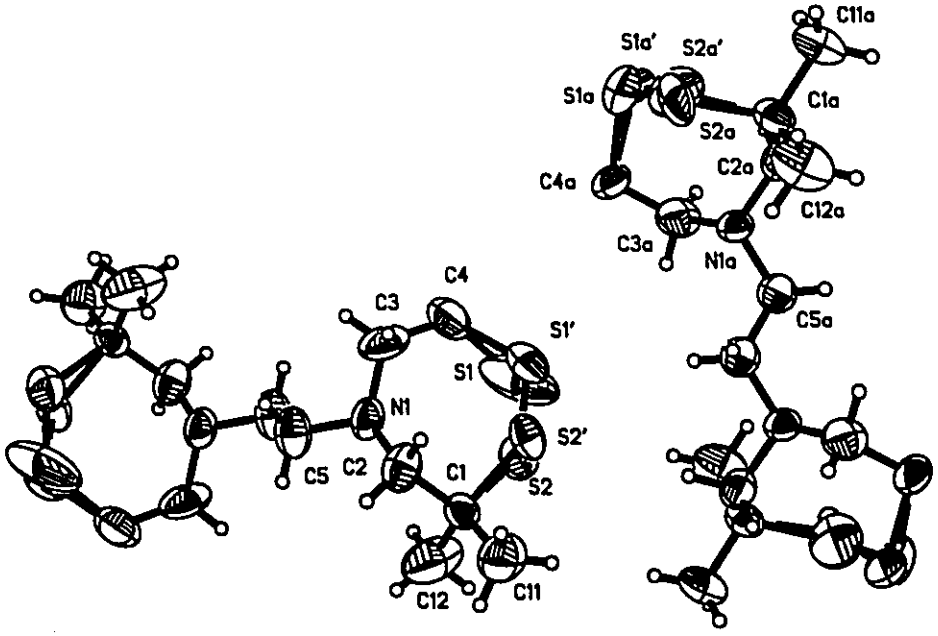

Figure 5.3. The crystal structure of 1,2-di-(N- (3,3-dimethyl-1,2-dithia-5-aza-cycloheptyl) ethane **(12)**

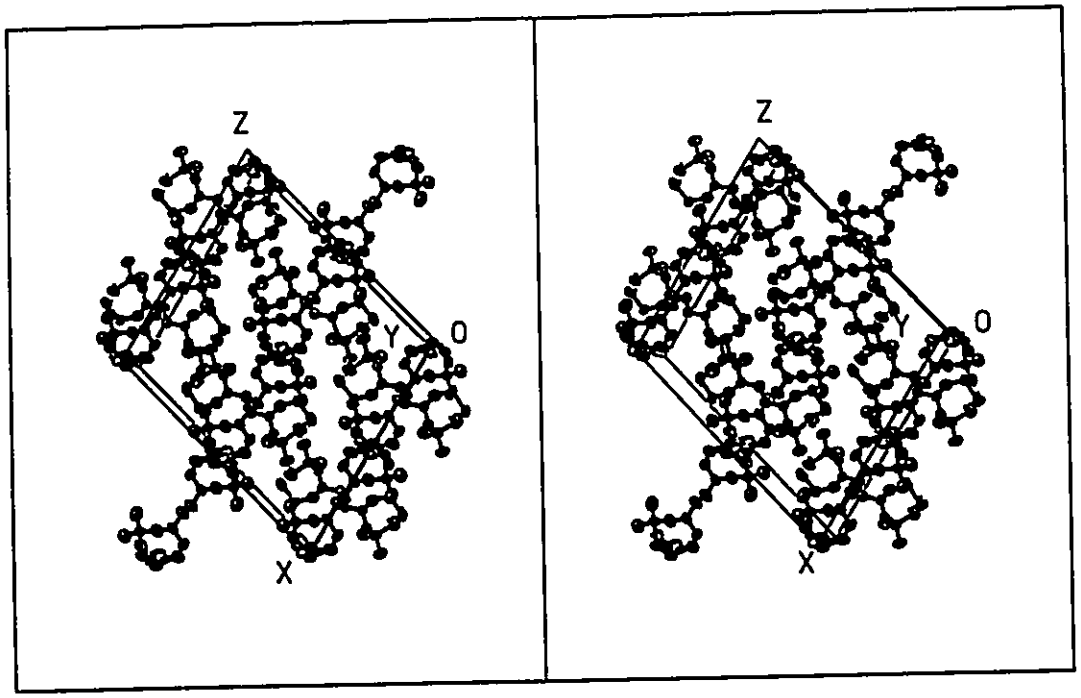

Figure 5.4. The packing diagram for 1,2-di-(N-(3,3-dimethyl-1,2-dithia-5-aza-cycloheptyl) ethane **(12)**

5.3.4. Compound (13):

In addition to 1,2-di-(N-(3,3-dimethyl-1,2-dithia-5-aza-cycloheptyl) ethane **(12)**, a second major product **(13)** was isolated in a pure form. Attempts to grow single crystals of this compound were not successful. The ligand was characterized by ^{1}H and ^{13}C NMR spectroscopy, which was presented in section 5.2.2. $^{1}H/^{1}H$ and $^{1}H/^{13}C$ correlation NMR spectra were also obtained to aid in the assignment. Unlike **(12)**, compound **(13)** seemed less symmetric and more rigid as reflected by the ^{13}C spectrum. Twelve signals were observed indicating that all the carbon atoms were not equivalent except for the four methyl carbons which showed only two signals. In **(12)** all four methyl carbons gave one singlet. The ^{13}C chemical shifts in **(13)** fall in the same range that was observed for **(12)** and each ^{13}C signal correlated nicely with a proton signal in the $^{1}H/^{13}C$ correlation spectrum, except for the two quaternary carbon atoms. The ^{1}H NMR spectrum showed a pattern that was similar to that observed for **(12)**, with two exceptions. (a) two methyl proton signals rather than one were observed. (b) a singlet, corresponding to two protons, was observed at 3.98ppm. The chemical shift for this signal is rather high for these compounds. However, this signal correlated with the ^{13}C signal at 59.82ppm. Finally a deuterium exchange experiment was carried out, and revealed the absence of any exchangeable protons, such as an -SH or an -NH proton. Based on the available spectroscopic data, compound **(13)** was tentatively assigned the structure shown in reaction scheme 5.1.. Another

possibility is the similar compound **(14)** shown below.

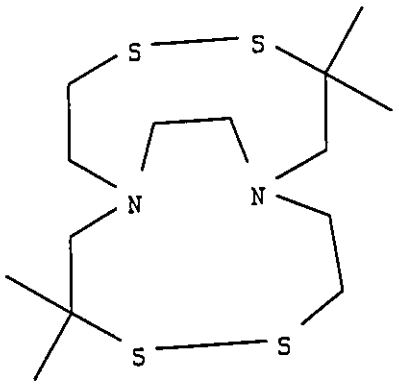

14

5.3.5. Attempted syntheses of TcN2S4 complexes:

Several attempts were made to make technetium complexes of 1,2-di-(N-(3,3-dimethyl-1,2-dithia-5-aza-cycloheptyl) ethane **(12)**. Reactions of this ligand with $Tc(tu)Cl_3$, $[(t\text{-}Bu)_4N][TcOCl_4]$ and NH_4TcO_4 were investigated. In each case, the reaction led to a mixture of products which could not be separated and hence were not characterized. It is very likely that the sulfur atoms were not all involved in the chelation with technetium. Instead, they might form intermolecular disulfide linkages. This process is then likely to lead to a mixture of polymeric products.

Chapter 6

6.1. Introduction:

In chapter 3, it was illustrated that the reduction of 3,3,10,10-tetramethyl-1,2-dithia-5,9-diazacyclodeca-4,9-diene **(2)** led to two products, 3,3,10,10-tetramethyl-1,2-dithia-5,9-diazacyclodecane **(4)** and the bicyclic **(3)**, as was shown in reaction scheme **3.1**. Kung *et al.* [102, 103] have reported the synthesis of the 11-membered ring N2S2 ligand corresponding to **(4)** by the reduction of the corresponding diimine. They did not report whether the bicyclic product corresponding to **(3)** was obtained. It is the objective of this chapter to study the sodium borohydride reduction of the 11-membered ring diimine 3,3,11,11-tetramethyl-1,2-dithia-5,9-diazacycloundeca-4,9-diene **(15)**. Compound **(15)** differs from compound **(2)** by having three methylene groups between the two nitrogen atoms instead of two making an 11-membered ring. Reaction scheme **6.1.** illustrates the reactions described in this chapter.

6.2. Experiments

6.2.1. Preparation of 2,2-dithio-bis(2-methylpropanal) (1):

This compound was prepared as described in section **3.2.1** [85].

6.2.2. Preparation of 3,3,11,11-tetramethyl-1,2-dithia-5,9-diazacycloundeca-4,9-diene (15):

To a solution of the dialdehyde **(1)** (4.00g, 19.2mmoL) in heptane (160.0mL),

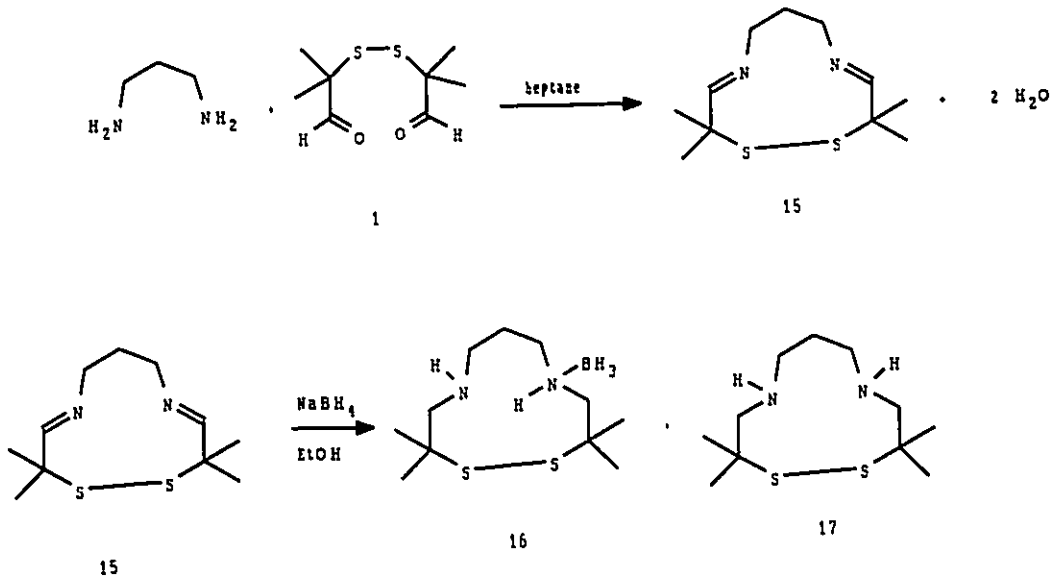

Figure 6.1. Reaction Scheme 6.1

1,3-diaminopropane (1.6mL, 19.2mmoL) and p-toluene sulfonic acid (0.10g) were added. The mixture was heated gently to boiling for 3hr. It was then stirred at room temperature for another 18hr. The solvent was removed under reduced pressure. The remaining oily residue was washed with water (50.0mL). It was then partitioned between water (3 x 15.0mL) and methylene chloride (3 x 15.0mL). The methylene chloride portions were combined and dried with anhydrous sodium sulfate. The methylene chloride was removed under reduced pressure. Yield (2.89g, 11.8mmoL, 61%); EIMS: 244 (41, $M^{\cdot+}$), 211 (11, $M^{\cdot+}$ - SH), 180 (73, $M^{\cdot+}$ -

S_2), 169 (45), 165 (100, $C_{10}H_{17}N_2^+$), 138 (58, $M^{\cdot+}$ - $S_2C(CH_3)_2$); CIMS: 245 (100, $M^{\cdot+}$ + 1), 183 (7, $M^{\cdot+}$ + 1 - S_2), 165 (8, $C_{10}H_{17}N_2^+$); ^{1}H NMR($CDCl_3$): δ 1.35 (s, 12H, 4 x CH_3), 1.86 (quintet, J = 6.8Hz, 2H, -$CH_2\underline{CH_2}CH_2$-), 3.40 (t, J = 6.7Hz, 4H, -$\underline{CH_2}CH_2\underline{CH_2}$-), 7.47 (s, 2H, 2 x -$\underline{CH}$=N); ^{13}C NMR ($CDCl_3$) (five signals were observed): δ (24.71, 4 x CH_3), (31.49, -$CH_2\underline{C}H_2CH_2$-), (51.43, 2 x $(CH_3)_2\underline{C}$S-), (57.85, -$\underline{C}H_2CH_2\underline{C}H_2$-), (166.46, 2 x -$\underline{C}$H=N-).

6.2.3. Reduction of 3,3,11,11-tetramethyl-1,2-dithia-5,9-diazacycloundeca-4,9-diene (15) with sodium borohydride:

To a suspension of the diimine **(15)** (1.00g, 4.1mmoL) in absolute ethanol (15.0mL), sodium borohydride (1.00g, 26.3mmoL) was added. The mixture was stirred at 25°C for 24hr, and then concentrated *in vacuo*. The residue was partitioned between water (15.0mL) and methylene chloride (15.0mL). The aqueous layer was washed with methylene chloride (3 x 10.0mL). The combined organic extracts were washed with water (2 x 10.0mL), dried over sodium sulfate and concentrated *in vacuo*. The residue was chromatographed on silica gel. Elution with methylene chloride-methanol (98:2) gave 3,3,11,11-tetramethyl-1,2-dithia-5,9-diazacycloundecane-5-borane **(16)**. Yield (0.20g, 0.76mmoL, 19%); Color: white solid; TLC: R_f = 0.81 CH_2Cl_2:CH_3OH (90:10); CIMS: 261 (36, $M^{\cdot+}$ - H), 249 (100, $M^{\cdot+}$ - BH_2); EIMS: 261 (100, $M^{\cdot+}$ - H), 252 (18), 195 (28), 163 (11), 139 (28), 111 (15), 99 (65), 85 (82, $C_3N_2BH_{10}^+$), 70 (32, $C_3N_2H_6^+$), 55 (36, $C_3NH_5^+$), 44 (50, $C_2NH_6^+$); ^{1}H NMR ($CDCl_3$): δ 1.18 (s, 3H, CH_3), 1.26 (s, 3H, CH_3), 1.40 (s, 3H, CH_3), 1.46 (s, 3H,

CH_3), 1.09 - 1.53 (m, BH_3), 2.35 - 2.76 (complex multiplet, 6H, 3 x CH_2), 2.98 - 3.13 (complex multiplet, 6H, 2 x CH_2, 2 x NH_2); ^{13}C NMR ($CDCl_3$): (10 signals were observed) δ (24.50, CH_3), (25.15, CH_3), (25.91, CH_3), (27.72, CH_3), (31.99, -$CH_2\underline{C}H_2CH_2$-), (49.49, 2 x $S\underline{C}(CH_3)_2$), (51.20, -$CH_2\underline{C}H_2NH$-), (59.16, $C(CH_3)_2\underline{C}H_2NH$), (63.60, $CH_2\underline{C}H_2NHBH_3$), (67.00, $C(CH_3)_2\underline{C}H_2NHBH_3$); IR (KBr pellet) ($\nu_{max}$ cm^{-1}): (3422, ν_{NH}), (3291, ν_{NH}), (3047 - 2835, ν_{CH}), (2356 - 2267, ν_{BH}). Single crystals of **(16)** were obtained by the slow evaporation of an ethyl acetate solution at room temperature. A second elution with methylene chloride-methanol (75:25) gave 3,3,11,11-tetramethyl-1,2-dithia-5,9-diazacycloundecane **(17)**. Yield: (0.60g, 2.42mmoL, 59%); Color: white oil; TLC: R_f = 0.15 CH_2Cl_2, CH_3OH (90:10); CIMS: 249 (100, $M^{\cdot+}$ + 1), 217 (6, $M^{\cdot+}$ - S); EIMS: 248 (10, $M^{\cdot+}$), 174 (8, M^+ - $SC(CH_3)_2$), 99 (65, $C_5N_2H_{11}^+$), 85 (84, $C_4N_2H_9^+$), 70 (52, $C_4NH_8^+$), 56 (57, C_3NH_6), 44 (100, C_2NH_6); ^1H NMR ($CDCl_3$): 1.27 (s, 12H, 4 x CH_3), 1.32 (s, 2H, 2 x NH), 1.63 (quintet, J = 6.7Hz, 2H, $CH_2\underline{C}H_2CH_2$), 2.56 (s, 4H, 2 x $C(CH_3)_2\underline{C}H_2NH$), 2.66 (t, J = 6.7Hz, 4H, $\underline{C}H_2CH_2\underline{C}H_2$).

6.3. Results and Discussion:

6.3.1. Synthesis:

The synthesis described in this chapter is similar to that presented in chapter **(3)**. Compound **(15)** differs from compound **(2)** by having three methylene groups between the two nitrogen atoms instead of two. It was synthesized in the same way as **(2)** except that 1,3-diaminopropane was used instead of ethylene

diamine. Treatment of compound **(15)** with sodium borohydride was shown by TLC to give two products. It was first believed that these two products would be the 11-membered ring diamine and the bicyclic compound corresponding to **(3)**, in analogy with what was observed in chapter **(3)**. Instead, chromatographic separation followed by X-ray structure determination showed that the second product was the borane adduct **(16)**. This was surprising because this adduct was not expected to be so stable. To confirm the X-ray results, compound **(16)** was further characterized by NMR, MS, and IR spectroscopy. The ^1H NMR showed four single peaks corresponding to the four methyl groups. The methylene hydrogen atoms caused two poorly resolved complex multiplets. The presence of the BH_3 group could not be conclusively confirmed by ^1H NMR because the BH_3 proton signal was split by the boron atom (^{11}B has a natural abundance of 80.2% and nuclear spin of 3/2) and overlapped with the four methyl signals. Both the CIMS and EIMS showed that the highest molecular weight peak was at 261 m/z instead of 263 m/z. This implies a favourable elimination of H_2. This is likely to be from the NH-BH_3 group because it was not observed in the mass spectra of any of the other ligands. The presence of BH_3, however, was conclusively confirmed by IR spectroscopy. The IR spectrum of **(16)** showed strong absorptions at 2356 - 2267cm^{-1} corresponding to $\nu_{B\text{-}H}$ which were well separated from the C-H absorptions.

The second product isolated from the sodium borohydride reduction of

3,3,11,11-tetramethyl-1,2-dithia-5,9-diazacycloundeca-4,9-diene (15) was 3,3,11,11-tetramethyl-1,2-dithia-5,9-diazacycloundecane (17) which was expected. Compound (17) was characterized by NMR and mass spectroscopy which were both consistent with the structure assignment. The ^1H NMR of (17) was different from that of the corresponding 10-membered ring (4) in that all four methyl groups showed one proton signal instead of two. Also, the two sets of $C(CH_3)_2\underline{CH_2}NH$ protons did not show any geminal coupling. This implies that the 11-membered ring is more fluxional than the 10-membered ring with respect to the NMR time scale. It should be mentioned that although the yield of the reaction products was only 78%, there was no evidence for the formation of the bicyclic product corresponding to (3). In fact, a mass spectrum of the product mixture showed peaks at 261m/z and 249m/z corresponding to (16) and (17), respectively. It did not show any peaks at 246m/z or 247m/z which otherwise would imply the presence of the bicyclic product. The lack of formation of the bicyclic product is likely to be because of the slower rate of formation of 6-membered rings in comparison to 5-membered rings [104].

6.3.2. Crystal Structure of 3,3,11,11-tetramethyl-1,2-dithia-5,9-diazacycloundecane-5-borane (16):

The structure of 3,3,11,11-tetramethyl-1,2-dithia-5,9-diazacycloundecane-5-borane (16) has been determined by X-ray diffraction. Single crystals were obtained from an ethyl acetate solution by slow evaporation at room temperature.

The crystal was mounted by gluing to a glass fibre. Automatic unit cell determination and data collection were performed on Rigaku AFC6R diffractometer with the use of CuKα (λ = 1.540598 Å) radiation. Unit cell parameters were refined by least square fit of positional parameters for 20 reflections ($10.7° \leq \theta \leq 52.3°$). Details of crystal data and solution refinement are listed in table 6.1. Table 6.2. lists the atomic coordinates and equivalent isotropic displacement coefficients for 3,3,11,11-tetramethyl-1,2-dithia-5,9-diazacycloundecane-5-borane **(16)**. The equivalent isotropic displacement coefficients for all atoms are within the expected values. The methyl carbon atoms show slightly higher temperature factors, as expected, because of thermal vibrations.

Table 6.1. Crystal Data and Solution refinement for 3,3,11,11-tetramethyl-1,2-dithia-5,9-diazacycloundecane-5-borane **(16)**:

Empirical Formula	$C_{11}H_{27}BN_2S_2$
Color; Habit	colorless plate
Crystal size (mm)	0.2 x 0.4 x 0.4
Crystal System	Orthorhombic
Space Group	Pbca
Unit Cell Dimensions	a = 10.250(2) Å b = 10.663(2) Å c = 27.883(6) Å
Volume	3048 (1) Å^3
Z	8
Formula weight	262.3
Density(calc.)	1.143 gcm^{-3}
Density (measured)	1.12(2) gcm^{-3}
Absorption Coefficient	2.975 mm^{-1}
F(000)	1152
Diffractometer Used	Rigaku AFC6R
Radiation	CuKα (λ = 1.540598 Å)
Temperature (K)	296
Monochromator	Highly oriented graphite crystal
2θ Range	7.0 to 119°
Scan Type	2θ - θ
Scan Speed	32°/min in ω, with up to 9 rescans

Scan Range (ω)	0.80° plus Kα-separation
Background Measurement	Stationary crystal and stationary counter at beginning and end of scan, each for 25% of total scan time
Standard Reflections	3 measured every 150 reflections
Index Ranges	$0 \le h \le 12, 0 \le k \le 12, 0 \le l \le 31$
Reflections Collected	2684
Independent Reflections	2263
Reflections Used	2263
Absorption Correction	DIFABS
System Used	Siemens SHELXTL PLUS (PC Version)
Solution	Direct Methods
Refinement Method	Full-Matrix Least-Squares
Quantity Minimized	$\Sigma w(\lvert F_o \rvert - \lvert F_c \rvert)^2$
Extinction Correction	$\chi = 0.00316(6)$, where $F^* = F [1 + 0.002 \chi F^2/\sin(2\theta)]^{-1/4}$
Hydrogen Atoms	Riding mode[1], fixed isotropic U
Weighting Scheme	$w^{-1} = \sigma^2(F)$
Number of Parameters Refined	146
Final R Indices	R = 14.96 %, wR = 6.13 %
Goodness-of-Fit	S = 1.17
Largest and Mean Δ/σ	0.033, 0.012
Data-to-Parameter Ratio	15.5:1
Largest Difference Peak	0.65 eÅ^{-3}
Largest Difference Hole	-0.68 eÅ^{-3}

Table 6.2. Atomic coordinates ($x10^4$) and equivalent isotropic displacement coefficients ($Å^2 \times 10^3$) for 3,3,11,11-tetramethyl-1,2-dithia-5,9-diazacycloundecane-5-borane **(16)**:

	x	y	z	U(eq)
S(1)	629(2)	3826(1)	2950(1)	57(1)
S(2)	1049(2)	4419(2)	3620(1)	58(1)
N(5)	709(4)	2248(4)	4394(1)	40(1)
N(9)	841(4)	1011(4)	3502(1)	40(1)
C(3)	-359(5)	4182(5)	4036(2)	47(2)
C(4)	198(5)	3536(5)	4481(2)	52(2)
C(6)	-296(5)	1235(5)	4489(2)	48(2)
C(7)	-14(6)	30(5)	4229(2)	53(2)
C(8)	-109(5)	107(5)	3690(2)	51(2)
C(10)	770(6)	1188(5)	2988(2)	50(2)
C(11)	1520(5)	2348(5)	2821(2)	45(2)
C(31)	-782(7)	5496(5)	4189(2)	78(3)
C(32)	-1476(5)	3494(5)	3791(2)	55(2)
C(111)	1540(6)	2351(6)	2272(2)	72(3)
C(112)	2882(5)	2399(5)	3021(2)	63(2)

B(1)	2084(6)	2035(7)	4678(2)	61(3)

* Equivalent isotropic U defined as one third of the trace of the orthogonalized U_{ij} tensor

Table 6.3 presents the bond lengths and table 6.4. presents the bond angles for 3,3,11,11-tetramethyl-1,2-dithia-5,9-diazacycloundecane-5-borane **(16)**. The compound has two different nitrogen atoms. N(5) is bound to a BH_3 group. The N(5)-B(1) bond distance is 1.632(7)Å as expected [105]. The distance between N(5) and N(9) is 2.817(7)Å, which is indicative of hydrogen bonding. This hydrogen bonding contributes to the unusual stability of the adduct. The two C-N bonds on the borated nitrogen atom (N(5)) are longer than the two corresponding C-N bonds on the second nitrogen atom (N(9)), (1.490(7) and 1.517(7) Å *vs* 1.467(6) and 1.449(7) Å). Also, within each pair of C-N bonds the ones that are next to the dimethyl substituted carbon atoms are shorter than those next to the methylene carbon atoms. The S-S, S-C and C-C bonds are normal. The C-C bonds range from 1.503(7) to 1.533(7) Å. All the bond angles are also within the expected range. The C(11)S(1)S(2)C(3) torsional angle is -107.3°. Table **6.6** shows the H-atom coordinates. The hydrogen atoms on B(1) and N(5) were found on the difference map and the positions of the rest of the hydrogen atoms were calculated. Figure **6.2.** shows the crystal structure and figure **6.3.** shows the packing diagram for 3,3,11,11-tetramethyl-1,2-dithia-5,9-diazacycloundecane-5-borane **(16)**.

Table 6.3. Bond lengths (Å) for 3,3,11,11-tetramethyl-1,2-dithia-5,9-diazacycloundecane-5-borane **(16)**:

S(1)-S(2)	2.019 (2)	S(1)-C(11)	1.856 (6)
S(2)-C(3)	1.869 (6)	N(5)-C(4)	1.490 (7)
N(5)-C(6)	1.517 (7)	N(5)-B(1)	1.632 (7)
N(9)-C(8)	1.467 (7)	N(9)-C(10)	1.449 (6)
C(3)-C(4)	1.530 (7)	C(3)-C(31)	1.528 (8)
C(3)-C(32)	1.521 (7)	C(6)-C(7)	1.503 (7)
C(7)-C(8)	1.509 (7)	C(10)-C(11)	1.529 (7)
C(11)-C(111)	1.533 (7)	C(11)-C(112)	1.504 (7)

Table 6.4. Bond angles (°) for 3,3,11,11-tetramethyl-1,2-dithia-5,9-diazacycloundecane-5-borane **(16)**:

S(2)-S(1)-C(11)	109.8(2)	S(1)-S(2)-C(3)	111.5(2)
C(6)-N(5)-C(4)	112.9(4)	C(6)-N(5)-B(1)	113.7(4)
C(4)-N(5)-B(1)	110.6(4)	C(8)-N(9)-C(10)	114.0(4)
S(2)-C(3)-C(4)	106.3(3)	S(2)-C(3)-C(31)	105.6(4)
S(2)-C(3)-C(32)	111.6(3)	C(31)-C(3)-C(4)	107.0(4)
C(32)-C(3)-C(4)	115.4(4)	C(32)-C(3)-C(31)	110.6(5)
N(5)-C(4)-C(3)	114.4(4)	N(5)-C(6)-C(7)	113.2(4)
C(6)-C(7)-C(8)	114.9(4)	N(9)-C(8)-C(7)	110.4(4)
N(9)-C(10)-C(11)	112.4(4)	S(1)-C(11)-C(10)	112.4(4)
S(1)-C(11)-C(111)	101.4(4)	S(1)-C(11)-C(112)	110.8(4)
C(10)-C(11)-C(111)	108.2(4)	C(112)-C(11)-C(10)	112.6(4)
C(112)-C(11)-C(111)	110.9(4)		

Table 6.5. Anisotropic displacement coefficients ($Å^2$ x 10^3) for 3,3,11,11-tetramethyl-1,2-dithia-5,9-diazacycloundecane-5-borane **(16)**:

	U_{11}	U_{22}	U_{33}	U_{12}	U_{13}	U_{23}
S(1)	65(1)	57(1)	49(1)	16(1)	-2(1)	10(1)
S(2)	63(1)	54(1)	58(1)	-19(1)	4(1)	-2(1)
N(5)	33(3)	47(3)	41(2)	-5(2)	0(2)	-4(2)
N(9)	27(3)	45(3)	48(2)	-6(2)	1(2)	5(2)
C(3)	37(3)	54(4)	49(3)	5(3)	-5(3)	-7(3)
C(4)	46(4)	67(4)	42(3)	4(3)	2(3)	-6(3)
C(6)	33(3)	67(4)	43(3)	-8(3)	4(3)	12(3)
C(7)	50(4)	47(3)	62(4)	-11(3)	3(3)	11(3)
C(8)	48(3)	50(3)	57(3)	-17(3)	6(3)	5(3)
C(10)	55(4)	48(3)	48(3)	1(3)	5(3)	-6(3)
C(11)	37(3)	49(4)	50(3)	2(3)	9(2)	7(3)
C(31)	81(6)	61(4)	93(5)	32(4)	-17(4)	-19(4)
C(32)	41(3)	66(4)	57(3)	2(3)	-8(3)	-4(3)
C(111)	71(5)	89(5)	56(4)	0(4)	14(3)	2(4)
C(112)	45(4)	54(4)	90(5)	-1(3)	10(3)	18(4)
B(1)	48(5)	52(5)	82(5)	-4(4)	-21(4)	5(4)

The anisotropic displacement exponent takes the form: $-2\pi^2(h^2a^{*2}U_{11} + ... + 2hka^*b^*U_{12} + ...)$

Table 6.6. H-Atom coordinates (x 10^4) and isotropic displacement coefficients ($Å^2$ x 10^3) for 3,3,11,11-tetramethyl-1,2-dithia-5,9-diazacycloundecane-5-borane **(16)**:

	x	y	z	U
H(4A)	-451	3505	4730	80
H(4B)	906	4046	4593	80
H(5)	871	2020	4075	50
H(6A)	-317	1080	4828	80
H(6B)	-1143	1535	4396	80
H(7A)	849	-248	4311	80
H(7B)	-617	-593	4345	80
H(8A)	-962	402	3601	80
H(8B)	19	-705	3550	80
H(9)	1533	774	3559	80
H(10A)	1121	454	2829	80
H(10B)	-125	1264	2899	80
H(31A)	-1016	5962	3906	106
H(31B)	-60	5895	4344	106
H(31C)	-1515	5458	4403	106
H(32A)	-1169	2692	3684	80

H(32B)	-1778	3969	3518	80
H(32C)	-2177	3388	4013	80
H(111A)	1986	3091	2166	100
H(111B)	661	2359	2152	100
H(111C)	1983	1621	2158	100
H(112A)	2861	2528	3361	80
H(112B)	3340	3083	2872	80
H(112C)	3329	1628	2952	80
H(B(1)A)	2066	966	4801	50
H(B(1)B)	1394	1895	5105	50
H(B(1)C)	2536	2812	4627	50

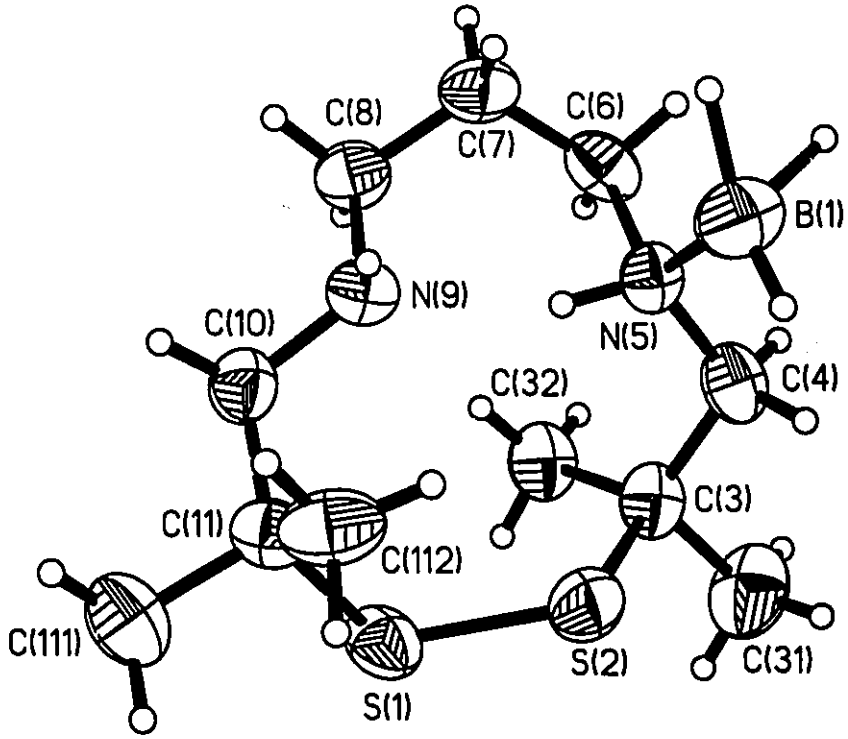

Figure 6.2. The Crystal structure of 3,3,11,11-tetramethyl-1,2-dithia-5,9-diazacycloundecane-5-borane

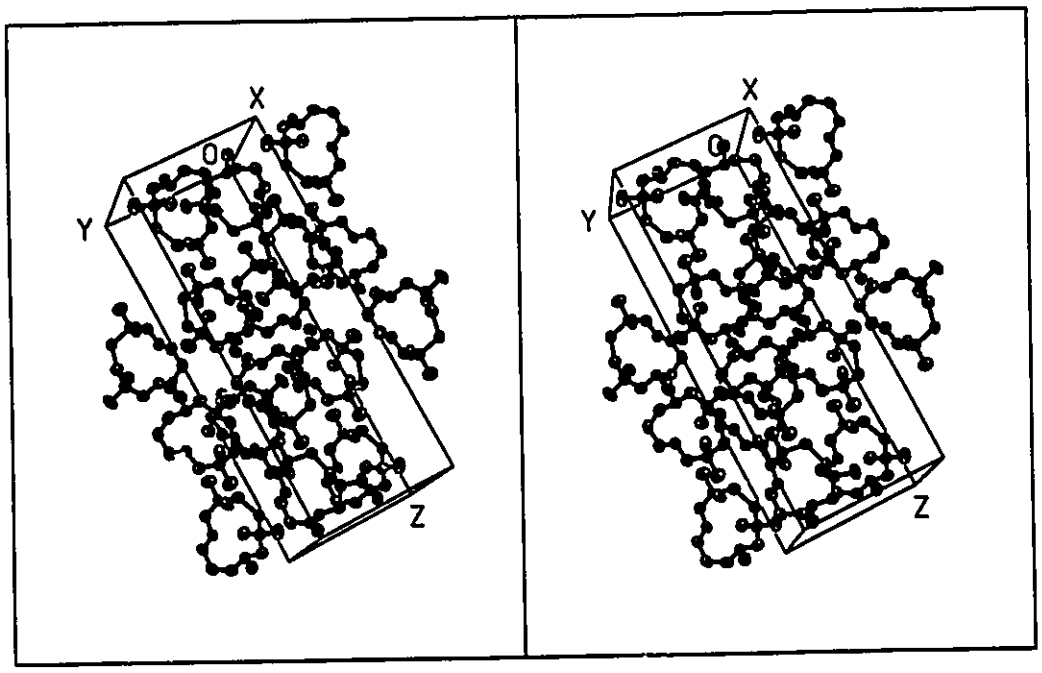

Figure 6.3. The Packing Diagram for 3,3,11,11-tetramethyl-1,2-dithia-5,9-diazacycloundecane-5-borane

CHAPTER 7

Summary

In the preceding chapters, results were presented that involved the study of diaminopolythiol ligands and their interaction with technetium and rhenium. Discussion of syntheses and full characterization of these ligands is the major part of this thesis. Methods of characterization included ^{1}H NMR, ^{13}C NMR, IR, Raman and mass spectroscopy. Double resonance NMR experiments were carried out for confirmation of the NMR assignments. Single crystal X-ray diffraction was used in cases where suitable crystals could be isolated.

The work described in chapter 3 involved the investigation of how the unexpected formation of oxo(2-(1'-methyl-1'-mercaptoethyl)-3-(5''-methyl-5''-mercapto-3''-dehydroazahexyl)-thiazolidinato-N^{3},$N^{3''}$,$S^{1''}$,$S^{5''}$)technetium(V) **(7)** took place. The complex was prepared by the Johns Hopkins group [71] and was thought to have the technetium atom bound to two nitrogen and three sulfur atoms giving a novel TcO(N2S3) complex. The crystal structure determination of the complex showed that the third sulfur atom was not bound to technetium; instead it formed an S-C bond to give a five-membered thiazolidine ring. It was shown in this work that the unexpected thiazolidine ring formation had taken place before complex formation.

It was demonstrated that the bicyclic 2,2,5,5-tetramethyl-3,4-dithia-7,10-

diazabicyclo[5.3.0]decane **(3)** was the major product in the sodium borohydride reduction of 3,3,10,10-tetramethyl-1,2-dithia-5,8-diazacyclodeca-4,8-diene **(2)**. The ligand, 3,3,10,10-tetramethyl-1,2-dithia-5,8-diazacyclodecane **(4)**, was only a minor product in this reaction. Compound **(3)** was shown to undergo further reduction to give **(4)** with the use of sodium borohydride under acidic conditions. The reaction of **(3)** with ethylene sulfide led to the isolation of the thiazolidine ring containing ligand, 2,2,5,5,-tetramethyl-3,4,13-trithia-7,10-diazabicyclo[8.3.0]tridecane **(5)**, which was subsequently characterized by single crystal X-ray diffraction.

The thiazolidine ring formation can be prevented if ethylene sulfide is replaced with 2-(triphenyl)thioethanoic acid **(8)**, as described in chapter 4. Reaction of 2,2,5,5-tetramethyl-3,4-dithia-7,10-diazabicyclo[5.3.0]decane **(3)** with 2-(triphenyl)thioethanoic acid **(8)** led to the isolation of N10-(triphenylmethylthioethanoyl)-2,2,5,5-tetramethy-3,4-dithia-7,10-diazabicyclo[5.3.0]decane **(9)** in a high yield. Compound **(9)** contained three sulfur and two nitrogen atoms available for metal chelation. It was characterized fully by various spectroscopic methods including single crystal X-ray diffraction. The protecting trityl group in **(9)** was removed successfully and the resultant ligand, N10-(thioethanoyl)-2,2,5,5-tetramethy-3,4-dithia-7,10-diazabicyclo[5.3.0]decane**(10)**, was added to $ReO(P(Ph)_3)_2Cl_3$. This reaction led to the unexpected formation of the novel asymmetric ReON2S2 complex, oxo(1,1-dimethyl-3-aza-6-amidooctane-

1,8-dithiolato)rhenium(V) **(11)**. The crystal structure determination of this complex showed that one ethylenethiol group was lost from the ligand in the process of the reaction and the final complex contained neither an N2S3 pentadentate ligand nor a thiazolidine ring containing ligand. In addition to single crystal X-ray diffraction, the complex **(11)** was characterized by IR and Raman spectroscopy.

In chapter 5, the investigation of the reaction of ethylene sulfide with 3,3,10,10-tetramethyl-dithia-5,8-diazacyclodecane **(4)** was described. It was found that this reaction led to the isolation of the N2S4 ligand, 1,2-di-(N-(3,3-dimethyl-1,2-dithia-5-aza-cycloheptyl) ethane **(13)**. Compound **(13)** was characterized by NMR spectroscopy and single crystal X-ray diffraction. Several attempts to make a technetium or rhenium complex of this ligand were not successful.

The sodium borohydride reduction of the 11-membered ring diimine, 3,3,11,11-tetramethyl-1,2-dithia-5,9-diazacycloundeca-4,9-diene **(15)**, was found to be different from that of the 10-membered ring diimine, 3,3,10,10-tetramethyl-1,2-dithia-5,8-diazacyclodeca-4,8-diene **(2)**. As described in chapter **(6)**, the reduction of **(15)** does not lead to the formation of a bicyclic product, in contrast to what was observed in the case of compound **(2)**. Instead, much to our surprise, the borane, adduct 3,3,11,11-tetramethyl-1,2-dithia-5,9-diazacycloundecane-5-borane **(16)**, was isolated. The characterization techniques of compound **(16)** included single crystal X-ray diffraction. The presence of the BH_3 group in the ligand was confirmed by use of IR spectroscopy which showed clearly the B-H stretching

absorption at 2356-2267 cm^{-1}.

There are many opportunities for further research. The bicyclic 2,2,5,5-tetramethyl-3,4-dithia-7,10-diazabicyclo[5.3.0]decane (3) has a secondary amino group which can readily form an amide linkage, as was demonstrated in chapter (4). Biologically active molecules can be added to this ligand through an amide bond formation. This might lead to the isolation of new technetium radiopharmaceuticals. In addition, compound (3) can be readily alkylated with the use of alkyl halides. Preliminary results, reaction 7.1., have shown that 2-

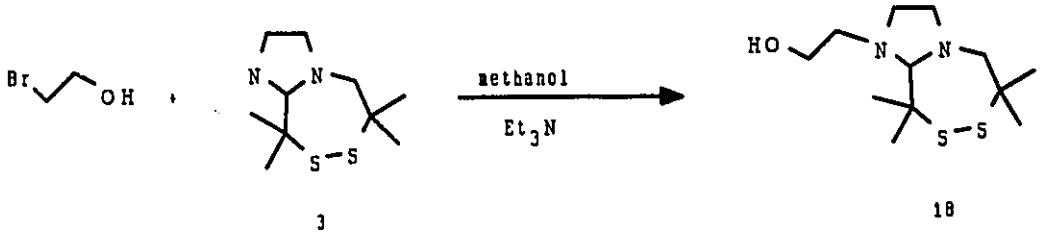

Figure 7.1. Reaction 7.1

bromoethanol reacts readily with compound (3) to give (18) in 70% yield. Compound (18) is potentially an N2S2O ligand, but, more important, is the fact that reaction 7.1 demonstrates that compound (3) can undergo alkylation. Addition of biologically important fragments to compound (3) by use of alkylation reactions is feasible.

References

1 E. Deutsch, K. Libson, S. Jurisson and L. F. Lindoy, Prog. Inorg. Chem., **30**, 75, (1983).

2 C. Perrier and E. Segré, J. Chem. Phys., **5**, 712 (1937).

3 C. Perrier and E. Segré, J. Chem. Phys., **7**, 155 (1939).

4 C. Perrier and E. Segré, Nature, **24**, 159 (1947).

5 R. C. Weast, M. J. Astle and W. H. Beyer, eds, CRC Handbook of Chemistry and Physics, CRC Press, 66 Ed, p. 37B, (1985-1986).

6 S. Kasina, A. R. Fritzberg, D. L. Johnson and D. J. Eshima, J. Nucl. Med., **29**, 1933 (1986).

7 R. F. Schneir, G. Subramanian, T. A. Feld, J. G. McAfee, C. Zapf-Longo, E. Palladino and F. D. Thomas, J. Nucl. Med., **25**, 233 (1984).

8 M. C. Lagunas-Solar, P. M. Kiefer, O. F. Carvacho, C. A. Lagunas, and Y. P. Cha, Appl. Radiat. Isot., **42**, 634 (1991) [ALASBIN 1989].

9 P. Richards, W. D. Tucker and S. C. Srivastava, Int. J. Appl. Isot., **33**, 793 (1982).

10 E. Deutsch, W. R. Heineman, J. P. Zodda and C. C. Williams, Int. J. Appl. Radiat. Isot., **33**, 843 (1982).

11 E. Deutsch, Radiopharmaceuticals II: Proceedings of the Second Symposium on Radiopharmaceuticals, Society of Nuclear Medicine, New

York, 130 (1979).

12 N. D. Heindel, H. D. Burns, T. Honda and L. W. Brady, eds., The Chemistry of Radiopharmaceuticals, Masson, New York, 155 (1978).

13 E. Deutsch, M. Nicolini and H. W. Wagner,jr, Eds., Technetium in Chemistry and Nuclear Medicine, Cortina International, Verona, (1983).

14 M. J. Clarke and L. Podbielski, Coord. Chem. Rev., **78**, 253, (1987).

15 M. Nicolini, G. Bandoli and U. Mazzi, eds., Technetium in Chemistry and Nuclear Medicine 2, Cortina International, Verona, (1986).

16 C. J. Jones, Comp. Coord. Chem., V. 6, Eds. G. Wilkinson, J.A. McCleverty, and R.D. Gillard. 963 - 1009, (1987).

17 S. Jurisson, D. Berning, Wei Jia and Dangshe Ma, Chem. Rev., **93**, 1137 (1993).

18 L. Astheimer, J. Hauck, H. J. Schenk and K.Schwochau, J. Chem. Phys., **63**, 1988 (1975).

19 E. Deutsch, W. R. Heineman, R. Hurst, J. C. Sullivan, W. Mular and G. Sheffield, J. Chem. Soc. Chem. Commun., 1038 (1978).

20 T. G. Tji, H. A. Vink, W. J. Gelsema and C. L. Deligny, Appl. Radiat. Isot., **41**, 17, (1990).

21 C. S. John, E. O. Schlemper, P. Hosain, C. H. Paik and R. C. Reba, Nucl. Med. Biol., **19**, 269 (1992).

22 E. Deutsch, R. C. Elder, B. A. Lange, M. J. Vaal and D. G. Lay, Proc. Natl.

Acad. Sci. USA, 73, 4287 (1976).

23 F. A. Cotton, A. Davison, V. W. Day, L. D. Gage and H. S. Trop, Inorg. Chem., 18, 3024, (1979).

24 R. W. Thomas, A. Davison, H. S. Trop and E. Deutsch, Inorg. Chem., 19, 2840, (1980).

25 A. Davison, H. S. Trop, B. V. Depamphilis and A. G. Jones, Inorg. Synth., 21, 160 (1982).

26 A. Davison, A. G. Jones and M. J. Abrams, Inorg. Chem., 20, 4300 (1981).

27 A. Davison, C. Orvig, J. S. Trop, M. Sohn and B. V. Dephamphilis, Inorg. Chem., 19, 19, (1980).

28 J. G. H. DuPreez, T. I. A. Gerber and O. Knoesen, Inorg. Chim. Acta, 109, L17, (1985).

29 T. Nicholson, J. Thornback, L. O'Connell, G. Morgan, A. Davison and A. G. Jones, Inorg. Chem., 29, 89, (1990).

30 G. Bandoli, D. A. Clemente, U. Mazzi, J. Chem. Soc., Dalton Trans., 2, 125, (1976).

31 F. Tisato, C. Bolzati, A. Duatti, G. Bandoli and F. Refosco, Inorg. Chem., 32, 2042 (1993).

32 M. J. Abrams, A. Davison, R. Faggiani, A. G. Jones and C. J. L. Lock, Inorg. Chem., 23, 3284, (1984).

33 H. Spies, U. Abram, E. Uhlemann and E. Ludwig, Inorg. Chim. Acta, 109,

L3 (1985).

34 T. Konno, J. R. Kirchhoff, M. J. Heeg, W. R. Heineman and E. Deutsch, J. Chem. Soc. Dalton Trans., 3069 (1992).

35 T. Konno, M. J. Heeg, and E. Deutsch, Inorg. Chem., **27**, 4113 (1988).

36 T. Konno, J. R. Kirchhoff, W. R. Heineman and E. Deutsch, Inorg. Chem., **28**, 1174, (1989).

37 T. Konno, M. J. Heeg and E. Deutsch, Inorg. Chem., **28**, 1694, (1989).

38 T. Konno, M. J. Heeg, J. A. Stuckey, J. R. Kirchhoff, W. R. Heineman and E. Deutsch, Inorg. Chem., **31**, 1173, (1992).

39 C. M. Archer, J. R. Dilworth, R. M. Thompson, M. McPartlin, D. C. Povey and J. D. Kelly, J. Chem. Soc. Dalton Trans., 461 (1993).

40 R. M. Pearlstein, W. M. Davis, A. G. Jones and A. Davison, Inorg. Chem., **28**, 3332 (1989).

41 A. Davison, A. G. Jones, C. Orvig, and M. Sohn, Inorg. Chem., **20**, 1629 (1981).

42 D. Brener, A. Davison, J. Lister-James, and A. G. Jones, Inorg. Chem., **23**, 3793 (1984).

43 R. Faggiani, C. J. L. Lock, L. A. Epps, A. V. Kramer, and D. Brune, Acta Cryst. C**44**, 777 (1988).

44 E. Deutsch, M. Nicolini, H. N. Wagner, jr, eds., Technetium in Nuclear Medicine, Cortina International, Verona, (1983).

45 H. K. Kung, M. Molnar, J. Billings, R. Wicks, and M. Blau, J. Nucl. Med., 25, 326, (1984).

46 A. Davison, M. Sohn, C. Orvig, A. G. Jones and M. R. LaTegola, J. Nucl. Med., 20, 641 (1979).

47 N. Bryson, J. C. Dewan, J. Lister-James, A. G. Jones and A. Davison, Inorg. Chem., 27, 2154 (1988).

48 A. R. Fritzberg, W. C. Klingensmith, W. P. Whitney and C. C. Kuni, J. Nucl. Med., 22, 258, (1981).

49 W. C. Klingensmith, J. P. Gerhold, A. R. Fritzberg, V. M. Spitzer, C. C. Kuni, C. J. Singer and R. Weil, J. Nucl. Med., 23, 377 (1982).

50 A. R. Fritzberg, S. Kasina, D. Eshima, D. L. Johnson, A. G. Jones, J. Lister-James, A. Davison and J. W. Brodack, J. Nucl. Med., 25, 16 (1984).

51 C. E. Costello, J. W. Brodack, A. G. Jones, A. Davison, D. L. Johnson, S. Kasina and A. R. Fritzberg, J. Nucl. Med., 24, 353, (1983).

52 T. N. Rao, D. Adhikesavalu, A. Camerman and A. R. Fritzberg, J. Am. Chem. Soc., 112, 5798 (1990).

53 T. N. Rao, D. I. Brixner, A. Srinivasan, S. Kasina, J. L. Vanderheyden, D. W. Wester and A. R. Fritzberg, Appl. Radiat. Isot., 42, 525 (1991).

54 A. R. Fritzberg, W. P. Whitney, J. Stevens, W. C. Klingensmith and C. C. Kuni, J. Nucl. Med., 23, 17 (1983).

55 W. C. Klingensmith, A. R. Fritzberg, V. M. Spitzer, D. L. Johnson, C. C.

Kuni, M. R. Williamson, G. Washer and R. Weil, J. Nuucl. Med., 25, 42 (1984).

56 A. R. Fritzberg, P. G. Abrams, P. L. Beaumier, S. Kasina, A. C. Morgan, T. N. Rao, J. M. Reno, J. A. Sanderson, A. Srinivasan, D. S. Wilbur, and J-L. Vanderheyden, Proc. Natl. Acad. Sci., 85, 4025 (1988).

57 S. Kasina, T. N. Rao, A. Srinivasan, J. A. Sanderson, J. N. Fitzner, J. M. Reno, P. L. Beaumier and A. R. Fritzberg, J. Nucl. Med., 32, 1445 (1991).

58 This test was carried out at McMaster's Department of Nuclear Medicine.

59 J. L. Corbin and D. E. Work, J. Org. Chem., 41, 489 (1976).

60 H. D. Burns, R. F. Dannals, and T. E. Dannals, J. Label. Comp., 18, 54 (1981).

61 S. M. N. Efange, H.F. Kung, J. Billings, Y. -Z. Guo, and M. Blau, The J. Nucl. Med., 28, 1012 (1987).

62 K. M. Tramposch, H. K. Kung, M. Blau, The J. Med. Chem., 26, 121 (1983).

63 S. Z. Lever, H. D. Burns, T. M. Kervitsky, H. W. Goldfarb, D. F. Wong, D. V. Woo, L. A. Epps, A. V. Kramer, H. N. Wagner Jr., J. Nucl. Med., 26, 1286 (1985).

64 U. Scheffel, H. W. Goldfarb, S. Z. Lever, R. L. Gungon, H. D. Burns, and H. N. Wagner, Jr, J. Nucl. Med., 29, 73 (1988).

65 H. F. Kung, B. Liu and S. Pan, Appl. Radiat. Isot., 40, 677 (1989).

66 H. F. Kung, C. C. Yu, J. Billings, M. Molnar and M. Blau, J. Med. Chem.,

28, 1280 (1985).

67 R. H. Mach, H. F. Kung, P. Jungwiwattanaporn, and Y. -Z. Guo, Tet. Lett., **30**, 4069 (1989).

68 R. H. Mach, H. F. Kung, Y. -Z. Guo, P. Jungwiwattanaporn and A. Alavi, J. Nucl. Med., **29**, 935 (1988).

69 G. S. Jones, H. W. Strauss and D. R. Elmaleh, J. Nucl. Med., **29**, 935 abs. (1988).

70 R. H. Mach, H. F. Kung, Y-Z Guo and P. Jungwiwattanaporn, Nucl. Med. Biol., **18**, 215 (1991).

71 L. A. Epps, A. V. Kramer, H. D. Burns, S. Z. Keva and H. W. Golfarb, Johns Hopkins University, unpublished results.

72 K. Schwochau, Radiochim. Acta, **32**, 139 (1983).

73 C. J. L. Lock and G. Wilkinson, Chem. and Indust., 40 (1962).

74 M. Freni and V. Valenti, J. Inorg. Nucl. Chem., **16**, 240 (1961).

75 G. E. Boyd, J. Chem. Educ., **36**, 3 (1959).

76 M. J. Buerger, X-ray Crystallography, John Wiley and Sons, New York, (1942).

77 P. Luger, Modern X-ray Analysis on Single Crystals, Walter de Gruyter, Berlin (1980).

78 G. H. Stout and L. H. Jensen, X-ray Structure Determination, John Wiley and Sons, New York (1989).

79 J. P. Glusker and K. N. Trueblood, Crystal Structure Analysis; A Primer, 2nd ed., Oxford University Press, New York (1985).

80 S. French and K. Wilson, Acta Cryst., A34, 517 (1978).

81 J. C. Calabrese and R. M. Burnett, TAPER, Nicolet XRD Corp., Locally modified by Z. Tun and called PSISCAN (1980).

82 N. Walker and D. Stuart, Acta Cryst., A39, 158 (1983).

83 D. J. Cromer and T. T. Waber, International Tables for X-ray Crystallography, Vol. IV, Kynoch Press, Birmingham (1974).

84 G. M. Sheldrick, SHELXTL PLUS Release 4.21/V, Siemens Analytical Instrument Inc. Madison, WI (1990).

85 J. J. D'Amico and W. E. Dahl, J. Org. Chem., 40, 1224 (1975).

86 A. V. Joshua, J. R. Scott, S. M. Sondhi, R. G. Ball and J. W. Lown, J. Org. Chem., 52, 2447 (1987).

87 S. M. Sondhi, P. Kolodziejczyk, R. G. Ball and J. W. Lown, J. Org. Chem., 53, 4310 (1988).

88 K. Shiba, H. Mori, H. Matsuda, S. Tsuji, K. Kinuya and K. Hisada, Appl. Radiat. Isot., 42, 1159 (1991).

89 K. D. Karlin and S. J. Lippard, J. Am. Chem. Soc., 98, 6951 (1976).

90 P. Ferruti and E. Ranucci, Makromol. Chem., Rapid Commun., 8, 549, (1987).

91 R. Faggiani, C. J. L. Lock, L. A. Epps, A. V. Kramer, and D. Brune, Acta

Cryst. C44, 777 (1988).

92 R. Faggiani, H. E. Howard-Lock, C. J. L. Lock and R. Orgias, Can. J. Chem., **69**, 1 (1991).

93 H. E. Howard-Lock, C. J. L. Lock, P. S. Smalley, Can. J. Chem., **63**, 2411 (1985).

94 M. Goodman and K. C. Stueben, J. Am. Chem. Soc., **81**, 3980 (1959).

95 H. A. Staab, Angew. Chem. Int. Ed., **1**, 360 (1962).

96 L. M. Gustavson, T. N. Rao, D. S. Jones, A. R. Fritzberg and A. R. Srinivasan, Tet. Lett., **32**, 5485 (1991).

97 T. N. Rao, L. M. Gustavson, A. Srinivasan, S. Kasina and A. R. Fritzberg, Nucl. Med. Biol., **19**, 889 (1992).

98 L. C. Francesconi, G. Graczyk, S. Wehrli, S. N. Shaikh, D. McClinton, S. Liu, J. Zubieta and H. F. Kung, Inorg. Chem., **32**, 3114 (1993).

99 T. W. Jackson, M. Kojima and R. M. Lambrecht, Aust. J. Chem., **46**, 1093 (1993).

100 A. Najafi, M. M. Alauddin, M. E. Siegel and A. L. Epstein, Nucl. Med. Biol., **18**, 179 (1991).

101 A. Najafi, M. M. Alauddin, A. Sosa, G. Q. Ma, D. C. P. Chen, A. L. Epstein and M. E. Siegel, Nucl. Med. Biol., **19**, 205 (1992).

102 R. H. Mach, H. F. Kung, P. Jungwiwattanaporn and Y. -Z. Guo, Nucl. Med. Biol. **18**, 215 (1991).

103 R. H. Mach, H. F. Kung, Org. Mass Spectr., 26, 528 (1991).

104 M. S. Newman, Steric Effects in Organic Chemistry, New York, p.115, (1959).

105 S. H. Bauer, J. Am. Chem. Soc., 59, 1804 (1937).